

AD\_\_\_\_\_

Award Number: DAMD17-99-1-9090

TITLE: Isolation of Signaling Molecules Involved in Angiogenic  
Pathways Mediated Alpha V Integrins

PRINCIPAL INVESTIGATOR: Marina Cardo-Vila

CONTRACTING ORGANIZATION: The University of Texas  
M.D. Anderson Cancer Center  
Houston, Texas 77030

REPORT DATE: May 2004

TYPE OF REPORT: Annual Summary

PREPARED FOR: U.S. Army Medical Research and Materiel Command  
Fort Detrick, Maryland 21702-5012

DISTRIBUTION STATEMENT: Approved for Public Release;  
Distribution Unlimited

The views, opinions and/or findings contained in this report are those of the author(s) and should not be construed as an official Department of the Army position, policy or decision unless so designated by other documentation.



**REPORT DOCUMENTATION PAGE**Form Approved  
OMB No. 074-0188

Public reporting burden for this collection of information is estimated to average 1 hour per response, including the time for reviewing instructions, searching existing data sources, gathering and maintaining the data needed, and completing and reviewing this collection of information. Send comments regarding this burden estimate or any other aspect of this collection of information, including suggestions for reducing this burden to Washington Headquarters Services, Directorate for Information Operations and Reports, 1215 Jefferson Davis Highway, Suite 1204, Arlington, VA 22202-4302, and to the Office of Management and Budget, Paperwork Reduction Project (0704-0188), Washington, DC 20503

**1. AGENCY USE ONLY**  
(Leave blank)**2. REPORT DATE**  
May 2004**3. REPORT TYPE AND DATES COVERED**  
Annual Summary (1 Nov 00-30 Apr 04)**4. TITLE AND SUBTITLE**

Isolation of Signaling Molecules Involved in Angiogenic Pathways Mediated Alpha V Integrins

**5. FUNDING NUMBERS**

DAMD17-99-1-9090

**6. AUTHOR(S)**

Marina Cardo-Vila

**7. PERFORMING ORGANIZATION NAME(S) AND ADDRESS(ES)**The University of Texas M.D. Anderson Cancer Center  
Houston, Texas 77030

E-Mail: mcardovi@mdanderson.org

**8. PERFORMING ORGANIZATION  
REPORT NUMBER****9. SPONSORING / MONITORING  
AGENCY NAME(S) AND ADDRESS(ES)**U.S. Army Medical Research and Materiel Command  
Fort Detrick, Maryland 21702-5012**10. SPONSORING / MONITORING  
AGENCY REPORT NUMBER****11. SUPPLEMENTARY NOTES**

Original contains color plates. All DTIC reproductions will be in black and white.

**12a. DISTRIBUTION / AVAILABILITY STATEMENT**

Approved for Public Release; Distribution Unlimited

**12b. DISTRIBUTION CODE****13. ABSTRACT (Maximum 200 Words)**

Angiogenic vasculature selectively expressed  $\alpha v\beta 3$  and  $\alpha v\beta 5$  integrins but they are not expressed in normal vasculature. They are cell adhesion molecules that play an important role in the regulation of angiogenesis. There are at least two cytokine-dependent pathways that lead to angiogenesis in vivo which can be distinguished by their dependency on specific  $\alpha v$  integrins. Here we aim to define what molecules are involved in  $\alpha v\beta 3$ - and  $\alpha v\beta 5$ -selective angiogenic signaling. We hypothesize that: i) different molecules associate with each of these integrins after angiogenesis is triggered by defined cytokines; ii) the assembly of specific molecules with the  $\beta 3$  or  $\beta 5$  cytoplasmic domains results in selective signaling. The strategy used to approach these questions is based on the panning of phage peptide libraries of  $\beta 3$  and  $\beta 5$  cytoplasmic domains. Selected peptides are used to characterize candidate molecules mimicked by the peptides using biochemistry techniques. Finally, by using micro-injection-based techniques and internalizable forms of the synthetic peptides, we studied the effect of the integrin cytoplasmic domain binding peptides in cell adhesion, migration, apoptosis and proliferation upon stimulation with factors that can activate endothelial cells in vitro. We established that a cell death process induced by  $\beta 5$ -binding peptide is sensitive to modulation by growth factors and by protein kinase C (PKC), and it cannot be triggered in  $\beta 5$  null cells. Finally, we show that the  $\beta 5$ -binding peptide is a mimic of annexin V. Our results suggest a functional link between the  $\alpha v\beta 5$  integrin, annexin V, and a novel programmed cell death mechanism. These studies will shed light into molecular basis of selective signal transduction pathways initiated by  $\alpha v\beta 3$  and  $\alpha v\beta 5$ . New assays aimed to inhibit of angiogenesis, and ultimately, new strategies to treat breast cancer may result from this work.

**14. SUBJECT TERMS**

Angiogenesis, Integrins, Signal Transduction

**15. NUMBER OF PAGES**

67

**16. PRICE CODE****17. SECURITY CLASSIFICATION  
OF REPORT**

Unclassified

**18. SECURITY CLASSIFICATION  
OF THIS PAGE**

Unclassified

**19. SECURITY CLASSIFICATION  
OF ABSTRACT**

Unclassified

**20. LIMITATION OF ABSTRACT**

Unlimited



## Table of Contents

Cover.....	1
SF 298.....	2
Table of Contents.....	3
Introduction.....	4
Body.....	5
Key Research Accomplishments.....	20
Reportable Outcomes.....	21
Conclusions.....	23
References.....	24
Appendices.....	31



## INTRODUCTION

The growth of new capillaries from pre-existing vessels, named angiogenesis, contributes to the development and progression of a variety of physio-pathological conditions, as malignant tumor growth and metastasis (Folkman, 1992; Weinstat-Saslow, D. and Steeg, P.S, 1994, Folkman, 1995). In the absence of angiogenesis, local tumor expansion is suppressed at a few millimeters and cells lack routes for distant hematogenous spread. Clinical studies have demonstrated that the degree of angiogenesis is correlated with the malignant potential of several cancers, including breast cancer and malignant melanoma (Horak et al., 1992; Carrau et al., 1995; Meitar et al., 1996; Takebayashi et al., 1996 Sung et al., 1998).

Although cell surface receptors of the integrin family were initially characterized for their contribution to cell adhesion and migration (Hynes, 1992), recent report suggest their contribution to cancer progression by mediating cellular functions such as tumor cell proliferation, invasion, survival and apoptosis (Hynes, 1999; Giancotti and Ruoslahti, 1999; Pariese et al., 2000, Elicieri and Cheresch, 2001)

Vascular integrins such as  $\alpha v\beta 3$  and  $\alpha v\beta 5$  are selectively expressed in angiogenic vasculature but they are not expressed in normal vasculature (Brooks et al., 1994; Drake et al., 1995; Clark et al., 1995; Pasqualini et al., 1997; Arap et al., 1998). Moreover,  $\alpha v$  integrin antagonists have been shown to block the growth of neovessels (Brooks et al., 1994a, 1994b, 1995, 1997; Hammes et al., 1996); in these experiments, endothelial cell apoptosis was identified as the explanation for the inhibition of angiogenesis (Brooks et al., 1994a, b, 1995; Varner et al., 1995). Even though, both  $\alpha v\beta 3$  and  $\alpha v\beta 5$  integrins bind to vitronectin, they probably mediate different post-ligand binding events. For instance, in the absence of exogenous soluble factors, the integrin  $\alpha v\beta 5$  fails to promote cell adhesion, spreading, migration, and angiogenesis. On the other hand, the  $\alpha v\beta 3$  integrin can induce such events without additional stimulation by cytokines (Klemke et al., 1994; Lewis et al., 1996; Friedlander et al., 1995).

The uses of phage libraries have provided a rapid means to identify extracellular integrin ligands (Koivunen et al, 1999). The large molecular diversity represented in phage peptide libraries facilitates the identification of motifs that map to protein interaction sites (Kolonin et al., 2001; Giordano et al., 2001). For example, RGD-containing peptides with high affinity for  $\alpha v$  integrins have been isolated by phage display and shown to be useful tools for targeting tumor vasculature in vivo (Koivunen et al., 1995; Pasqualini et al, 1997; Zetter, 1997).

Cellular control of the adhesive interactions and their translation into dynamic cellular responses, such as cell spreading or migration, requires the integrin cytoplasmic tails. The diverse cytoplasmic domain sequences within the various integrin subunits are critical for integrin-mediated signaling into the cell (outside-in signaling) and for activation of ligand binding affinity (inside-out signaling) (Clark and Brugge, 1995; Clark and Hynes, 1997; Howe et al., 1998; Schlaepfer and Hunter, 1998). Often, it is the association of specific molecules with integrin cytoplasmic domains that initiates signal transduction cascades



(Schwartz et al., 1995; Shattil and Ginsberg, 1997; Schlaepfer and Hunter, 1998; Liu et al., 2000; Aplin and Juliano, 2001). Expression of chimeric integrins showed that the cytoplasmic domains of the integrin  $\beta$  subunits are critical for integrin-mediated signaling into the cell (outside-in signaling) and activation of integrin-ligand binding affinity (inside-out signaling; Hynes, 1992; Schwartz et al., 1995; Lafrenie and Yamada, 1996; Shattil and Ginsberg, 1997).

Only a limited number of proteins that bind to integrin cytoplasmic domains have been identified. These proteins, such as paxillin and ICAP-1, mainly associate with the  $\beta 1$  chain (reviewed in Shattil and Ginsberg, 1997). Cytohesin-1 and filamin associate with the cytoplasmic domain of  $\beta 2$  (Kolanus et al., 1996; Sharma et al., 1995).

The  $\beta 5$  cytoplasmic domain has been reported to control cell migration and proliferation (Pasqualini and Hemler, 1994; Klemke et al. 1994; Clark and Hynes, 1997). In addition, it has also been reported that the control of  $\alpha v\beta 5$  -dependent cell migration and tube formation of endothelial cells is through a pathway regulated by PKC (Tang et al., 1999). However,  $\alpha v\beta 5$ -dependent mechanisms for cytoplasmic domain control of cell signaling are not well understood. Theta-associated protein 20 (TAP 20), a cytoplasmic protein related to endonexin, is a key player in this process and associates with the  $\beta 5$  cytoplasmic. Unlike cytoskeletal proteins such as talin or the cytosolic protein receptor for activated protein kinase C (RACK1; Mochly-Rosen et al., 1995; Liliental and Chang, 1998), which associate with the cytoplasmic domains of several integrin  $\beta$  subunits, TAP 20 is the only protein known to interact exclusively with the  $\beta 5$  cytoplasmic domain.

To gain insight into the mechanisms regulating  $\alpha v\beta 5$  signaling, we sought to identify molecules that specifically interact with the cytoplasmic domain of  $\beta 5$  by screening a random peptide library using phage display. The extraordinary molecular diversity represented in phage display libraries facilitates identification of motifs that mimic protein interaction sites (Kallen et al., 2000; Kolonin et al., 2001; Giordano et al., 2001). Because peptides that bind to the  $\beta 5$  cytoplasmic domain probably mimic the effects of  $\alpha v\beta 5$  -associated molecules, we hypothesized that such peptides could interfere with  $\alpha v\beta 5$  -mediated cell functions upon cell internalization.

In summary, our proposed studies are likely to contribute to a better understanding of the biochemical mechanisms that are related to the integrin-mediated signaling events involved in controlling tumor growth and angiogenesis. These processes involve cell adhesion to the extracellular matrix and integrin-mediated signaling. Thus, the work proposed here may lead to novel therapeutic approaches in diseases such as cancer, rheumatoid arthritis, and retinopathies.

## **PROPOSAL BODY**

The tasks originally approved for this proposal are listed below.



1. To select peptides that bind specifically to  $\beta 3$  or to  $\beta 5$  integrin cytoplasmic domains.
2. To investigate whether phosphorylation events can modulate the interaction of the selected peptides with integrin cytoplasmic domains
3. To determine the biological properties of the cytoplasmic domain-binding peptides

In this final report, we show that we had successfully isolated peptides that bind specifically to  $\beta 3$  or  $\beta 5$  cytoplasmic domains. We provide functional data that strongly support the notion that our isolated peptides affect integrin function in a selective, specific and dose-dependent fashion. We demonstrate that phage display is a powerful tool that not only can be used to identify sequences that specifically bind the target protein, but it can also be used, with a combination of protein purification, to identify the protein that contains the sequence. We also determined biological properties of the cytoplasmic-binding peptide. Our findings are likely to contribute to a better understanding of the biochemical mechanisms that are related to the integrin-mediated signaling events involved in controlling tumor growth and angiogenesis.

*Phage display library screenings produce peptides that interact selectively with integrin cytoplasmic domains*

#### Panning of phage peptide libraries on $\beta 3$ or $\beta 5$ cytoplasmic domains.

We have isolated  $\beta 3$  (Figure 1) and  $\beta 5$  cytoplasmic domain-binding peptides (Figure 2), by screening multiple phage libraries with recombinant GST fusion proteins that contain either GST- $\beta 3$ cyto or GST- $\beta 5$ cyto coated onto microtiter wells. Immobilized GST was used as a negative control for enrichment during the panning on each cytoplasmic domain. Phage were sequenced from randomly selected clones after three rounds of panning as described elsewhere (Koivunen et al., 1994, 1995; Pasqualini et al., 1995). We successfully isolated distinct sequences that interact specifically with the  $\beta 3$  or with the  $\beta 5$  cytoplasmic domains (Figure 3A and 3B).

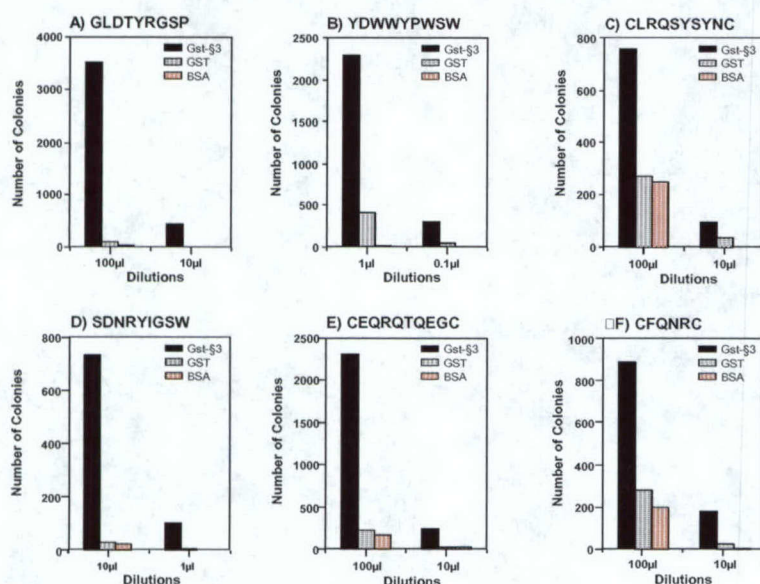


**Figure 1. Binding of  $\beta 3$  cytoplasmic domain-selected phage to immobilized proteins.** GST fusion proteins or GST alone were coated on microtiter wells at 10  $\mu$ g/ml and used to bind phage expressing the peptides (each phage is identified by the peptide sequence it displays, i.e. GLDTRYGSP; YDWWYPWSW; CLRQSYNSC; SDNRYIGSW; CEQRQTQEGC; CFQNRRC). The data represent the mean colony counts from triplicate wells, with standard error less than 10% of the mean.



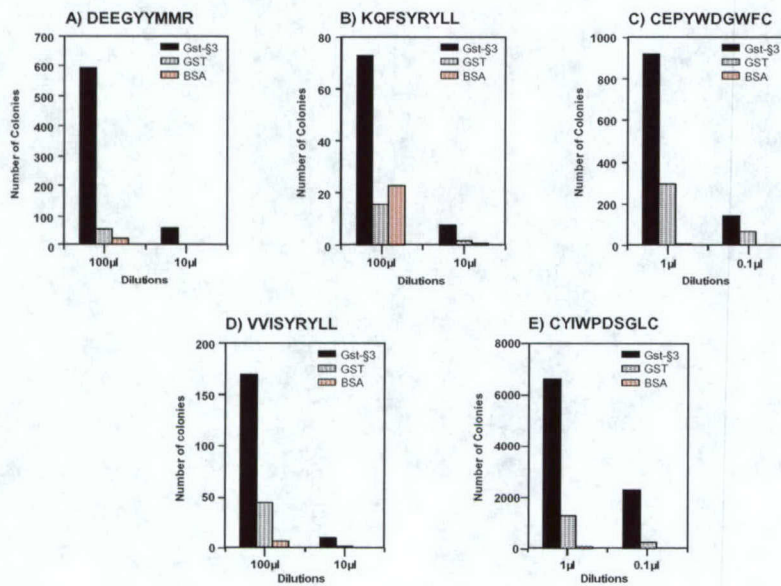
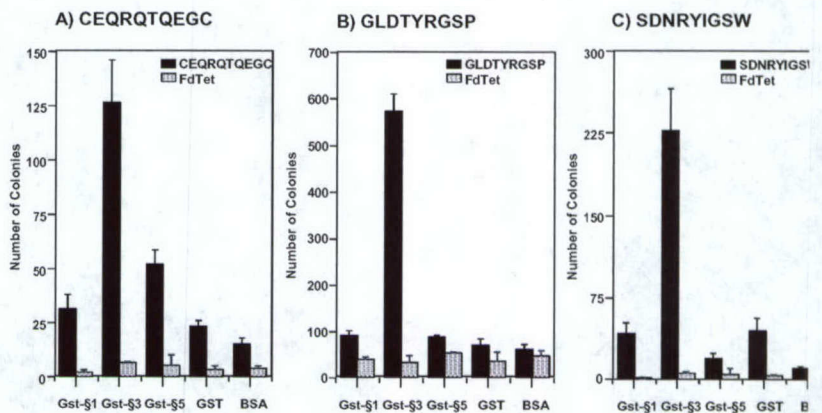


**Figure 2. Binding of  $\beta 5$  cytoplasmic domain-selected phage to immobilized proteins.** GST fusion proteins or GST alone were coated on microtiter wells at 10  $\mu$ g/ml and used to bind each phage expressing the peptides shown in Table 3 (each phage is identified by the peptide sequence it displays). (A) VVISYSMPD; (B) KQFSYRYLL; (C) CYIWPDSGLC; (D) CEPYWDGWFC (E) DEEGYYMMR. The data represent the mean colony counts from triplicate wells, with standard error less than 10% of the mean.

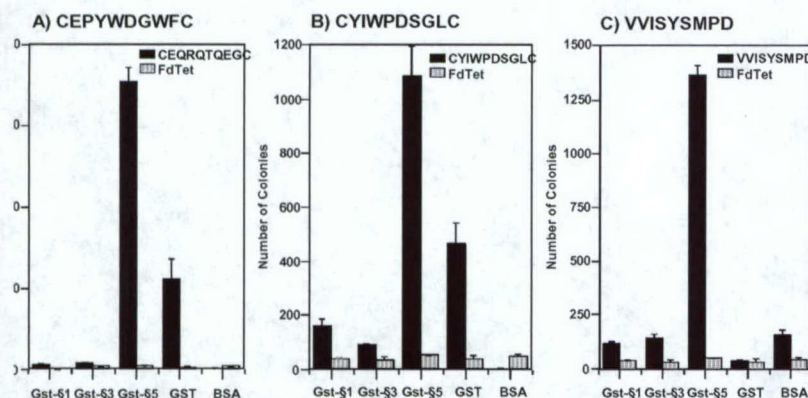
**Figure 3A. Binding of  $\beta 3$  cytoplasmic domain-selected phage to  $\beta 1$ ,  $\beta 3$  and  $\beta 5$  immobilized proteins.** GST fusion proteins or GST alone were coated on microtiter wells at 10  $\mu$ g/ml and used to bind each phage expressing the peptides shown in Table 3 (each phage is identified by the peptide sequence it displays). The data represent the mean colony counts from triplicate wells with standard error less than 10% of the mean. Fd-tet insertless phage was used as a negative control.

**Figure 3B. Binding of  $\beta 5$  cytoplasmic domain-selected phage to  $\beta 1$ ,  $\beta 3$  and  $\beta 5$  immobilized proteins.** GST fusion proteins or GST alone were coated on microtiter wells at 10  $\mu$ g/ml and



used to bind each phage expressing the peptides shown in Table 3 (each phage is identified by the peptide sequence it displays). The data represent the mean colony counts from triplicate wells, with standard error less than 10% of the mean. Fd-tet insertless phage was used as a negative control.

**Characterization of the synthetic peptides corresponding to the sequences displayed by the integrin-cytoplasmic domain-binding phage**  
We selected specific phage for further studies on the basis of their binding properties. We used synthetic peptides corresponding to the sequence displayed





by the phage to perform inhibitory studies (Figure 4A and B). This assay is important because it determines whether phage binding is entirely mediated by the peptide displayed by the phage. As expected, we found that the synthetic peptides can inhibit the binding of the corresponding phage in a dose-dependent manner. A control peptide containing unrelated amino acids had no effect on phage binding when tested at identical concentrations.

**Figure 4A. Binding of the cytoplasmic-domain binding phage to  $\beta 3$  immobilized protein and inhibition with the synthetic peptide.**

Phage were incubated on wells coated with GST- $\beta 3$ cyto in the presence of increasing concentrations of the corresponding synthetic peptide or a control peptide. The data represent the mean colony counts from triplicate wells, with standard error less than 10% of the mean.

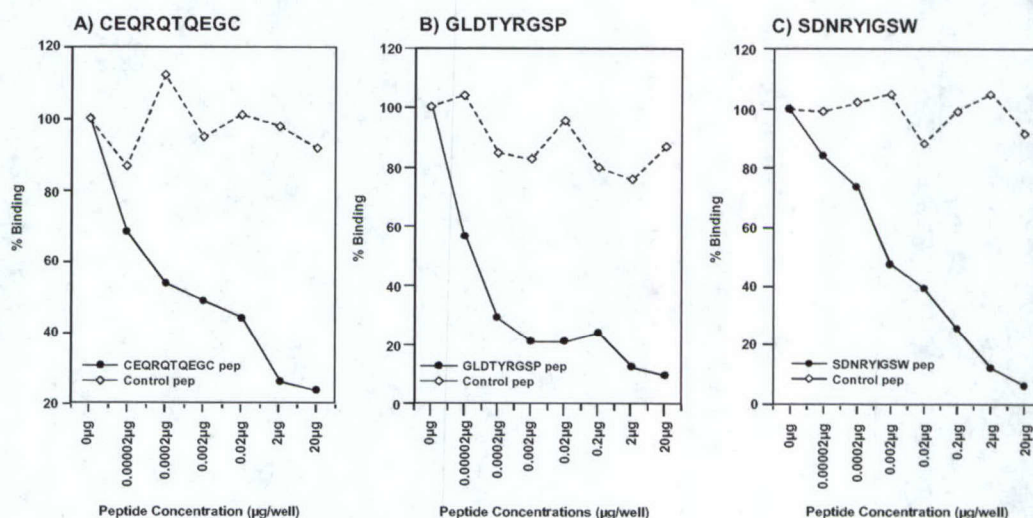
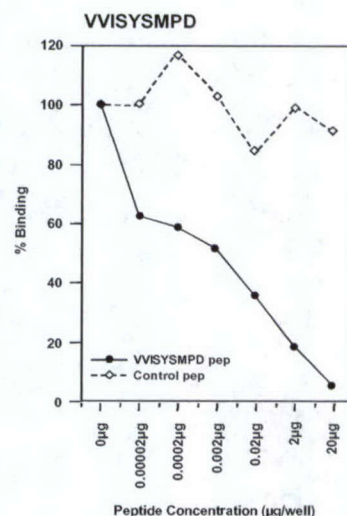


**Figure 4B. Binding of the cytoplasmic-domain binding phage to  $\beta 5$  immobilized protein and inhibition with the synthetic peptide.** Phage were incubated on wells coated with GST- $\beta 5$ cyto in the presence of increasing concentrations of the corresponding synthetic peptide or a control peptide. The data represent the mean colony counts from triplicate wells, with standard error less than 10% of the mean.



### A selective $\beta 5$ domain binding peptide identified by Phage Display

Because events involving tyrosine phosphorylation of key molecules are essential during the signal transduction of integrins (Jenkins et al., 1998; Lin et al., 1997) we used



recombinant fusion protein containing  $\beta 5$  cytoplasmic domain for panning of phage libraries displaying tyrosine-containing peptides. We isolated  $\beta 5$  cytoplasmic domain-binding peptides by screening a phage library displaying the motif  $X_4YX_4$  (where X is any amino acid and Y is a tyrosine) with an immobilized recombinant fusion protein containing the  $\beta 5$ -cytoplasmic domain. Immobilized glutathione-S-transferase (GST) and bovine serum albumin (BSA) were used as negative controls. After three rounds of selection with a significant enrichment for phage binding to  $\beta 5$ , fusion protein peptides inserts from randomly selected  $\beta 5$ -bound phage were sequenced. The most common motif (VVISYSMPD) was characterized further. To determine the specificity of its interaction with the  $\beta 5$  cytoplasmic domain, phage displaying the VVISYSMPD peptide was tested for binding to GST- $\beta 1$ , - $\beta 3$ , or - $\beta 5$  cytoplasmic domain fusion proteins. As shown in (Figure 3B), the VVISYSMPD phage interacted only with GST- $\beta 5$  and not with GST- $\beta 1$  and GST- $\beta 3$ . Phage lacking a peptide insert (Fd-tet) did not bind to any of the three immobilized fusion proteins. To determine whether binding of VVISYSMPD-displaying phage was mediated by peptide sequence alone, we synthesized VVISYSMPD peptide and assayed its ability to inhibit phage binding. As expected, VVISYSMPD peptide inhibited binding of the corresponding phage in a dose-dependent manner. A control peptide with an unrelated sequence had no effect on phage binding. As additional negative controls, we engineered phage to display three scrambled versions of the VVISYSMPD sequence (ISYVMDSVP, VISVYPDMS, and ISDPYVVSM). We clearly show that these peptides do not bind to GST- $\beta 1$ , - $\beta 3$ , or - $\beta 5$  (Figure 5). Thus, we showed that the VVISYSMPD peptide binds to the cytoplasmic domain of the  $\beta 5$  integrin and that the interaction is specific.

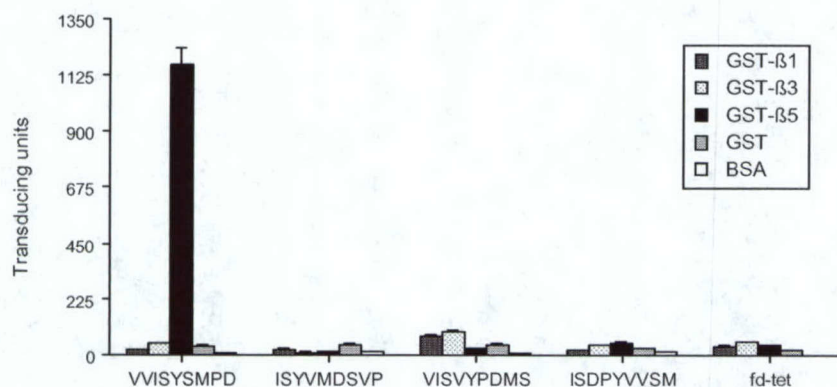


**Figure 5. Phage displaying scramble sequence of VVISYSMPD peptide did not bind specifically to the  $\beta 5$  Integrin Cytoplasmic Domain.** Integrin cytoplasmic domain GST fusion proteins or GST alone were coated on microtiter wells at 10  $\mu\text{g/ml}$  and incubated with  $\beta 5$  cytoplasmic domain-binding phage (VVISYSMPD) or the scramble sequences (ISYVMDSVP, VISVYPDMS, and ISDPYVVSM). Fd-tet (insertless) phage were used as a negative control.

#### *Phosphorylation events modulate the interaction of the selected peptides with cytoplasmic domains*

Events involving phosphorylation are important in regulating signal transduction. We used the phage display system to evaluate the effect of tyrosine phosphorylation at two



levels: (i) recombinant fusion proteins containing  $\beta 3$  or  $\beta 5$  cytoplasmic domains were used for panning of phage libraries displaying tyrosine-containing peptides or (ii) the cytoplasmic domains themselves were phosphorylated before phage selection was performed. Experiments were performed to investigate the capacity of specific tyrosine kinases to modulate the interaction of the selected peptides with the cytoplasmic domains. This strategy is interesting because it can reveal the effect of phosphorylation on their binding properties at different levels.

#### *Biological properties of the cytoplasmic domain-binding peptides*

We performed several assays in the presence and absence of the cytoplasmic domain-binding peptides to assess the effects of these peptides on cell function.

#### **Apoptosis triggered by the $\beta 5$ -cytoplasmic domain binding peptide**

We successfully internalized the  $\beta 5$ -cytoplasmic domain binding peptide using a penetratin chimera. Penetratin is a 16-residue peptide corresponding to amino acids 43–58 of the homeodomain of the *Drosophila* Antennapedia transcription factor. Penetratin can move hydrophilic compounds across the plasma membrane and targets oligopeptides to the cytoplasm without apparent degradation (Derossi et al., 1994). This internalization occurs at both 37°C and 4°C (Joliot et al., 1991a, 1991b; Le Roux et al., 1993; Bloch-Gallego et al., 1993). Similar penetratin fusion peptides (penetratin chimeras) have been shown to be internalized into cells in culture and elicit peptide-specific biological responses (Theodore et al., 1995; Bonfanti et al., 1997; Holinger et al., 1999). Penetratin and penetratin fused to VVISYSMPD (Pen-VVISYSMPD) were synthesized and labeled with biotin. To analyze the biological effects of  $\beta 5$ -binding peptides, we used human umbilical vein endothelial cells (HUVECs) as a model system. HUVECs express high levels of the  $\beta 5$  integrin and respond to proangiogenic cytokines. In fact,  $\beta 5$ -mediated signaling pathways can be activated by VEGF in endothelial cells (Eliceiri, 2001; Stupack and Cheresh, 2002). Penetratin, penetratin chimeras, and a control biotinylated peptide were incubated with HUVEC monolayer for 1 hr. Cells were then fixed and stained with streptavidin-fluorescein isothiocyanate (FITC) to confirm internalization of the peptide.

The internalizing form of the VVISYSMDP peptide induced apoptosis upon VEGF stimulated quiescent HUVEC cells. Cell death was analyzed by using propidium iodide (PI)/fluorescence-activated cell sorting (FACS) (Figure 6) analysis as well detected by the binding of annexin V to the cell surface (Figure 7) (Fadok et al., 1992). A DNA laddering assay confirmed that DNA fragmentation occurred in cells treated with Pen-VVISYSMPD. Caspase activity was required for induction of cell death. Treatment with z-VAD prevented over 50% of the Pen-VVISYSMPD-induced cell death. In contrast, the caspase-8 inhibitor z-IETD had no such effect. These results show that apoptosis induced by Pen-VVISYSMPD in HUVECs requires caspase activation, although caspase-8 is not involved in that process

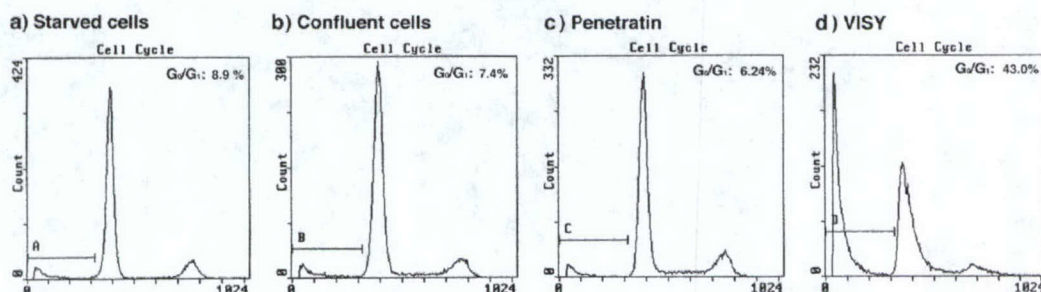




**Figure 6. Penetratin peptide chimera binding to the  $\beta 5$  cytoplasmic domain induces programmed cell death in HUVEC.** A) Phase contrast of VEGF stimulated HUVECs cultured in apoptosis assay. B)  $10^6$  HUVEC were harvest in complete media. After that time, 15 $\mu$ M penetratin peptides chimera were added to the culture for four, eight and twelve hours. The cells were stained with Propidium Iodide (PI) and induction of apoptosis was analyzed by cytometric analysis. a) 24 hours starved cells. b) Confluent cells in complete media. c) 15 $\mu$ M of penetratin was incubated for four hours. d) 15 $\mu$ M of VISY-penetratin chimera was incubated for four hours. At eight hours and twelve hours points showed a similar percentage of G<sub>0</sub>/G<sub>1</sub>.

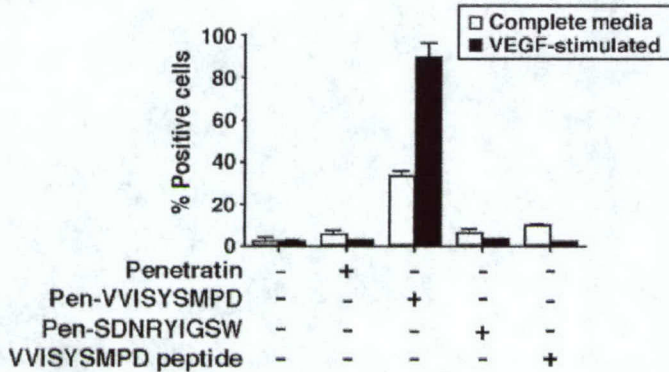


**Figure 7. Apoptosis detection by annexin V staining.** Cells were harvested after treatment with internalizing peptides as indicated, and stained with ApoAlert.

Programmed cell death is involved in many diseases as well as in wound healing and in tissue remodeling (Reed, 2001). Disruption of integrin-mediated cell-matrix interactions may lead to caspase-dependent apoptosis; two pathways, anoikis (Frisch and Francis, 1994) and integrin-mediated death (IMD; Stupack et al., 2001), have been described. By definition, anoikis requires loss of cell adhesion (Frisch and Francis, 1994; Frisch and Ruoslahti, 1997; Frisch and Screaton, 2001; Howe et al., 2002; Meredith et al, 1998; Aoudjit and Vuori, 2001). Given that cells treated with the VVISYSMDP peptide undergo apoptosis while still attached, it is unlikely that our observations can be explained by the general phenomenon of anoikis. On the other hand, IMD occurs when  $\beta 3$ -mediated interactions are blocked in adherent cells. However, IMD is induced by the cytoplasmic domains of  $\beta 1$  or  $\beta 3$  (but not  $\beta 5$ ) and it results from recruitment of caspase-8 to the membrane and its subsequent activation (Stupack et al., 2001). In contrast, the VVISYSMDP peptide binds only to the  $\beta 5$  cytoplasmic domain (but not to  $\beta 1$  or  $\beta 3$ ). Finally, caspase 8 activity is not required for VVISYSMDP-induced cell death. Taken together, these observations indicate that VVISYSMDP-induced apoptosis is a programmed cell death mechanism not as yet described.

#### **$\beta 5$ integrin-null fibroblasts resistant to Pen-VVISYSMPD-induced apoptosis**

We tested whether the  $\beta 5$  integrin subunit was required for apoptosis induction by the VVISYSMPD peptide, we compared the effects of internalizing peptides on fibroblasts isolated from  $\beta 5$  integrin-null mice (Huang et al., 2000) and wild-type mice. Penetratin, VVISYSMPD, or Pen-VVISYSMPD were added to the culture media. Marked cell death was observed in wild-type fibroblasts treated with Pen-VVISYSMPD, while fibroblasts lacking the  $\beta 5$  integrin were not affected. Treatment with penetratin or the non-internalizing VVISYSMPD peptide did not induce cell death (Figure 8). Cell viability was quantified (MTT) assay. These results showed that apoptosis induction by the membrane-permeable form of the VVISYSMPD peptide does not occur in the absence of the  $\beta 5$  integrin subunit.



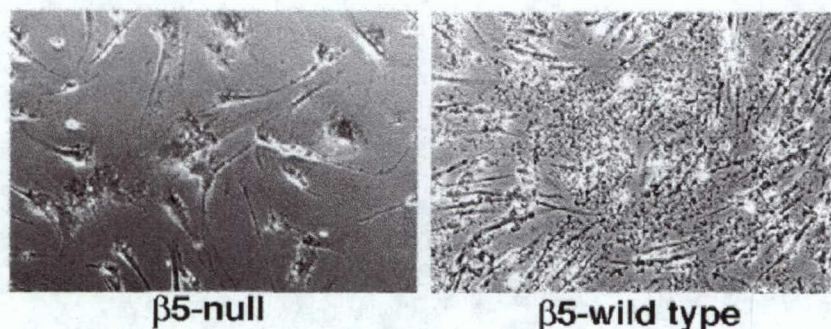


**Figure 8. Cell death induced by Pen-VVISYSMPD requires  $\beta 5$  expression** Fibroblasts from  $\beta 5$ -null mice or from wild-type were incubated with 15  $\mu$ M Pen-VVISYSMPD peptide. The cells were visualized by phase contrast (100 x magnification).

To reinforce that VVISYSMPD-triggered cell death requires the expression of  $\beta 5$ , we used a different cell system in which  $\beta 5$  integrin-negative cells (CS-1) were transfected with  $\beta 5$ . We showed that VVISYSMPD-triggered cell death does not occur in the absence of the  $\beta 5$  subunit (Figure 9), and does occur in  $\beta 5$ -transfected cells. Cell viability was quantified by MTT assay. These results show that apoptosis induction by the membrane-permeable form of the VVISYSMPD peptide does not occur in the absence of the  $\beta 5$  integrin subunit.

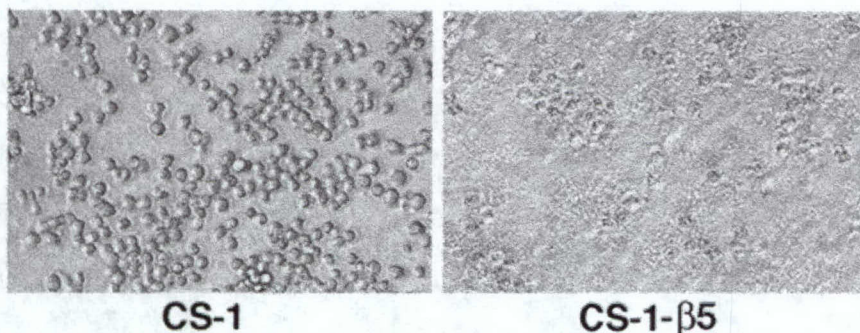


**Figure 9. Expression of  $\beta 5$  cytoplasmic domain is required.** CS-1 or CS-1- $\beta 5$  cells were incubated with RPMI alone (1, 4), Pen-VVISYSMPD (2, 5) or penetratin at a concentration of 15  $\mu$ M (3, 6) and visualized by phase contrast (100 x magnification).

#### **Purification of $\beta 5$ -mimicked band to identify the target protein**

We reasoned that the VVISYSMPD peptide could mimic a  $\beta 5$  integrin-associated molecule. To test this hypothesis, we generated a polyclonal antibody against the peptide. The anti-VVISYSMPD serum recognized the immobilized VVISYSMPD peptide in a concentration-dependent manner. Reactivity was abrogated by preincubation with the synthetic VVISYSMPD peptide, but not with an unrelated control peptide (data not shown). When tested on Western blots of total cell extracts, the anti-VVISYSMPD polyclonal antibody reacted with a specific 36-kDa protein.

We used the anti-VVISYSMPD antibody to probe protein samples from cell extracts processed by sequential gel filtration and anion exchange column chromatography to identify the target antigen. A 36-kDa protein was enriched after the final purification step



(Figure 10A) and was recognized by the anti-VVISYSMPD antibody on Western blots (Figure 10B).

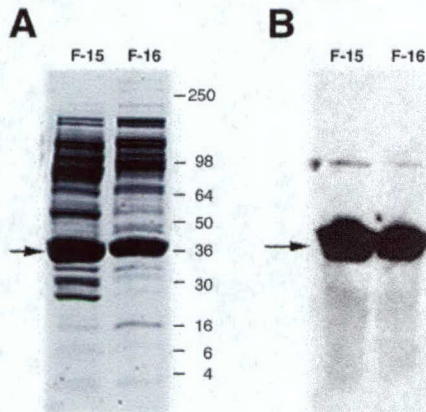


**Figure 10. Identification of the Protein Mimicked by the VVISYSMPD Peptide**

(A) Coomassie blue staining of proteins obtained from cell extracts after ion exchange chromatography followed by molecular weight fractionation. The arrow indicates the protein excised and processed by MALDI-TOF mass spectroscopy of F-15 and F-16. (B) Western blot analysis of fractions containing purified proteins using the anti-VVISYSMPD rabbit antiserum (generated by immunizing rabbits with VVISYSMPD-KLH).

Mass spectrometry analysis revealed seven unique peptides derived from the purified 36kDa protein that matched the annexin V protein sequence (Cookson et al., 1994) in a BLAST homology search (Figure 11).

```

1 MAQVLRGTVT DFPGFDERAD AETLRKAMKG LGTDEESILT LLTSRSNAQR QEISAAPFKTL FGRDLDDLK
71 SELTGKFEKL IVALMKPSRL YDAYELKHAL KGAGTNEKVL TEIIASRTPE ELRAIKQVYE EYGSSLEDD
141 VVGDTSGYYQ RMLVLLQAN RDPDAGIDEA QVEQDAQALF QAGELKWGTD EEKFITIFGT RSVSHLRKVF
211 DKYMTISGFQ IEETIDRETS GNLEQLLLAV VKSIRSIPAY LAETLYAMK GAGTDDHTLI RVMVSRSEID
281 LFNIRKEFRK NFATSLYSMI KGDTS GDYKK ALLLLCGEDD
      S YSM D
      +* *** *
      VVIS-YSM -D

```

**Figure 11. The amino acid sequence of the full-length h-annexin V from the NCBI database** (accession number AAB60648). Boxed in orange are the seven peptides obtained by mass spectrometry from the purified protein shown in Fig 4A. The region of similarity with the VVISYSMPD peptide is underlined; identical (\*) and conserved (+) amino acids are indicated.

To confirm that the purified protein was annexin V, we reprobed the membrane containing the fractions enriched for the 36-kDa protein (Figure 12) with a commercial antibody against annexin V, which readily detected the same 36-kDa antigen (Figure 9B). These results show that annexin V is the protein recognized by the anti-VVISYSMPD polyclonal antibody.

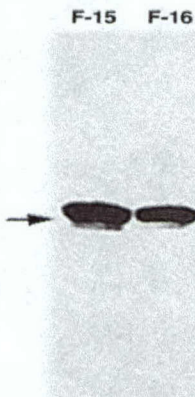


**Figure 12. Annexin V is the purified protein.** The same Western blot (Figure 9B) was stripped and reprobed with a polyclonal anti-human annexin V antibody.



Analysis of a three-dimension model of annexin V based on its structure (Sopkova et al., 1993) shows that the motif containing the  $\beta 5$ -binding peptide is exposed on the surface of the molecule (Figure 13). Annexin V belongs to a family of proteins defined by their ability to bind calcium and phospholipids via a series of tandem motifs that form the core of the protein (Dubois et al., 1996). All annexins contain a putative PKC binding site, but only annexin V has been shown to function as a PKC inhibitor (Schlaepfer et al., 1992; Dubois et al., 1998). Thus, we sought to determine whether inhibition of PKC would interfere with the induction of apoptosis by the VVISYSMPs peptide.

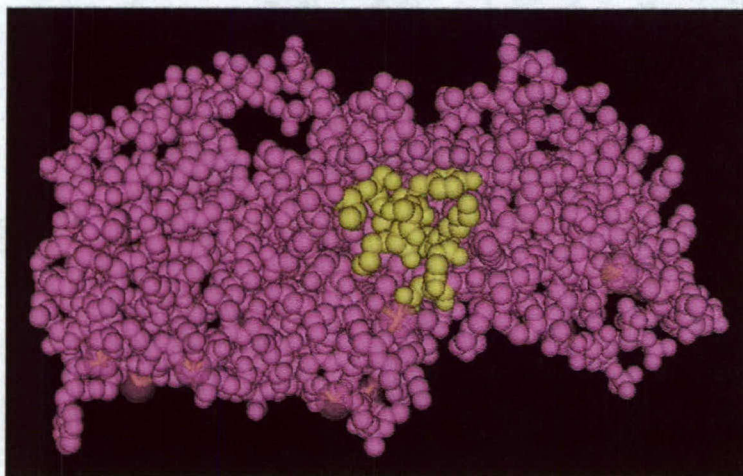


**Figure 13.** Annexin V structure showing the location of the sequence containing the  $\beta 5$ -binding peptide (in yellow).

#### **Localization of Annexin V and the $\alpha v\beta 5$ Integrin in Pen-VVISYSMPD Untreated and Treated HUVECs**

Double immunofluorescence staining of  $\beta 5$  (shown in green) and annexin V (shown in red) in VEGF-stimulated cells (HUVECs) was used to evaluate the localization of these two proteins in proliferating and dying cells by immunofluorescence (Figure 14).  $\beta 5$  (shown in green) and annexin V (shown in red) colocalize (yellow) in VEGF-stimulated cells. Loss of the cytoplasmic membrane integrity (likely due to massive apoptosis induction) was seen 3 hr after treatment with Pen-VVISYSMPD, yet cells remain attached.



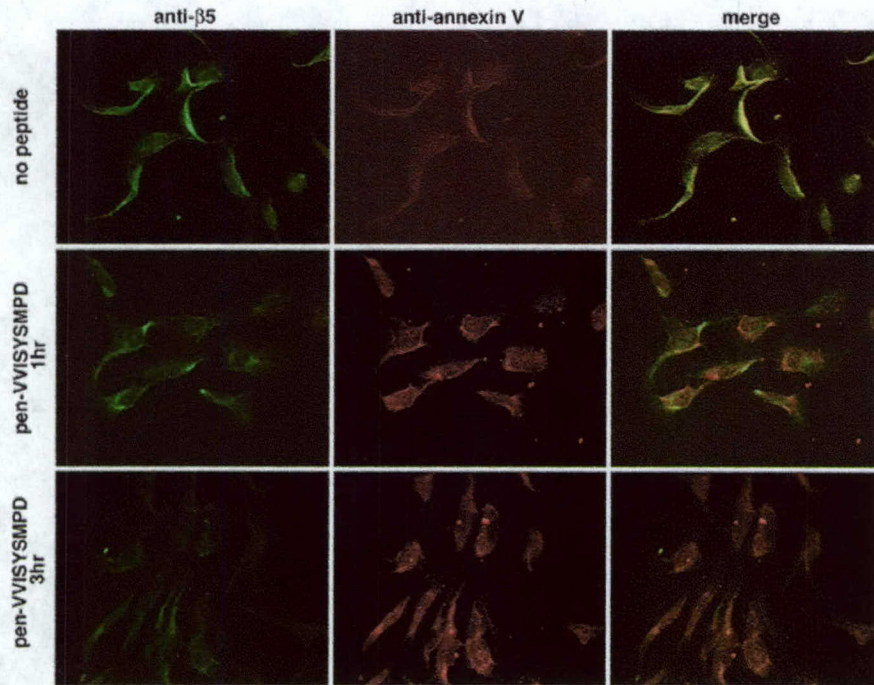


**Figure 14. Localization of Annexin V with  $\alpha v \beta 5$  Integrin and a PKC Inhibitor Modulates the apoptotic Effects in Pen-VVISYSMPD Untreated and Treated HUVECs.** Double immunofluorescence staining of  $\beta 5$  (shown in green) and annexin V (shown in red) in VEGF-stimulated cells (HUVECs). Colocalization of  $\beta 5$  cytoplasmic domain and annexin V appears in yellow in the merged images (top right panel).  $\beta 5$  and annexin V no longer co-localize after incubation with Pen-VVISYSMPD for 1 hr (middle panels) or 3 hr (lower panels).

#### **PKC Activity Is Required for VVISYSMPD-Induced Cell Death**

The role of annexin in signal transduction and the mechanism(s) by which annexin V inhibits PKC activity remain elusive. It has been proposed that the identification of a protein that regulates the relative concentrations of annexin V and PKC near the membrane may control PKC signaling events (Dubois et al., 1996). However, such a protein has not yet been identified. On the other hand, PKC signaling regulates  $\beta 5$  function and controls cell survival in endothelial cells (Tang et al., 1999; Lewis et al., 1996). Serine/threonine kinases are activated upon integrin stimulation, and inhibitors of PKC block cell attachment and spreading in vitro (Vuori and Ruoslahti, 1993; Nakamura and Nishizuka, 1994; Chen et al., 1994). The C-terminal domain of annexin V associates with and inhibits PKC in the presence of  $Ca^{2+}$  (Schlaepfer et al., 1992; Raynal et al., 1993; Rothhut et al., 1995; Dubois et al., 1995). These observations led us to hypothesize that PKC regulates  $\beta 5$ -dependent apoptosis induced by Pen-VVISYSMPD. We demonstrated that the PKC inhibitors Myr-PKC $\square/\square$ , calphostin C, and Ro31-8220 inhibit VVISYSMPD-induced cell death, but not PKC $\epsilon$ , and Myr PKC $\square$  (Figure 15A). These results also show that conventional PKCs play a key role in VVISYSMPD-mediated cell death.



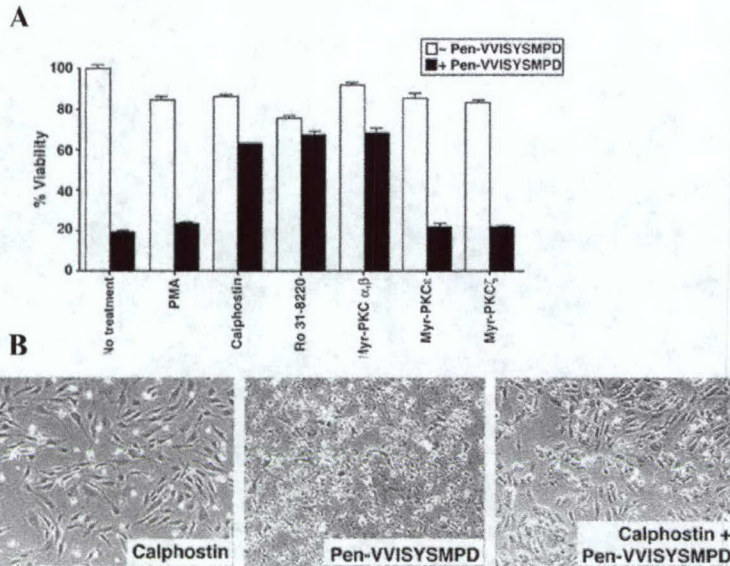


**Figure 15. Effect on Annexin V and  $\alpha v \beta 5$  Integrin with a PKC Inhibitors** **A)** VEGF-stimulated HUVECs were incubated with PKC inhibitors (Myr-PKC $\square/\square$ , calphostin C, Ro 31-8220, Myr-PKC $\epsilon$ , Myr-PKC $\zeta$ ) or PMA in the presence or absence of pen-VVISYSMPD. Cell viability was evaluated by the MTT assay 24 hr later. **B)** The PKC inhibitor calphostin C delays apoptosis induced by Pen-VVISYSMPD in HUVECs.

High concentrations of calphostin C induced cell death (Zhu et al., 1998). However, at low concentrations (1-10 nM), we show that calphostin C inhibited PKC activity without significant induction of cell death (Figure 15B). Apoptosis induced by the VVISYSMPD peptide was markedly reduced in the presence of low concentrations of calphostin C (Figure 16A). A [ $^3$ H]-thymidine incorporation assay revealed that cell proliferation was completely blocked by Pen-VVISYSMPD. Apoptosis induction was evaluated, there were more viable cells in the wells exposed to both Pen-VVISYSMPD and calphostin C than in monolayers treated with only Pen-VVISYSMPD (Figure 16B). These data show that VVISYSMPD-induced apoptosis is blocked by inhibition of PKC, suggesting that PKC activity regulates the proapoptotic effects of the VVISYSMPD peptide.

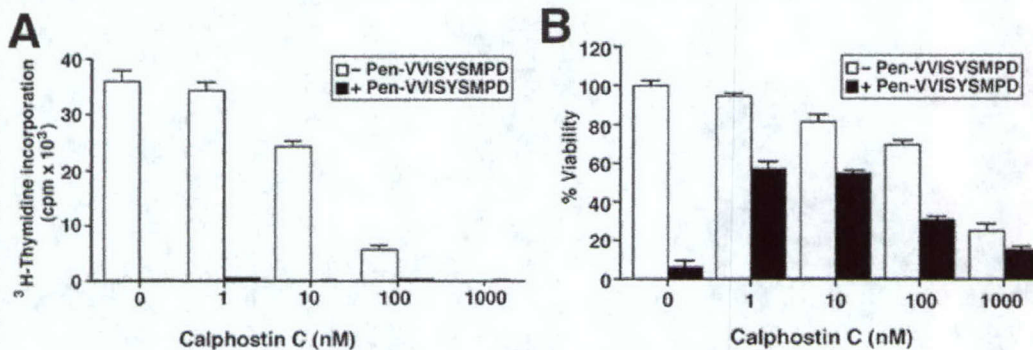


**Figure 16. Calphostin C inhibits apoptosis induced by the Pen-VVISYSMPD peptide.** **A)** HUVECs were incubated with increasing concentrations of calphostin C with or without 12  $\mu$ M Pen-VVISYSMPD. After an overnight incubation, proliferation was assessed by measuring [ $^3$ H]-thymidine incorporation. **B)** Quantification of cell viability after incubation with Pen-VVISYSMPD in the presence of increasing concentrations of calphostin C.



### Annexin V Associates with the $\beta 5$ Integrin Cytoplasmic Domain

We performed reciprocal co-immunoprecipitation using antibodies against the  $\beta 5$  integrin or annexin V to show that annexin V associates with  $\beta 5$  integrin *in vivo*. We then probed immunoprecipitates on Western blots with a well-characterized anti- $\beta 5$  antibody. A specific band corresponding to the  $\beta 5$  integrin subunit was detected (Figure 17). These data demonstrate that annexin V associates with  $\beta 5$  integrin in cells.

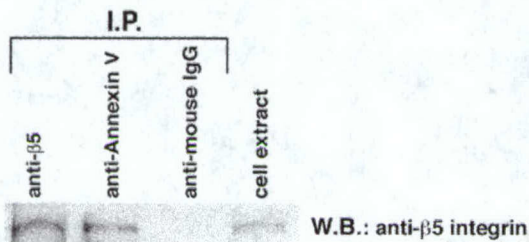


**Figure 17. Annexin V Associates to with the  $\beta 5$  Integrin Cytoplasmic Domain.** HUVECs were lysed with RIPA buffer containing  $\text{Ca}^{2+}$ , and immunoprecipitation was performed with an anti- $\beta 5$  integrin antibody (lane 1), an anti- annexin V antibody (lane 2), or anti-mouse IgG as a negative control (lane 3).  $\beta 5$  integrin was detected by Western blot analysis by a monoclonal antibody. A crude cell extract is shown in lane 4.

We used protein binding assays to show that the interaction between annexin V and the  $\beta 5$  integrin cytoplasmic domain was specific (Figure 18). Recombinant annexin V was incubated with GST- $\beta 5$ , or with  $\beta 1$  or  $\beta 3$  GST fusion proteins as negative controls. Because  $\text{Ca}^{2+}$  is required for the association between annexin V, PKC and phospholipids (Mira et al., 1997), we tested whether  $\text{Ca}^{2+}$  would also enhance the interaction between annexin V and  $\beta 5$ . Bound annexin V was detected with a specific antibody against annexin V. A highly specific interaction between annexin V and the GST- $\beta 5$  cytoplasmic domain was observed (Figure 18).  $\text{Ca}^{2+}$  was required for the interaction, since annexin V binding was not detected when  $\text{Ca}^{2+}$ -free buffers were used. The interaction between the  $\beta 5$  cytoplasmic domain and annexin V was specifically inhibited by the VVISYSMPD peptide. Thus, the VVISYSMPD peptide mimics the binding site through which annexin V associates with the cytoplasmic domain of the  $\beta 5$  integrin subunit.

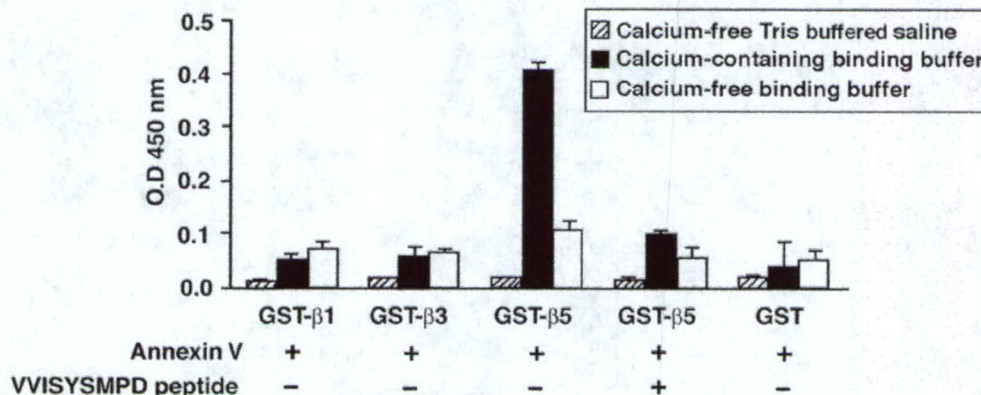


**Figure 18. Annexin V binds to the  $\beta 5$  cytoplasmic domain.** Binding of recombinant human annexin V was determined spectrophotometrically by an anti-human annexin V polyclonal antibody.

We ruled out the possibility that the VVISYSMPD peptide might induce apoptosis by directly inhibiting PKC, we tested whether the peptide binds to the enzyme. If the peptide



interacted with PKC, it might also affect the interaction between annexin V and PKC. Phage binding assays eliminated both possibilities, as no binding of VVISYSMPD-displaying phage to PKC was detected; the  $\beta 5$ -GST protein was used as a positive control (Figure 19A).

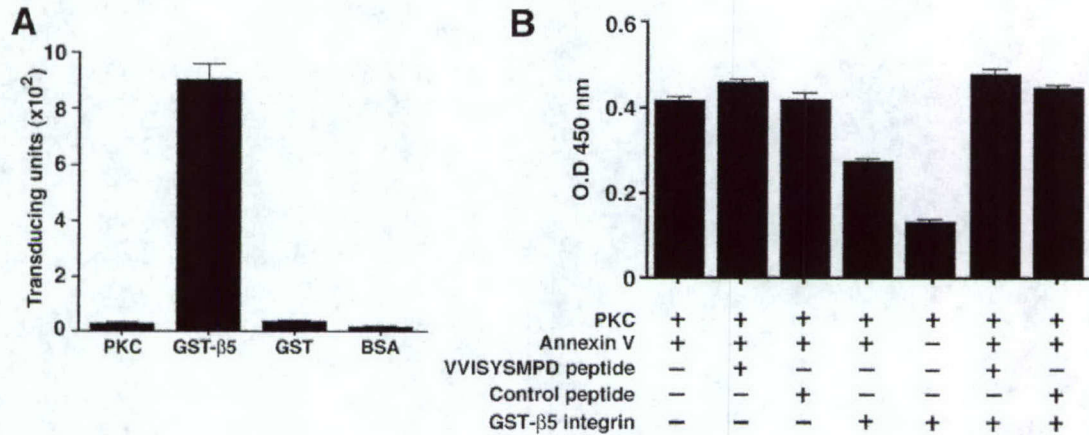


**Figure 19. Inhibition of Annexin V to PKC by  $\beta 5$  cytoplasmic domain.** **A)** The VVISYSMPD peptide does not bind to PKC. Purified PKC was coated on microtiter wells at 250 ng/ml and incubated with phage displaying the VVISYSMPD peptide. GST- $\beta 5$ -coated wells were used as a positive control and wells coated with GST or BSA as negative controls. **B)** The  $\beta 5$  integrin cytoplasmic domain inhibits binding of annexin V to PKC. Microtiter-plate wells coated with PKC were incubated with annexin V with or without GST- $\beta 5$  cytoplasmic domain and VVISYSMPD peptide or with an unrelated control peptide.

Annexin V had been shown to bind to PKC (Schlaepfer et al., 1992), and we examined whether the VVISYSMPD peptide could interfere with this interaction. Protein-protein binding assays showed that the VVISYSMPD peptide did not affect the binding of annexin V to PKC (Figure 19 B). In contrast, the GST- $\beta 5$  integrin cytoplasmic domain blocked the binding of annexin V to PKC by about 40%. Importantly, the interaction between annexin V and PKC was rescued when VVISYSMPD peptide and GST- $\beta 5$  were incubated jointly. Taken together, these results showed that binding of annexin V to the cytoplasmic domain of  $\beta 5$  integrin is blocked by VVISYSMPD peptide.

Interestingly, PMA did not prevent VVISYSMPD-induced cell death, because it facilitated PKC binding to annexin V (Figure 20). Consistent with this result, a specific inhibitor of conventional PKCs (Myr peptide) blocked binding of annexin V to PKC (Figure 20) and inhibited VVISYSMPD-induced cell death. These results supported a key role for PKC activity and subsequent inhibition by annexin V in the VVISYSMPD-induced cell death process.

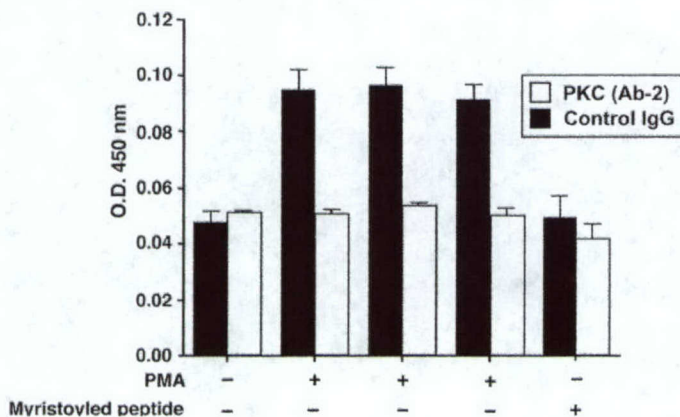




**Figure 20. Annexin V binds to activated PKC.** HUVECs incubated with PMA or with the Myr peptide for the indicated times were used as the source of immunocaptured PKC. Binding of annexin V to PKC was analyzed by incubating each sample well with 1.5 µg/ml recombinant human annexin V. Bound annexin V was detected spectrophotometrically with an anti-human annexin V polyclonal antibody. Control IgG was used as a negative control.

We observed that PKC activity was required for annexin V binding; yet it was through annexin V-dependent PKC inhibition that cell death were induced by the  $\beta 5$ -cytoplasmic domain binding peptide. Moreover, based on experiments performed with specific PKC inhibitors, conventional PKCs mediated VVISYSMPD-induced cell death.

### **$\beta 5$ cytoplasmic-binding peptide Inhibits Neovascularization In Vitro and In Vivo**

We determined whether pro-angiogenic factors modulate apoptosis induced by Pen-VVISYSMPD, we evaluated cell death after stimulation with factors that activate endothelial cells. HUVECs treated with Pen-VVISYSMPD in the presence of VEGF or basic fibroblast growth factor (bFGF) underwent rapid apoptosis compare to the controls (Figure 21). Penetratin or the VVISYSMPD peptide alone were used as negative controls and had no effect under identical conditions. Therefore, cell death induced by Pen-VVISYSMPD is markedly enhanced by pro-angiogenic growth factors. These observations led us to hypothesize that Pen-VVISYSMPD might function as an inhibitor of angiogenesis.

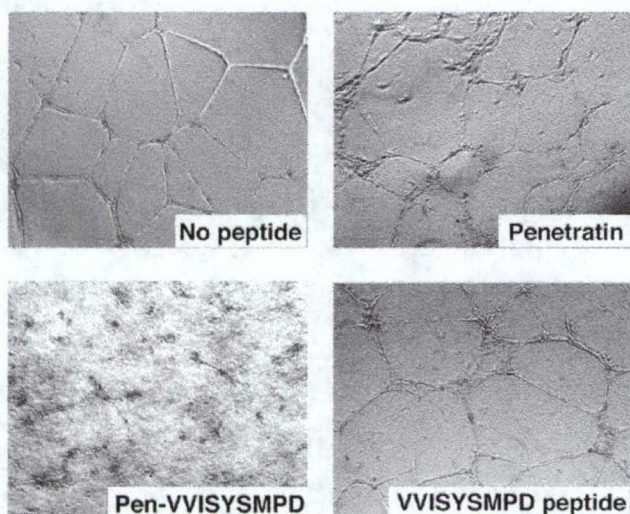


**Figure 21. Pen-VVISYSMPD inhibited vascular network formation.** HUVECs were plated in Matrigel-coated plates and photographed 24 hr after incubation with penetratin, Pen-VVISYSMPD, or the VVISYSMPD peptide alone (magnification 4 $\times$ ).

In response to specific stimuli, endothelial cells plated on Matrigel develop into networks of capillary-like structures. VEGF-stimulated HUVECs plated in Matrigel were used as a model of neovascularization. By using this model, we showed that incubation with Pen-VVISYSMPD completely inhibits the formation of a vascular network, while penetratin or the VVISYSMPD peptide alone did not have any effects. Subcutaneous implantation of Matrigel plugs containing a combination of bFGF plus VEGF in nude mice induces vessel growth within 5 days. Pen-VVISYSMPD completely inhibited angiogenesis induced by both growth factors, while penetratin alone had no effect (Figure 22). These results clearly showed that the  $\beta 5$  cytoplasmic domain-binding peptide inhibits neovascularization.



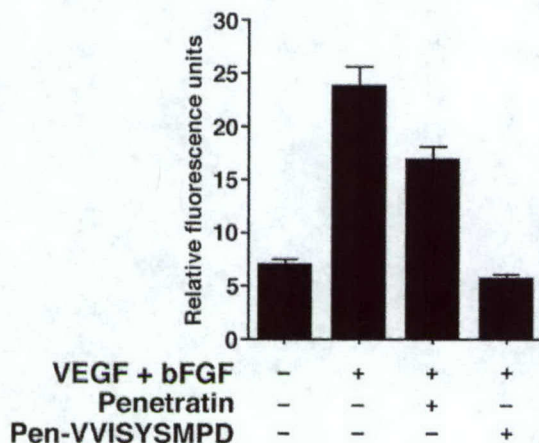


**Figure 22. Pen-VVISYSMPD-induced Cell Death Results in Angiogenesis Inhibition In Vivo** Matrigel supplemented with growth factors was injected into mice in the presence of absence of penetratin or Pen-VVISYSMPD. Neovascularization within the Matrigel plugs was determined by measurement of the levels of injected FITC-labeled lectin that were subsequently recovered after ground the plugs.

Consistent with these observations, we found that pro-angiogenic factors (VEGF and bFGF) enhance Pen-VVISYSMPD-induced cell death. VEGF was very effective in accelerating VVISYSMPD mediated cell death. While bFGF was also effective, it was less potent than VEGF under the experimental conditions tested. Finally, Pen-VVISYSMPD had little effect on non-proliferating endothelial cells cultured in medium without growth factors. Endothelial cell viability in this experiment was evaluated (Figure 23).

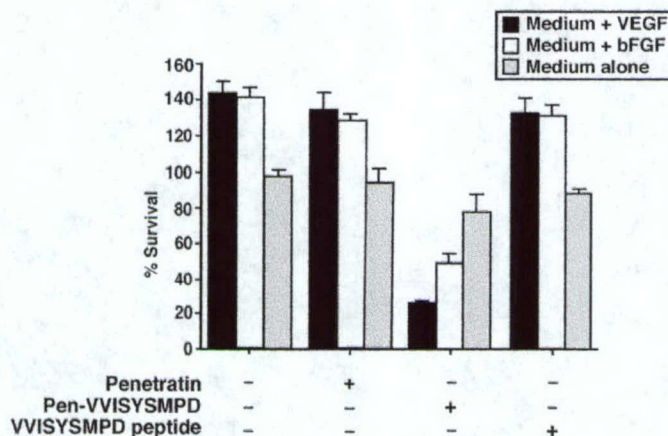


**Figure 23. Angiogenic factors (VEGF and bFGF) enhance Pen-VVISYSMPD-induced cell death.** Endothelial cell viability was evaluated by the MTT assay

#### KEY RESEARCH ACCOMPLISHMENTS:

- We have isolated peptides that selectively bind to  $\beta 3$  or  $\beta 5$  cytoplasmic domains by panning of phage peptide libraries on recombinant fusion proteins containing  $\beta 3$  or  $\beta 5$  cytoplasmic domains. We have synthesized membrane-permeable forms of the cytoplasmic domain-binding peptides to determine their effect on  $\beta 3$  or  $\beta 5$  integrin-mediated signaling and subsequent cellular responses.
- We have used recombinant fusion proteins containing  $\beta 3$  or  $\beta 5$  cytoplasmic domains for panning of phage libraries displaying tyrosine-containing peptides. The libraries were phosphorylated *in vitro* with different kinases. We have



studied the capacity of specific tyrosine kinases to phosphorylate isolated cytoplasmic domains and cytoplasmic domain-binding peptides by mass spectroscopy. The effect of phosphorylation on their binding properties was investigated.

- We have determined that a  $\beta 5$  cytoplasmic domain-binding peptide induces apoptosis upon cell internalization. We have proved that this peptide requires  $\beta 5$  integrin expression to mediate its biological effects.
- We have generated and characterized antibodies that recognize  $\alpha v \beta 3$  and  $\alpha v \beta 5$ -binding peptides. We have used affinity chromatography assays to purify a protein that has been identified by mass spectrometry.
- We have identified the  $\beta 5$  cytoplasmic binding peptide as an annexin V in a BLAST homology search, and 3D structure viewer data base showed an exposed surface where the  $\beta 5$  cytoplasmic domain has homology. We showed a colocalization on the VEGF-stimulated cells of  $\beta 5$  cytoplasmic domain and Annexin V. We have been proved that annexin V associates with  $\beta 5$  integrin by immunoprecipitation and Western Blot.
- We demonstrated for the first time a connection between the regulation of PKC activity by annexin V, and the induction of cell death in a  $\beta 5$ -dependent manner. Our data reveal a structural basis for the regulation of PKC-mediated cell survival and provides insights into the mechanism of action of annexin V.
- We have shown the  $\beta 5$  cytoplasmic domain binding peptide is able to inhibit new blood vessel formation, both in vitro and in vivo. Cell death induced by Pen-VVISYSMPD is markedly enhanced by pro-angiogenic growth factors. These observations led us to hypothesize that Pen-VVISYSMPD might function as an inhibitor of angiogenesis.

## REPORTABLE OUTCOMES:

### Manuscripts:

Cardo-Vila M, Arap W, Pasqualini R. Alpha v beta 5 integrin-dependent programmed cell death triggered by a peptide mimic of annexin V. *Mol Cell*. 2003 May;11(5):1151-62.

Arap W, Kolonin MG, Trepel M, Lahdenranta J, Cardo-Vila M, et al. Steps toward mapping the human vasculature by phage display. *Nat Med*. 2002 Feb, 8(2) 121-7.



Giordano, R.J. Cardo-Vila, M, Lahdenranta, J., Pasqualini, R. and Arap, W. Biopanning and rapid analysis of selective interactive ligands. Nat Med. 2001 Nov; 7(11):1249-53.

Cardo-Vila M, Arden KC, Cavenee WK, Pasqualini R, Arap W. Is annexin 7 a tumor suppressor gene in prostate cancer? Pharmacogenomics J. 2001;1(2):92-4.

#### **Abstracts:**

Annual AACR meeting.

Cardó-Vila M, Arap W and Pasqualini R.

*Contrasting properties of integrin cytoplasmic domains revealed by phage Display.* 2002 San Francisco, CA, USA

Era of Hope meeting.

Cardó-Vila M, Arap W and Pasqualini R

*Isolation of signaling molecule involved in angiogenesis mediated by beta 5 integrin cytoplasmic domain.* 2002 Orlando FL, USA

Gordon Conference: Angiogenesis and microcirculation.

Cardó-Vila M, Arap W and Pasqualini R

*Contrasting signaling properties of integrin cytoplasmic domains in angiogenesis.* 2003. Salve Regina-Newport RI, USA

#### **Awards**

2002            AACR. Scholar-in-Training Award

#### **Book Chapter Publications**

Vidal, C., Cardó-Vila, M., Lahdenranta, J., Arap, W., and Pasqualini, R. (2003).

Targeting blood vessels in vivo by using phage display libraries. In Targeted Therapy for Cancer, K. N. Syringos, and K. J. Harrington, eds. (Nyw York, NY, Oxford University Press Inc.), pp. 250-255.

#### **Degrees Obtained**

Ph.D. in Biology. July 25<sup>th</sup>, 2003.

Thesis defense program: Immunology.

Thesis title: "*Functional role of extracellular matrix proteins and their receptors in apoptosis and cell survival*"

#### **Patents and Licenses**



PCT/US01/27702

Entitled "Methods and Compositions for In Vitro Targeting"

Filed 9/7/01

## CONCLUSIONS

Even though breast cancer is one of the most common cancers in women in the US, there is no universally agreed strategy for its management. Several lines of research have recently converged to explore vascular targeting by taking advantage of the differences between the newly formed vessels in tumors and the mature vessels in normal tissues. Our approach is particularly novel because it directly selects for peptides that can interfere with cell signaling and angiogenesis specifically at the level of receptors that are upregulated during angiogenesis. We studied the effect of  $\beta 3$  and  $\beta 5$  integrin cytoplasmic domain-binding motifs in cell adhesion, migration, and proliferation upon stimulation with factors that activate endothelial cells. Peptides are generally accepted as probes for integrin functions in vitro and in vivo. Moreover, drugs based on peptides that specifically block individual integrins are being developed. Blocking ligand binding by the  $\alpha v\beta 3$  (or  $\alpha v\beta 5$ ) integrin with RGD peptides or antibodies shows promise as an anti-angiogenic therapy. Such treatments cause apoptosis in activated endothelial cells that are in the process of forming new blood vessels, while not harming established blood vessels. These latter observations imply that  $\alpha v$  integrin(s), while accessible to soluble peptides and antibodies in neovasculature, are engaged in endothelial cell interactions with the underlying extracellular matrix. Here we show that we isolated a  $\beta 5$ -binding peptide mimics of annexin V, a cytosolic signaling protein known to inhibit PKC activity and to be involved in signal transduction, is associated specifically with the  $\beta 5$  cytoplasmic domain. Upon internalization, this peptide very effectively activates apoptosis. This induction of apoptosis requires caspase activity and the  $\beta 5$  integrin subunit. Furthermore, the apoptosis triggered by this peptide is modulated by growth factors and PKC antagonists. Our results provide a mechanistic basis for the involvement of  $\alpha v\beta 5$  integrin, proangiogenic cytokines, and annexin V in the regulation of endothelial cell survival and vascular remodeling.

Several observations attested to the specificity of the  $\alpha v\beta 5$ -cytoplasmic domain directed peptide and its pro-apoptotic properties. First, only cells expressing  $\beta 5$  could be killed by treatment with the Pen-VVISYSMPD chimera, whereas chimeras carrying another peptide with different integrin specificity did not trigger cell death. Second, the difference between cell death when the VEGF stimulated endothelial cells was impressive compared to unstimulated cells. Our findings contribute to a better understanding of the biochemical mechanisms that are related to the integrin-mediated signaling events involved in controlling tumor growth and angiogenesis. These processes involve cell adhesion to the extracellular matrix and integrin-mediated signaling.

Finally, peptides that affect endothelial and tumor cell proliferation and invasion were derived from this work, suggesting novel therapeutic strategies for the treatment of diseases such as cancer and diabetic retinopathy. Appreciation for the diversity of cancer biology and the importance of vascular heterogeneity in the development of breast cancer has just begun to be realized. In our view, the results we presented delineate the



uniqueness of the blood vessels in breast cancer, and how targeted therapies affecting such vessels can have significant therapeutic effects. We believe that our accomplishments are entirely consistent with the DOD directives of promotion of translational, organ-specific research, such as the BCRP Program. Personally, the dissertation research award from Department of the Army for Breast Cancer Research has had a significant impact on my career. It has provided me with the means of concentrating in cancer research, thus the funding period has been very productive time for my research. It has also brought additional potential and credibility on the future of my research.

## REFERENCES

- Aoudjit, F., and K. Vuori. 2001. Matrix attachment regulates Fas-induced apoptosis in endothelial cells: a role for c-flip and implications for anoikis. *J. Cell Biol.* **152**:633-43.
- Aplin, A.E., and R.L. Juliano. 2001. Regulation of nucleocytoplasmic trafficking by cell adhesion receptors and the cytoskeleton. *J. Cell Biol.* **155**:187-91.
- Arap, W, Pasqualini, R. and Ruoslahti, E. 1998. Cancer treatment by targeted drug delivery to tumor vasculature. *Science* **279**: 377-380.
- Bloch-Gallego E, Le Roux I, Joliot AH, Volovitch M, Henderson CE, Prochiantz A. 1993. Antennapedia homeobox peptide enhances growth and branching of embryonic chicken motoneurons in vitro. *J Cell Biol.* **120**, 485-92.
- Bonfanti, M., Taverna, S., Salmons, M., D'Incalci, M., and Broggin, M. 1997. p21WAF1-derived peptides linked to an internalization peptide inhibit human cancer cell growth. *Cancer Res.* **57**, 1442-1446.
- Brooks, P.C., Clark, R.A. and Cheresh, D.A. 1994. Requirement of vascular integrin  $\alpha v \beta 3$  for angiogenesis. *Science* **264**:569-571.
- Brooks, P.C., Montgomery, A.M., Rosenfeld, M., Reinsfeld, R.A., Hu, T., Klier, G. and Cheresh, D.A. 1994. Integrin  $\alpha v \beta 3$  antagonists promote tumor regression by inducing apoptosis of angiogenic blood vessels. *Cell* **79**:1157-1164.
- Brooks, P.C., Stromblad, S., Klemke, R., Visscher, D., Sarkar, F.H. and Cheresh, D.A. Anti-integrin  $\alpha v \beta 3$  blocks human breast cancer growth and angiogenesis in human skin. *J. Clin. Invest.* **96**:1815-1822, 1995.
- Brooks, P.C., Klemke, R.L., Schon, S., Lewis, J.M., Schwartz, M.A. and Cheresh, D.A. 1997. Insulin-like growth factor receptor cooperates with integrin  $\alpha v \beta 5$  to promote tumor cell dissemination in vivo. *J. Clin. Invest.* **99**:1390-1398.



- Carrau, R.L. et al. 1995. Tumor angiogenesis as a predictor of tumor aggressiveness and metastatic potential in squamous cell carcinoma of the head and neck. *Invasion Metastasis* **15**, 197-202.
- Chen, Q., Kinch, M.S., Lin, T.H., Burridge, K., and Juliano, R.L. (1994). Integrin-mediated cell adhesion activates mitogen-activated protein kinases. *J. Biol. Chem.* **269**, 26602-26605.
- Clark, E.A., and J.S. Brugge. 1995. Integrins and signal transduction pathways: the road taken. *Science*. **268**:233-9.
- Clark, E.A., and R.O. Hynes. 1997. 1997 keystone symposium on signal transduction by cell adhesion receptors. *Biochim. Biophys. Acta*. **1333**:R9-16.
- Cookson, B.T., Engelhardt, S., Smith, C., Bamford, H.A., Prochazka, M., and Tait, J.F. 1994. Organization of the human annexin V (ANX5) gene. *Genomics* **20**, 463-467.
- Derossi, D., A.H. Joliot, G. Chassaing, and A. Prochiantz. 1994. The third helix of the Antennapedia homeodomain translocates through biological membranes. *J. Biol. Chem.* **269**:10444-50.
- Dubois, T., Oudinet, J.P., Russo-Marie, F., and Rothhut, B. 1995. In vivo and in vitro phosphorylation of annexin II in T cells: potential regulation by annexin V. *Biochem. J.* **310**, 243-248.
- Dubois, T., Oudinet, J.P., Mira, J.P., and Russo-Marie, F. 1996. Annexins and protein kinases C. *Biochim. Biophys. Acta* **1313**, 290-294.
- Dubois, T., Mira, J.P., Feliars, D., Solito, E., Russo-Marie, F., and Oudinet, J.P. 1998. Annexin V inhibits protein kinase C activity via a mechanism of phospholipid sequestration. *Biochem. J.* **330**, 1277-1282.
- Drake, C.J., Cheresh, D.A. and Little, C.D. 1995. An antagonist of integrin  $\alpha v \beta 3$  prevents maturation of blood vessels during embryonic neovascularization. *J. Cell Sci.* **108**:2655-61.
- Eliceiri, B.P., and D.A. Cheresh. 2001. Adhesion events in angiogenesis. *Curr. Opin. Cell Biol.* **13**:563-8.
- Eliceiri, BP. 2001. Integrin and growth factor receptor crosstalk. *Circ. Res.* **89**, 1104-1110.
- Fadok, V.A., Voelker, D.R., Campbell, P.A., Cohen, J.J., Bratton, D.L., and Henson P.M. 1992. Exposure of phosphatidylserine on the surface of apoptotic lymphocytes triggers specific recognition and removal by macrophages. *J. Immunol.* **148**, 2207-2216.



- Folkman, J. 1992. The role of angiogenesis in tumor growth. *Semin. Cancer Biol.* 3, 65-71.
- Folkman, J. Angiogenesis in cancer, vascular, rheumatoid and other disease. *Nature Med.* 1, 27-31 (1995).
- Friedlander, M., Brooks, P.C., Sharffer, R.W., Kincaid, C.M., Varner, J.A. and Cheresch, D.A. 1995. Definition of two angiogenic pathways by distinct  $\alpha$  integrins. *Science* 270:1500-1502.
- Frisch, S.M., and H. Francis. 1994. Disruption of epithelial cell-matrix interactions induces apoptosis. *J. Cell Biol.* 124:619-26.
- Frisch, S.M., and E. Ruoslahti. 1997. Integrins and anoikis. *Curr. Opin. Cell Biol.* 9:701-6.
- Frisch, S.M., and R.A. Screaton. 2001. Anoikis mechanisms. *Curr. Opin. Cell Biol.* 13:555-62.
- Giancotti, F.G., and E. Ruoslahti. 1999. Integrin signaling. *Science.* 285:1028-32.
- Giordano, R.J., M. Cardo-Vila, J. Lahdenranta, R. Pasqualini, and W. Arap. 2001. Biopanning and rapid analysis of selective interactive ligands. *Nat. Med.* 7:1249-53.
- Hammes, H.-P., Brownlee, M., Joonczyk, A., Sutter, A. and Preissner, K.T. 1996. Subcutaneous injection of a cyclic peptide antagonist of vitronectin receptor-type integrins inhibits retinal neovascularization. *Nature Med.* 5:529-533.
- Holinger, E.P., Chittenden, T., and Lutz, R.J. 1999. Bak BH3 peptides antagonize Bcl-xL function and induce apoptosis through cytochrome c-independent activation of caspases. *J Biol. Chem.* 274, 13298-13304.
- Horak, E.R. et al. 1992. Angiogenesis, assessed by platelet/endothelial cell adhesion molecule antibodies, as indicators of node metastases and survival in breast cancer. *Lancet* 340, 1120-1124.
- Howe, A., A.E. Aplin, S.K. Alahari, and R.L. Juliano. 1998. Integrin signaling and cell growth control. *Curr. Opin. Cell Biol.* 10:220-31.
- Howe, A.K., Aplin, A.E., and Juliano, R.L. 2002. Anchorage-dependent ERK signaling-mechanisms and consequences. *Curr. Opin. Genet. Dev.* 12, 30-35.
- Huang, X., M. Griffiths, J. Wu, R.V. Farese, Jr., and D. Sheppard. 2000. Normal development, wound healing, and adenovirus susceptibility in beta5-deficient mice. *Mol. Cell Biol.* 20:755-9.



- Hynes, R.O. 1992. Integrins: versatility, modulation, and signaling in cell adhesion. *Cell*. **69**:11-25.
- Hynes, R.O. (1999). Cell adhesion: old and new questions. *Trends Cell Biol.* 9, M33-37.
- Jenkins, A.L. et al. 1998. Tyrosine phosphorylation of the  $\beta 3$  cytoplasmatic domain mediates integrin-cytoskeletal interactions. *J. Biol. Chem* **273**:13878-13885.
- Joliot AH, Triller A, Volovitch M, Pernelle C, Prochiantz A. 1991. alpha-2,8-Polysialic acid is the neuronal surface receptor of antennapedia homeobox peptide. *New Biol.* Nov;3(11):1121-34.
- Joliot A, Pernelle C, Deagostini-Bazin H, Prochiantz A. 1991. Antennapedia homeobox peptide regulates neural morphogenesis. *Proc Natl Acad Sci U S A.* **88**:1864-8.
- Kallen KJ, Grotzinger J, Rose-John S. 2000. New perspectives on the design of cytokines and growth factors. *Trends Biotechnol.* **18**:455-61. Review.
- Klemke, R.L., Yebra, M., Bayna, E.M. and Cheresch, D.A. 1994. Receptor tyrosine kinase signaling required for integrin  $\alpha v \beta 5$  -directed cell motility but not adhesion on vitronectin. *J. Cell Biol.* **127**:859-866.
- Koivunen, E., Wang, B., Dickinson, C.D. and Ruoslahti, E. 1994. Peptides in cell adhesion research. *Methods Enzymol.* **245**:346-369.
- Koivunen, E., B. Wang, and E. Ruoslahti. 1995. Phage libraries displaying cyclic peptides with different ring sizes: ligand specificities of the RGD-directed integrins. *Biotechnology (N Y).* **13**:265-70.
- Koivunen, E., B.H. Restel, D. Rajotte, J. Lahdenranta, M. Hagedorn, W. Arap, and R. Pasqualini. 1999. Integrin-binding peptides derived from phage display libraries. *Methods Mol. Biol.* **129**:3-17.
- Kolanus, W. and Zeitlmann, L. 1998. Regulation of integrin function by inside-out signaling mechanisms. *Curr. Topics Microbiol. Immunol.* **231**:33-49.
- Kolonin, M., R. Pasqualini, and W. Arap. 2001. Molecular addresses in blood vessels as targets for therapy. *Curr. Opin. Chem. Biol.* **5**:308-13.
- Lafrenie, R.M. and Yamada, K.M. 1996. Integrin-dependent signal transduction. *J. Cell. Biochem.* **61**:543-553.
- Le Roux I, Joliot AH, Bloch-Gallego E, Prochiantz A, Volovitch M. 1993. Neurotrophic activity of the Antennapedia homeodomain depends on its specific DNA-binding properties. *Proc Natl Acad Sci U S A.* **90**:9120-4.



- Lewis, J.M., Cheresch, D.A. and Schwartz, M.A. 1996. Protein kinase C regulates  $\alpha v\beta 5$ -dependent cytoskeletal associations and focal adhesion kinase phosphorylation. *J. Cell Biol.* **134**:1323-1332.
- Liliental J, Chang DD. 1998 Rack1, a receptor for activated protein kinase C, interacts with integrin beta subunit. *J Biol Chem.* **273**, 2379-83.
- Lin, T.H., Aplin, A.E., Shen, Y., Chen Q., Schaller, M.D., Romer L., Aukhil, I. and Juliano, R.L. 1997. Integrin-mediated activation of MAP kinase is independent of FAK: evidence for dual integrin signalling pathways in fibroblast. *J. Cell Biol.* **136**:1385-1395.
- Liu, S., D.A. Calderwood, and M.H. Ginsberg. 2000. Integrin cytoplasmic domain-binding proteins. *J. Cell Sci.* **113**:3563-71.
- Meitar, D., Crawford, S.E., Rademaker. A.W. & Cohn, S.L. 1996. Tumor angiogenesis correlates with metastatic disease, N-myc amplification, and poor outcome in human neuroblastoma. *J. Clin. Oncol.* **14**, 405-414.
- Meredith, J., Jr., Z. Mu, T. Saido, and X. Du. 1998. Cleavage of the cytoplasmic domain of the integrin beta3 subunit during endothelial cell apoptosis. *J. Biol. Chem.* **273**:19525-31.
- Mira, J.P., Dubois, T., Oudinet, J.P., Lukowski, S., Russo-Marie, F., and Geny, B. 1997. Inhibition of cytosolic phospholipase A2 by annexin V in differentiated permeabilized HL-60 cells. Evidence of crucial importance of domain I type II  $\text{Ca}^{2+}$ -binding site in the mechanism of inhibition. *J. Biol. Chem.* **272**, 10474-10482.
- Mochly-Rosen D, Smith BL, Chen CH, Disatnik MH, Ron D. 1995. Interaction of protein kinase C with RACK1, a receptor for activated C-kinase: a role in beta protein kinase C mediated signal transduction. *Biochem Soc Trans.* **23**:596-600. Review.
- Nakamura, S., and Nishizuka, Y. 1994. Lipid mediators and protein kinase C activation for the intracellular signaling network. *J. Biochem. (Tokyo)* **115**, 1029-1034.
- Pasqualini, R., and M.E. Hemler. 1994. Contrasting roles for integrin beta 1 and beta 5 cytoplasmic domains in subcellular localization, cell proliferation, and cell migration. *J. Cell Biol.* **125**:447-60.
- Pasqualini, R., Koivunen, E. and Ruoslahti, E. 1995 A peptide isolated from phage display libraries is a structural and functional mimic of an RGD-binding site on integrins. *J. Cell Biol.* **130**:1189-1196.
- Pasqualini, R., E. Koivunen, and E. Ruoslahti. 1997. Alpha v integrins as receptors for tumor targeting by circulating ligands. *Nat. Biotechnol.* **15**:542-6.



- Raynal, P., Hullin, F., Ragab-Thomas, J.M., Fauvel, J., and Chap, H. 1993. Annexin 5 as a potential regulator of annexin 1 phosphorylation by protein kinase C. In vitro inhibition compared with quantitative data on annexin distribution in human endothelial cells. *Biochem. J.* 292, 759-765.
- Reed, J.C. 2002. Apoptosis-based therapies. *Nat. Rev. Drug Discov.* 1:111-21.
- Rothhut, B., Dubois, T., Feliers, D., Russo-Marie, F., and Oudinet, J.P. 1995. Inhibitory effect of annexin V on protein kinase C activity in mesangial cell lysates. *Eur. J. Biochem.* 232, 865-872.
- Schlaepfer, D.D., Jones, J., and Haigler, H.T. 1992. Inhibition of protein kinase C by annexin V. *Biochemistry* 31, 1886-1891.
- Schlaepfer, D.D., and T. Hunter. 1998. Integrin signalling and tyrosine phosphorylation: just the FAKs? *Trends Cell Biol.* 8:151-7.
- Schwartz, M.A., M.D. Schaller, and M.H. Ginsberg. 1995. Integrins: emerging paradigms of signal transduction. *Annu. Rev. Cell Dev. Biol.* 11:549-99.
- Sharma, C.P., Ezzell, R.M. and Arnaout, M.A. 1995. Direct interaction of filamin (ABP-280) with the  $\beta 2$ -integrin subunit CD18. *J. Immunol.* 154:3461-3470.
- Shattil, S.J., and M.H. Ginsberg. 1997. Perspectives series: cell adhesion in vascular biology. Integrin signaling in vascular biology. *J. Clin. Invest.* 100:1-5.
- Sopkova, J., Renouard, M., and Lewit-Bentley, A. 1993. The crystal structure of a new high-calcium form of annexin V. *J. Mol. Biol.* 234, 816-825.
- Stupack, D.G., X.S. Puente, S. Boutsaboualoy, C.M. Storgard, and D.A. Cheresh. 2001. Apoptosis of adherent cells by recruitment of caspase-8 to unligated integrins. *J. Cell Biol.* 155:459-70.
- Stupack, D.G., and Cheresh, D.A. 2002. ECM remodeling regulates angiogenesis: endothelial integrins look for new ligands. *Sci. STKE* 12, PE7. Review.
- Sung V, Stubbs JT 3rd, Fisher L, Aaron AD, Thompson EW. 1998. Bone sialoprotein supports breast cancer cell adhesion proliferation and migration through differential usage of the  $\alpha(v)\beta 3$  and  $\alpha(v)\beta 5$  integrins. *J Cell Physiol.* 17: 482-94.
- Takebayashi, Y., Aklyma, S., Yamada, K., S. & Aikou, T. Angiogenesis as an unfavorable prognostic factor in human colorectal carcinoma. *Cancer* 78, 226-231 (1996).



Tang, S., Y. Gao, and J.A. Ware. 1999. Enhancement of endothelial cell migration and in vitro tube formation by TAP20, a novel beta 5 integrin-modulating, PKC theta-dependent protein. *J. Cell Biol.* **147**:1073-84.

Theodore, L., D. Derossi, G. Chassaing, B. Llibat, M. Kubes, P. Jordan, H. Chneiweiss, P. Godement, and A. Prochiantz. 1995. Intraneuronal delivery of protein kinase C pseudosubstrate leads to growth cone collapse. *J. Neurosci.* **15**:7158-67.

Varner, J.A., Brooks, P.C. and Cheresch DA. 1995. REVIEW: the integrin  $\alpha v \beta 3$ : angiogenesis and apoptosis. *Cell Adh. Comm.* **3**:367-374.

Vuori, K., and Ruoslahti, E. 1993. Activation of protein kinase C precedes alpha 5 beta 1 integrin-mediated cell spreading on fibronectin. *J. Biol. Chem.* **268**, 21459-21462.

Weinstat-Saslow, D. & Steeg, P.S. 1994. Angiogenesis and colonization in the tumor metastatic process: basic and applied advances. *FASED J.* **8**, 401-407.

Zetter, B.R. 1997. On target with tumor blood vessel markers. *Nat. Biotechnol.* **15**:1243-4.

Zhu, D.M., Narla, R.K., Fang, W.H., Chia, N.C., and Uckun, F.M. 1998. Calphostin C triggers calcium-dependent apoptosis in human acute lymphoblastic leukemia cells. *Clin. Cancer Res.* **4**, 2967-2976.



## APPENDICES

Copy of each manuscript:

- 1- Cardo-Vila M, Arap W, Pasqualini R. Alpha v beta 5 integrin-dependent programmed cell death triggered by a peptide mimic of annexin V. Mol Cell. 2003 May;11(5):1151-62.....
- 2- Arap W, Kolonin MG, Trepel M, Lahdenranta J, Cardo-Vila M, et al. Steps toward mapping the human vasculature by phage display. Nat Med. 2002 Feb, 8(2) 121-7.....
- 3- Giordano, R.J. Cardo-Vila, M, Lahdenranta, J., Pasqualini, R. and Arap, W. Biopanning and rapid analysis of selective interactive ligands. Nat Med. 2001 Nov; 7(11):1249-53.....
- 4- Cardo-Vila M, Arden KC, Cavenee WK, Pasqualini R, Arap W. Is annexin 7 a tumor suppressor gene in prostate cancer? Pharmacogenomics J. 2001; 1(2):92-4.....





SCIENCE @ DIRECT

Register or Login: user name

Password:

Go

Home

Journals

Books

Abstract Databases

My Profile

Alerts

Help

Quick Search:

within All Full-text Sources

Go

Search Tips

welcome Web Edit

# Molecular Cell

Volume 11, Issue 5, May 2003, Pages 1151-1162

doi:10.1016/S1097-2765(03)00138-2

Cite or Link Using DOI

Copyright © 2003 Cell Press.

## Article

# $\alpha$ v $\beta$ 5 Integrin-Dependent Programmed Cell Death Triggered by a Peptide Mimic of Annexin V

Marina Cardó-Vila, Wadih Arap and Renata Pasqualini  

M.D. Anderson Cancer Center, The University of Texas, 1515 Holcombe Boulevard, Houston, TX 77030, USA

Received 16 July 2002; Revised 14 February 2003; accepted 19 February 2003 Published: May 22, 2003 Available online 16 April 2004.

## Abstract

The diverse cytoplasmic domain sequences within the various integrin subunits are critical for integrin-mediated signaling into the cell (outside-in signaling) and for activation of ligand binding affinity (inside-out signaling). Here we introduce an approach based on phage display technology to identify molecules that specifically interact with the cytoplasmic domain of the  $\beta$ 5 integrin subunit. We show that a peptide selected for binding specifically to the  $\beta$ 5 cytoplasmic domain (VVISYSMPD) induces apoptosis upon internalization. The cell death process induced by VVISYSMPD is sensitive to modulation by growth factors and by protein kinase C (PKC), and it cannot be triggered in  $\beta$ 5 null cells. Finally, we show that the VVISYSMPD peptide is a mimic of annexin V. Our results suggest a functional link between the  $\alpha$ v $\beta$ 5 integrin, annexin V, and programmed cell death. We propose the term "endothanatos" to designate this phenomenon.

## Article Outline

### This Document

- SummaryPlus
- ▶ Full Text + Links
  - Full Size Images
  - PDF (811 K)

### Actions

- E-mail Article



- Introduction
- Results and Discussion
  - Identification of a Specific  $\beta 5$  Cytoplasmic Domain Binding Peptide
  - An Internalizing Version of the VVISYSMPD Peptide Triggers Apoptosis
  - $\beta 5$  Integrin Null Fibroblasts Are Resistant to VVISYSMPD-Induced Apoptosis, Whereas Transfection of CS-1 Cells with  $\beta 5$  Confers Sensitivity to VVISYSMPD
  - The VVISYSMPD Peptide Is a Mimic of Annexin V
  - Localization of Annexin V and the  $\alpha v\beta 5$  Integrin in Pen-VVISYSMPD Untreated and Treated HUVECs
  - PKC Activity Is Required for VVISYSMPD-Induced Cell Death
  - Annexin V Associates with the  $\beta 5$  Integrin Cytoplasmic Domain
  - Angiogenic Growth Factors Enhance VVISYSMPD- Induced Programmed Cell Death In Vitro and In Vivo
  - Conclusions
- Experimental Procedures
  - Reagents
  - Cell Culture
  - Phage Display Screenings and Phage Binding Assays
  - Peptide Internalization and Visualization
  - Double Immunofluorescence
  - Proliferation and Cell Viability Assays
  - Apoptosis Assays
  - Protein-Protein Interaction Assays
  - Western Blot Analysis and Immunoprecipitation
  - Protein Biochemistry and High-Pressure Liquid Chromatography
  - In Vitro and In Vivo Neovascularization Assays
- Acknowledgements
- References

---

## Introduction

Cell surface receptors of the integrin family are important regulators of cell behavior. Integrins mediate cell adhesion, proliferation, migration, and survival (Hynes 1992; Hynes 1999; Giancotti and Ruoslahti 1999 and Eliceiri and Cheresch 2001).

The diverse cytoplasmic domain sequences within the various integrin subunits are critical for integrin-mediated signaling into the cell (outside-in signaling) and for activation of ligand binding affinity (inside-out signaling) (Clark and Brugge 1995; Clark and Hynes 1997; Howe et al. 1998 and Schlaepfer and Hunter 1998). Often, it is the association of specific molecules with integrin cytoplasmic domains that initiates signal transduction cascades (Schwartz et al. 1995; Shattil and Ginsberg 1997; Schlaepfer and Hunter 1998; Liu et al. 2000 and Aplin and Juliano 2001).

The  $\beta 5$  cytoplasmic domain has been reported to control cell migration and proliferation (Pasqualini and Hemler 1994; Klemke et al. 1994; Clark and Hynes 1997 and Aplin et al. 1998). Certain postadhesion events are regulated through a pathway that requires both  $\alpha v\beta 5$



and PKC activity (Tang et al., 1999). However,  $\alpha_v\beta_5$ -dependent mechanisms for cytoplasmic domain control of cell signaling are not well understood. To date, the theta-associated protein 20 (TAP 20) is the only molecule known to interact exclusively with the  $\beta_5$  cytoplasmic domain (Liu et al., 2000).

Extensive data have been generated based on the use of phage libraries to identify extracellular integrin ligands (Koivunen et al., 1999). The large molecular diversity represented in phage peptide libraries facilitates the identification of motifs that map to protein interaction sites (Kolonin et al. 2001 and Giordano et al. 2001). For example, RGD-containing peptides with high affinity for  $\alpha_v$  integrins have been isolated by phage display and shown to be useful tools for targeting tumor vasculature in vivo (Koivunen et al. 1995; Pasqualini et al. 1997 and Zetter 1997).

We reasoned that peptides that bind to the  $\beta_5$  cytoplasmic domain might mimic signal transduction properties of  $\alpha_v\beta_5$ -associated proteins. Here we introduce an approach based on phage display technology to identify molecules that specifically interact with the cytoplasmic domain of the  $\beta_5$  integrin subunit.

We show that a peptide mimicking annexin V binds to the  $\beta_5$  cytoplasmic domain and triggers apoptosis. Annexin V is a cytosolic signaling protein known to inhibit PKC activity (Dubois et al., 1996); we demonstrate that annexin V binds only to the active form of PKC. Induction of programmed cell death by this peptide is modulated by growth factors and by PKC antagonists. Caspase activity and the expression of the  $\beta_5$  integrin subunit are also required. These results establish a connection between annexin V, cell adhesion, and apoptosis.

## Results and Discussion

Cell adhesion through integrins affects cell survival. We have uncovered a programmed cell death pathway triggered by internalization of VVISYSMPD, a  $\beta_5$  cytoplasmic domain binding peptide that mimics annexin V and affects PKC-dependent signaling.

### Identification of a Specific $\beta_5$ Cytoplasmic Domain Binding Peptide

We isolated  $\beta_5$  cytoplasmic domain binding peptides by screening a phage library displaying the motif  $X_4YX_4$  (X, any amino acid; Y, tyrosine) on a recombinant fusion protein containing the  $\beta_5$  cytoplasmic domain. Immobilized glutathione-S-transferase (GST) and BSA were used as negative controls for enrichment during multiple rounds of panning; phage were sequenced from randomly selected clones after three rounds of screening (data not shown). Phage displaying the sequences DEEGYYMMR, FQFSYRYLL, SDWYYPWSW, DWPSYYEL, and VVISYSMPD were recovered with high frequency during the screening. The most commonly displayed peptide sequence (VVISYSMPD) was characterized further. We first determined the specificity of the phage peptide interaction with the  $\beta_5$  cytoplasmic domain. Phage displaying the sequence VVISYSMPD, or scrambled versions of the peptide, were tested for binding to GST- $\beta_1$ , - $\beta_3$ , or - $\beta_5$  cytoplasmic domains. The VVISYSMPD phage interacted only with GST- $\beta_5$  and not with GST- $\beta_1$  or GST- $\beta_3$  (Figure 1A). In contrast, control insertless phage (Fd-tet), or phage displaying the scrambled versions of the VVISYSMPD peptide, did not bind to any of the immobilized proteins. Next, we showed



that the synthetic VVISYSMPD peptide specifically inhibited binding of the corresponding phage in a dose-dependent manner; a control peptide with an unrelated sequence had no effect (Figure 1B). Thus, we show that the VVISYSMPD peptide binds to the cytoplasmic domain of the  $\beta 5$  integrin and that the interaction is specific.

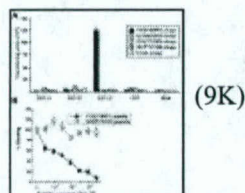


Figure 1. Phage Displaying the VVISYSMPD Peptide Binds Specifically to the  $\beta 5$  Integrin Cytoplasmic Domain (A) Integrin cytoplasmic domain GST fusion proteins or GST alone were coated on microtiter wells at 10  $\mu\text{g/ml}$  and incubated with  $\beta 5$  cytoplasmic domain binding phage (VVISYSMPD). Phage displaying scrambled versions of the VVISYSMPD peptide (ISYVMDSP, VISYVPDMS, and ISDPYVSM) or fd-tet (insertless) phage were used as negative controls. (B) Binding of VVISYSMPD phage to the  $\beta 5$  integrin cytoplasmic domain and inhibition with the corresponding synthetic peptide. Phage displaying VVISYSMPD were incubated on wells coated with the GST- $\beta 5$  integrin cytoplasmic domain in the presence of increasing concentrations of VVISYSMPD peptide or an unrelated negative control peptide sequence (SDNRYIGSW).

### An Internalizing Version of the VVISYSMPD Peptide Triggers Apoptosis

To determine whether the VVISYSMPD peptide interferes with  $\beta 5$  integrin signaling, we designed and synthesized an internalizing version of this peptide by using the penetratin system for intracellular delivery. Penetratin is a peptide containing 16 amino acids that is part of the third helix of the antennapedia protein homeodomain (Derossi et al. 1998). Because penetratin (Pen) has translocating properties, it is capable of carrying hydrophilic compounds across the plasma membrane and delivering them directly to the cytoplasm without degradation (Derossi et al., 1994). We fused VVISYSMPD or a control unrelated peptide to penetratin and added a biotin moiety to visualize internalization. We used human umbilical vein endothelial cells (HUVECs) to test the effect of the internalizing peptide because these cells (1) express the  $\alpha v\beta 5$  integrin (as determined by FACS analysis with specific antibodies; Pasqualini et al., 1993), and (2) respond to growth factors such as VEGF, which activates  $\beta 5$ -dependent signaling (Byzova et al. 2000 and Eliceiri and Cheresch 2001). Pen-VVISYSMPD and a negative control were internalized and remained in the cytoplasm of HUVECs (Figure 2A). Penetratin alone was also internalized and uniformly distributed in the cytoplasm; biotinylated peptides lacking penetratin were not internalized (data not shown).

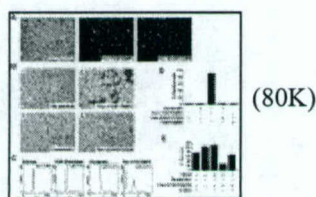




Figure 2. An Internalizing Version of the VVISYSMPD  $\beta 5$  Cytoplasmic Domain Binding Peptide Triggers Cell Death (A) Peptide internalization. Phase-contrast image of human umbilical cord endothelial cells (HUVECs) (left panel); cells incubated with the internalizing version of the VVISYSMPD peptide (Pen-VVISYSMPD) (middle panel); cells incubated with a control unrelated internalizing peptide, Pen-SDNRYIGSW (right panel). (B) Phase-contrast images showing the effect of penetratin-VVISYSMPD (Pen-VVISYSMPD) on endothelial cells. Cells were stimulated with VEGF and were monitored after an overnight incubation without peptide (B1), with Pen-VVISYSMPD (B2), with penetratin alone (B3), or with Pen-SDNRYIGSW (B4), at equimolar concentrations. (C) Internalization of Pen-VVISYSMPD leads to growth arrest of HUVECs at G<sub>0</sub>/G<sub>1</sub> and induces programmed cell death. Cells were stained with propidium iodide (PI), and their DNA was analyzed by FACS. (D) Apoptosis detection by annexin V staining. Cells were harvested after treatment with internalizing peptides, as indicated, and stained with ApoAlert. (E) Effect of caspase inhibitors on cell death mediated by the internalizable VVISYSMPD peptide was evaluated by MTT assay.

We next evaluated cell survival and proliferation in cells exposed to Pen-VVISYSMDP. Quiescent HUVECs were stimulated with basal medium containing VEGF. After an overnight incubation, most of the VEGF-stimulated cells treated with Pen-VVISYSMPD died (Figure 2 B2). No cell death was observed when HUVECs were untreated (Figure 2B1), treated with penetratin alone, or treated with an unrelated control peptide fused to penetratin (Figures 2B3 and 2B4). Moreover, incubation of VEGF-stimulated HUVECs with Pen-VVISYSMPD induced a subdiploid peak corresponding to apoptotic cells, whereas starvation or treatment with penetratin alone had little or no effect (Figure 2C).

An early step in the induction of programmed cell death is the inversion of phosphatidylserine in the cell membrane. Such a phenomenon can be detected in a standard apoptosis assay (Fadok et al., 1992). Again, treatment of VEGF-stimulated HUVECs with Pen-VVISYSMPD induced marked cell death, whereas treatment with control peptides did not (Figure 2D). A DNA laddering assay confirmed that DNA fragmentation occurred in cells treated with Pen-VVISYSMPD but not with controls (data not shown).

To evaluate whether caspase activity was required for induction of cell death, we incubated VEGF-stimulated HUVECs with penetratin or Pen-VVISYSMPD in the presence of the caspase inhibitor z-VAD. Treatment with z-VAD prevented over 50% of the Pen-VVISYSMPD-induced cell death (Figure 2E). In contrast, the caspase-8 inhibitor z-IETD had no such effect (data not shown). These results show that apoptosis induced by Pen-VVISYSMPD in HUVECs requires caspase activation, although caspase-8 is not involved in the cell death process.

As shown in Figure 2B, the internalizing form of the VVISYSMDP peptide induces apoptosis without affecting cell adhesion. To reinforce this finding, we performed two types of experiments. First, we preloaded cells (while in suspension) with the internalizing version of the VVISYSMPD peptide, and subsequently plated them on vitronectin, fibronectin, or collagen. Given that HUVECs undergo rapid cell death in the presence of the VVISYSMPD peptide, treated cells attached poorly under all the experimental conditions tested. These results support the hypothesis that VVISYSMPD does not interfere with  $\alpha v\beta 5$ -mediated adhesion to vitronectin, but rather induces cell death, a process resulting in impaired adhesion to any substrate (data not shown). We also observed that when cells are plated on collagen or fibronectin, the internalizing version of the VVISYSMPD peptide is still able to induce cell death. These data demonstrate that (1)  $\alpha v\beta 5$  binding to vitronectin is not required to trigger this process and (2) the interaction between VVISYSMPD and the  $\beta 5$  cytoplasmic



domain is not vitronectin dependent.

Programmed cell death is involved in many diseases as well as in wound healing and in tissue remodeling (Reed, 2002). Disruption of integrin-mediated cell-matrix interactions may lead to caspase-dependent apoptosis; two pathways, anoikis (Frisch and Francis, 1994) and integrin-mediated death (IMD) (Stupack et al., 2001), have been described. By definition, anoikis requires loss of cell adhesion (Frisch and Francis 1994; Frisch and Ruoslahti 1997; Frisch and Screaton 2001; Howe et al. 2002; Meredith et al. 1998 and Aoudjit and Vuori 2001). Given that cells treated with the VVISYSMPD peptide undergo apoptosis while still attached, it is unlikely that our observations can be explained by the general phenomenon of anoikis. On the other hand, IMD occurs when  $\beta 3$ -mediated interactions are blocked in adherent cells. However, IMD is induced by the cytoplasmic domains of  $\beta 1$  or  $\beta 3$  (but not  $\beta 5$ ), and it results from recruitment of caspase-8 to the membrane and its subsequent activation (Stupack et al., 2001). In contrast, the VVISYSMPD peptide binds only to the  $\beta 5$  cytoplasmic domain (but not to  $\beta 1$  or  $\beta 3$ ). Finally, caspase 8 activity is not required for VVISYSMPD-induced cell death. Taken together, these observations indicate that VVISYSMPD-induced apoptosis is a programmed cell death mechanism that has not previously been described.

### **$\beta 5$ Integrin Null Fibroblasts Are Resistant to VVISYSMPD-Induced Apoptosis, Whereas Transfection of CS-1 Cells with $\beta 5$ Confers Sensitivity to VVISYSMPD**

To test whether the  $\beta 5$  integrin subunit is required for apoptosis induction by the VVISYSMPD peptide, we compared the effects of internalizing peptides on fibroblasts isolated from  $\beta 5$  integrin null mice (Huang et al., 2000) and wild-type mice. Penetratin, VVISYSMPD, or Pen-VVISYSMPD was added to the culture media (Figure 3). Marked cell death was observed in wild-type fibroblasts treated with Pen-VVISYSMPD (Figure 3A5), while fibroblasts lacking the  $\beta 5$  integrin were not affected (Figure 3A2). Treatment with penetratin or the noninternalizing VVISYSMPD peptide did not induce cell death (Figures 3A1, 3A3, 3A4, and 3A6). Cell viability was quantified by the 3-[4,5-dimethylthiazol-2-yl]-2,5-diphenyltetrazolium bromide (MTT) assay (Figure 3B).

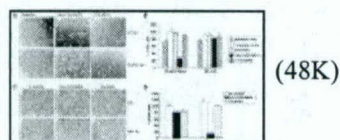


**Figure 3. Cell Death Induced by Pen-VVISYSMPD Requires  $\beta 5$  Expression**(A) Fibroblasts from  $\beta 5$  null mice (A1–A3) or from wild-type (A4–A6) were incubated with 15  $\mu$ M penetratin (A1 and A4), Pen-VVISYSMPD (A2 and A5), or the VVISYSMPD peptide (A3 and A6). The cells were visualized by phase contrast (100  $\times$  magnification).(B) Quantification of cell viability by using the MTT assay.(C) CS-1 or CS-1- $\beta 5$  cells were incubated with RPMI alone (C1 and C4), Pen-VVISYSMPD (C2 and C5), or penetratin at a concentration of 15  $\mu$ M (C3 and C6) and visualized by phase contrast (100  $\times$  magnification).(D) MTT assays were used to measure cell viability.



To reinforce that VVISYSMPD-triggered cell death requires the expression of  $\beta 5$ , we used a different cell system in which  $\beta 5$  integrin-negative cells (CS-1) were transfected with  $\beta 5$ . We showed that VVISYSMPD-triggered cell death does not occur in the absence of the  $\beta 5$  subunit (Figure 3C2) and does occur in  $\beta 5$ -transfected cells (Figure 3C5). Treatment with penetratin alone did not induce cell death (Figures 3C3 and 3C6). Cell viability was quantified by the MTT assay (Figure 3D).

These results show that apoptosis induction by the membrane-permeable form of the VVISYSMPD peptide does not occur in the absence of the  $\beta 5$  integrin subunit.

### The VVISYSMPD Peptide Is a Mimic of Annexin V

We reasoned that the VVISYSMPD peptide could mimic a  $\beta 5$  integrin-associated molecule. To test this hypothesis, we generated a polyclonal antibody against the peptide. The anti-VVISYSMPD serum recognized the immobilized VVISYSMPD peptide in a concentration-dependent manner. Reactivity was abrogated by preincubation with the synthetic VVISYSMPD peptide, but not with an unrelated control peptide (data not shown). When tested on Western blots of total cell extracts, the anti-VVISYSMPD polyclonal antibody reacted with a specific 36 kDa protein.

We used the anti-VVISYSMPD antibody to probe protein samples from cell extracts processed by sequential gel filtration and anion exchange column chromatography to identify the target antigen (see Experimental Procedures for details). A 36 kDa protein was enriched after the final purification step (Figure 4A) and was recognized by the anti-VVISYSMPD antibody on Western blots (Figure 4B). Mass spectrometry analysis revealed seven unique peptides derived from the purified 36 kDa protein that matched the annexin V protein sequence (Cookson et al., 1994) in a BLAST homology search (Figure 4D). To confirm that the purified protein was annexin V, we reprobed the membrane containing the fractions enriched for the 36 kDa protein (Figure 4B) with a commercial antibody against annexin V, which readily detected the same 36 kDa antigen (Figure 4C). These results show that annexin V is the protein recognized by the anti-VVISYSMPD polyclonal antibody. Analysis of a three-dimensional model of annexin V based on its structure (Sopkova et al., 1993) shows that the motif containing the  $\beta 5$  binding peptide is exposed on the surface of the molecule (Figure 4E).

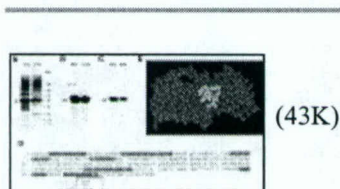


Figure 4. Identification of the Protein Mimicked by the VVISYSMPD Peptide (A) Coomassie blue staining of proteins obtained from cell extracts after ion exchange chromatography followed by molecular weight fractionation. The arrow indicates the protein excised and processed by MALDI-TOF mass spectrometry. (B) Western blot analysis of fractions containing purified proteins using the anti-VVISYSMPD rabbit antiserum (generated by immunizing rabbits with VVISYSMPD-KLH). (C) The same Western blot (Figure 4B) was stripped and reprobed with a polyclonal anti-human annexin V antibody. (D) The amino acid sequence of the full-length h-annexin V from the NCBI database (accession number AAB60648). Boxed in orange are the seven peptides obtained by mass spectrometry from the purified protein shown in Figure 4A. The



region of similarity with the VVISYSMPD peptide is underlined; identical (\*) and conserved (+) amino acids are indicated. (E) Annexin V structure showing the location of the sequence containing the  $\beta 5$  binding peptide (in yellow).

Annexin V belongs to a family of proteins defined by their ability to bind calcium and phospholipids via a series of tandem motifs that form the core of the protein (Dubois et al., 1996). All annexins contain a putative PKC binding site, but only annexin V has been shown to function as a PKC inhibitor (Schlaepfer et al. 1992 and Dubois et al. 1998). Thus, we sought to determine whether inhibition of PKC would interfere with the induction of apoptosis by the VVISYSMPD peptide.

### Localization of Annexin V and the $\alpha v\beta 5$ Integrin in Pen-VVISYSMPD Untreated and Treated HUVECs

Double immunofluorescence staining of  $\beta 5$  (shown in green) and annexin V (shown in red) in VEGF-stimulated cells (HUVECs) was used to evaluate the localization of these two proteins in proliferating and dying cells by immunofluorescence (Figure 5A).  $\beta 5$  (shown in green) and annexin V (shown in red) colocalize (yellow) in VEGF-stimulated cells (Figure 5A, upper panel). However, in cells treated with Pen-VVISYSMPD, annexin V is seen mainly in the cytoplasm (Figure 5A, middle panel). Loss of cytoplasmic membrane integrity (likely due to massive apoptosis induction) is seen 3 hr after treatment with Pen-VVISYSMPD. However, cells remained attached (Figure 5A, lower panels).

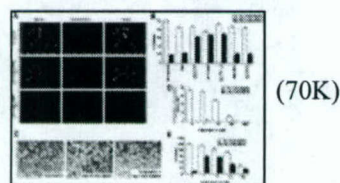


Figure 5. Localization of Annexin V with  $\alpha v\beta 5$  Integrin and a PKC Inhibitor Modulates the Apoptotic Effects in Pen-VVISYSMPD Untreated and Treated HUVECs (A) Double immunofluorescence staining of  $\beta 5$  (shown in green) and annexin V (shown in red) in VEGF-stimulated cells (HUVECs). Colocalization of the  $\beta 5$  cytoplasmic domain and annexin V appears in yellow in the merged images (top right panel).  $\beta 5$  and annexin V no longer colocalize after incubation with Pen-VVISYSMPD for 1 hr (middle panels) or 3 hr (lower panels). (B) VEGF-stimulated HUVECs were incubated with PKC inhibitors (Myr-PKC $\alpha/\beta$ , calphostin C, Ro 31-8220, Myr-PCK $\epsilon$ , Myr-PKC $\zeta$ ) or PMA in the presence or absence of Pen-VVISYSMPD. Cell viability was evaluated by the MTT assay 24 hr later. (C) The PKC inhibitor calphostin C delays apoptosis induced by Pen-VVISYSMPD in HUVECs. (D) HUVECs were incubated with increasing concentrations of calphostin C with or without 12  $\mu$ M Pen-VVISYSMPD. After an overnight incubation, proliferation was assessed by measuring [ $^3$ H]thymidine incorporation. (E) Quantification of cell viability after incubation with Pen-VVISYSMPD in the presence of increasing concentrations of calphostin C.

Furthermore, in order to define the VVISYSMPD peptide interacting site within the  $\beta 5$  cytoplasmic domain, we engineered phage particles displaying several sequences within the

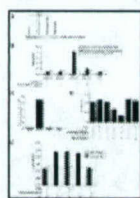


$\beta 5$  tail. Then, using phage binding assays with both the VVISYSMPD peptide and the native annexin V protein, we mapped the binding site within a short domain containing the sequence FQSERSRARYEMAS. This domain, as expected, is not present in other integrin cytoplasmic domains. In addition, we also demonstrated that the VVISYSMPD peptide had properties similar to the actual sequence present in annexin V by synthesizing the annexin V peptide SLYSMIKGD (Figure 4D) and showing that this peptide binds equally well to the cytoplasmic domain of  $\beta 5$  (data not shown).

### PKC Activity Is Required for VVISYSMPD-Induced Cell Death

The role of annexin in signal transduction and the mechanism(s) by which annexin V inhibits PKC activity remain elusive. It has been proposed that the identification of a protein that regulates the relative concentrations of annexin V and PKC near the membrane may control PKC signaling events (Dubois et al., 1996). However, such a protein has not yet been identified. On the other hand, PKC signaling regulates  $\beta 5$  function and controls cell survival in endothelial cells (Tang et al. 1999 and Lewis et al. 1996). Serine/threonine kinases are activated upon integrin stimulation, and inhibitors of PKC block cell attachment and spreading in vitro (Vuori and Ruoslahti 1993; Nakamura and Nishizuka 1994 and Chen et al. 1994). The C-terminal domain of annexin V associates with and inhibits PKC in the presence of  $\text{Ca}^{2+}$  (Schlaepfer et al. 1992; Raynal et al. 1993; Rothhut et al. 1995 and Dubois et al. 1995). These observations led us to hypothesize that PKC regulates  $\beta 5$ -dependent apoptosis induced by Pen-VVISYSMPD. To verify this hypothesis, we tested the effects of Pen-VVISYSMPD in the presence of different agents that interfere with PKC activity, namely, PMA, Myr-PKC $\alpha/\beta$ , calphostin C, Ro31-8220, PCK $\epsilon$ , and Myr PKC $\zeta$ . We demonstrated that the PKC inhibitors Myr-PKC $\alpha/\beta$ , calphostin C, and Ro31-8220 inhibit VVISYSMPD-induced cell death (Figure 5B). These results also show that conventional PKCs play a key role in VVISYSMPD-mediated cell death.

Because calphostin C is a well-established PKC inhibitor used extensively in the literature, we have expanded our studies by the use of this reagent (Figures 6C and 6D).



(16K)

Figure 6. Annexin V Associates with the  $\beta 5$  Integrin Cytoplasmic Domain and Binds to Activated PKC(A) HUVECs were lysed with RIPA buffer containing  $\text{Ca}^{2+}$ , and immunoprecipitation was performed with an anti- $\beta 5$  integrin antibody (lane 1), an anti-annexin V antibody (lane 2), or anti-mouse IgG as a negative control (lane 3).  $\beta 5$  integrin was detected by Western blot analysis by a monoclonal antibody. A crude cell extract is shown in lane 4.(B) Annexin V binds to the  $\beta 5$  cytoplasmic domain. Binding of recombinant human annexin V was determined spectrophotometrically by an anti-human annexin V polyclonal antibody.(C) The VVISYSMPD peptide does not bind to PKC. Purified PKC was coated on microtiter wells at 250 ng/ml and incubated with phage displaying the VVISYSMPD peptide. GST- $\beta 5$ -coated wells were used as a positive control, and wells coated with GST or BSA were used as negative controls.(D) The  $\beta 5$  integrin cytoplasmic domain inhibits binding of annexin V to PKC.



Microtiter plate wells coated with PKC were incubated with annexin V with or without the GST- $\beta 5$  cytoplasmic domain and VVISYSMPD peptide or with an unrelated control peptide. Binding of recombinant human annexin V to PKC was determined as described above. (E) HUVECs incubated with PMA or with the Myr peptide for the indicated times were used as the source of immunocaptured PKC. Binding of annexin V to PKC was analyzed by incubating each sample well with 1.5  $\mu$ g/ml recombinant human annexin V. Bound annexin V was detected spectrophotometrically with an anti-human annexin V polyclonal antibody. Control IgG was used as a negative control.

High concentrations of calphostin C induced cell death (Zhu et al., 1998). However, at low concentrations (1–10 nM), we show that calphostin C inhibits PKC activity without significant induction of cell death (Figure 5D). Apoptosis induced by the VVISYSMPD peptide was markedly reduced in the presence of low concentrations of calphostin C (Figure 5D). A [ $^3$ H]thymidine incorporation assay revealed that cell proliferation was completely blocked by Pen-VVISYSMPD (Figure 5D). However, when apoptosis induction was evaluated, there were more viable cells in the wells exposed to both Pen-VVISYSMPD and calphostin C than in monolayers treated with only Pen-VVISYSMPD (Figure 5E).

These data show that VVISYSMPD-induced apoptosis is blocked by inhibition of PKC, and they indicated that PKC activity regulates the proapoptotic effects of the VVISYSMPD peptide.

### Annexin V Associates with the $\beta 5$ Integrin Cytoplasmic Domain

The experimental evidence described above indicated that annexin V interacts with the  $\beta 5$  cytoplasmic domain. To show that annexin V associates with  $\beta 5$  integrin *in vivo*, we performed reciprocal coimmunoprecipitation with antibodies against the  $\beta 5$  integrin or annexin V and probed the immunoprecipitates on Western blots with a well-characterized anti- $\beta 5$  antibody. A specific band corresponding to the  $\beta 5$  integrin subunit was detected (Figure 6A). These data demonstrate that annexin V associates with  $\beta 5$  integrin in cells.

To show that the interaction between annexin V and the  $\beta 5$  integrin cytoplasmic domain is specific, we used protein binding assays (Figure 6B). Recombinant annexin V was incubated with GST- $\beta 5$ , or with  $\beta 1$  or  $\beta 3$  GST fusion proteins as negative controls. Because  $\text{Ca}^{2+}$  is required for the association between annexin V, PKC, and phospholipids (Mira et al., 1997), we tested whether  $\text{Ca}^{2+}$  would also enhance the interaction between annexin V and  $\beta 5$ . Three different buffers were used in the binding experiments: Tris-buffered saline, and a buffer that mimics cytoplasmic conditions (termed binding buffer) with or without  $\text{Ca}^{2+}$  (Figure 6B). Bound annexin V was detected with a specific antibody against annexin V. A highly specific interaction between annexin V and the GST- $\beta 5$  cytoplasmic domain was observed (Figure 6B).  $\text{Ca}^{2+}$  was required for the interaction, since annexin V binding was not detected when  $\text{Ca}^{2+}$ -free buffers were used. The interaction between the  $\beta 5$  cytoplasmic domain and annexin V was specifically inhibited by the VVISYSMPD peptide (Figure 6B), but not by a control peptide (data not shown). Thus, the VVISYSMPD peptide mimics the binding site through which annexin V associates with the cytoplasmic domain of the  $\beta 5$  integrin subunit.

To rule out the possibility that the VVISYSMPD peptide might induce apoptosis by its direct inhibition of PKC, we tested whether the peptide binds to the enzyme. If the peptide



interacted with PKC, it might also affect the interaction between annexin V and PKC. Phage binding assays eliminated both possibilities, as no binding of VVISYSMPD-displaying phage to PKC was detected; the  $\beta 5$ -GST protein was used as a positive control (Figure 6C).

Annexin V has been shown to bind to PKC (Schlaepfer et al., 1992), and we examined whether the VVISYSMPD peptide could interfere with this interaction. Protein binding assays showed that the VVISYSMPD peptide does not affect the binding of annexin V to PKC (Figure 6D). In contrast, the GST- $\beta 5$  integrin cytoplasmic domain blocked the binding of annexin V to PKC by about 40%. Importantly, the interaction between annexin V and PKC was rescued when VVISYSMPD peptide and GST- $\beta 5$  were incubated jointly. Taken together, these results show that binding of annexin V to the cytoplasmic domain of  $\beta 5$  integrin is blocked by VVISYSMPD peptide.

Interestingly, PMA does not prevent VVISYSMPD-induced cell death, because it facilitates PKC binding to annexin V (Figure 6E). Consistent with this result, a specific inhibitor of conventional PKCs blocks binding of annexin V to PKC (Figure 6E) and inhibits VVISYSMPD-induced cell death (Figure 5). These results support a key role for PKC activity and subsequent inhibition by annexin V in the VVISYSMPD-induced cell death process.

Having established that cell death induced by VVISYSMPD is modulated by PKC, we observed that PKC activity is required for annexin V binding; yet, it is through annexin V-dependent PKC inhibition that cell death is induced by the  $\beta 5$ -cytoplasmic domain binding peptide. Moreover, based on experiments performed with specific PKC inhibitors, conventional PKCs mediate VVISYSMPD-induced cell death.

### Angiogenic Growth Factors Enhance VVISYSMPD- Induced Programmed Cell Death In Vitro and In Vivo

To determine whether angiogenic factors modulate apoptosis induced by Pen-VVISYSMPD, we evaluated cell death after stimulation with factors that activate endothelial cells. HUVECs treated with Pen-VVISYSMPD in the presence of VEGF or basic fibroblast growth factor (bFGF) underwent rapid apoptosis in comparison to the controls (Figure 7C). Penetratin or the VVISYSMPD peptide alone were used as negative controls and had no effect under identical conditions. Therefore, cell death induced by Pen-VVISYSMPD is markedly enhanced by angiogenic growth factors. These observations led us to hypothesize that Pen-VVISYSMPD might function as an inhibitor of angiogenesis.

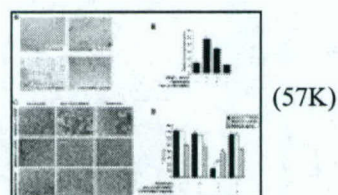


Figure 7. Pen-VVISYSMPD-Induced Cell Death Results in Angiogenesis Inhibition In Vitro and In Vivo(A) HUVECs were plated in Matrigel-coated plates and photographed 24 hr after incubation with penetratin, Pen-VVISYSMPD, or the VVISYSMPD peptide alone (magnification 4 $\times$ ). (B) Matrigel supplemented with growth factors was injected into mice in the presence or



absence of penetratin or Pen-VVISYSMPD. Neovascularization within the Matrigel plugs was determined by measurement of the levels of injected FITC-labeled lectin recovered by using a fluorimeter (485 nm). (C) Phase-contrast images showing the effect of Pen-VVISYSMPD on growth factor-stimulated HUVECs. Cells were monitored after an overnight incubation with either culture medium without growth factors, or after stimulation with VEGF or bFGF. Monolayers were treated with Pen-VVISYSMPD or penetratin alone, at equimolar concentrations. (D) Proangiogenic factors (VEGF and bFGF) enhance Pen-VVISYSMPD-induced cell death. Endothelial cell viability was evaluated by the MTT assay.

In response to specific stimuli, endothelial cells plated on Matrigel develop into networks of capillary-like structures. Using VEGF-stimulated HUVECs plated in Matrigel as a model of neovascularization, we showed that incubation with Pen-VVISYSMPD completely inhibits the formation of a vascular network, whereas penetratin or the VVISYSMPD peptide alone did not have any apparent effect (Figure 7A). To expand our findings, we also assessed the ability of the  $\beta 5$  integrin cytoplasmic domain binding motif to inhibit neovascularization in vivo. Subcutaneous implantation of Matrigel plugs containing a combination of bFGF plus VEGF in nude mice induces vessel growth within 5 days. When tested in this model, Pen-VVISYSMPD completely inhibited angiogenesis induced by both growth factors, while penetratin alone had no effect (Figure 7B). These results clearly show that the  $\beta 5$  cytoplasmic domain binding peptide inhibits neovascularization. Consistent with these observations, we found that the angiogenic factors (VEGF and bFGF) enhance Pen-VVISYSMPD-induced cell death (Figure 7C). VEGF is highly effective in accelerating VVISYSMPD-mediated cell death (Figure 7C, upper panel). Although bFGF is also effective, it is less potent than VEGF under the experimental conditions tested (Figure 7C, middle panel). Finally, Pen-VVISYSMPD has little effect on nonproliferating endothelial cells cultured in medium without growth factors (Figure 7C, lower panel). Endothelial cell viability in this experiment was also evaluated by the MTT assay (Figure 7D).

## Conclusions

We demonstrate that there is a connection between the regulation of PKC activity by annexin V and the induction of cell death in a  $\beta 5$ -dependent manner. Also in agreement with our findings is the recent serendipitous copurification of annexin V with the integrin  $\beta 5$  subunit (Andersen et al., 2002).

Our data reveal a structural basis for the regulation of PKC-mediated cell survival and provide insights into the mechanism of action of annexin V. We show that a short synthetic peptide mimic of annexin V induces cell death and that the mechanisms underlying this phenomenon were completely different from those of anoikis or of IMD. We propose the term "endothanatos" (death from inside) to designate this  $\beta 5$ -dependent cell death pathway.

## Experimental Procedures

### Reagents

GST fusion proteins expressing  $\beta 1$ ,  $\beta 3$ , or  $\beta 5$  integrin cytoplasmic domains cloned into the vector pGEX were purified according to the manufacturer's instructions (Amersham Pharmacia Biotech). Anti- $\beta 5$  integrin antibodies (IA9 and IVA4) were a kind gift from Dr. Martin Hemler, the anti-GST antibody was from Amersham Pharmacia Biotech, horseradish



peroxidase (HRP)-conjugated anti-rabbit and anti-goat secondary antibodies were purchased from Sigma-Aldrich. The anti-human annexin V antibody was produced by Hyphen BioMed and is distributed by diaPharma. Recombinant human VEGF was purchased from BD Pharmingen. Annexin V was purchased from Santa Cruz Biotechnology. Synthetic peptides, the keyhole limpet hemocyanin (KLH) conjugates, and penetratin chimeras were purchased from Anaspec.

## Cell Culture

Single-donor HUVECs were purchased from Clonetics and were cultured in complete endothelial media (EGM BulletKit, Clonetics) according to the manufacturer's instructions. Cells were used at passage 3 to 5. Starved HUVECs were grown in EBM-2 (endothelial basal media, serum-free, Clonetics). MDA-MB-435 cells were obtained from American Type Culture Collection (ATCC). Primary fibroblast cultures were established from mouse brain and grown in Dulbecco's modified Eagle's media (DMEM) from GIBCO containing 10% fetal calf serum (FCS). For assays using  $\beta 5$  null cells, confluent fibroblasts were plated in 12 wells ( $5 \times 10^4$  cells per well) in complete media and were allowed to attach (fibroblasts used in our experiments were not stimulated with specific growth factors). The medium was replaced by starvation medium; 24 hr later, peptides were added in complete media, and cells were incubated for 12 hr at 37°C. CS-1 (Farishian and Whittaker 1979 and Thomas et al. 1993) and CS-1 cells stably transfected with a  $\beta 5$ wt integrin subunit domain were described previously (Filardo et al., 1996). Cells were cultured in RPMI, 1% HEPES, 10% FCS, 2 mM L-glutamine, and 100 u/ml Penicillin/Streptomycin  $\text{SO}_4$ .

## Phage Display Screenings and Phage Binding Assays

A phage display random peptide library displaying the insert  $\text{X}_4\text{YX}_4$  (where X is any amino acid and Y is a tyrosine residue) was used in the screenings; phage input was  $3 \times 10^{10}$  transducing units (TU). GST fusion proteins were coated on microtiter wells as previous described (Smith and Scott 1993 and Koivunen et al. 1993). Phage binding assays on purified proteins were carried out as described (Giordano et al., 2001). GST- $\beta 1$ , GST- $\beta 3$ , GST- $\beta 5$ , and GST (at 1  $\mu\text{g}$  in 50  $\mu\text{l}$  phosphate buffered saline [PBS]) were immobilized on microtiter wells overnight at 4°C. Wells were washed twice with PBS, blocked with PBS/3% BSA for 2 hr at room temperature, and incubated with  $10^9$  TU of VVISYSMPD phage, scrambled versions of the VVISYSMPD peptide (ISYVMDSVP, VISVYPDMS, and ISDPYVVSM), or fd-tet phage in 50  $\mu\text{l}$  PBS/1.5% BSA. After 1 hr at room temperature, wells were washed ten times with PBS, and phage were recovered by bacterial infection. VVISYSMPD or SDNRYIGSW were used as synthetic peptides to evaluate competitive inhibition of phage binding. ELISA with polyclonal anti-GST (Amersham) confirmed the presence and concentration of the GST-fusion proteins on the wells. To test binding of the VVISYSMPD phage to PKC, microtiter-wells were coated at 4°C overnight with 250 ng/ml of purified PKC (Promega), GST- $\beta 5$  fusion protein (positive control), or GST or BSA (negative controls). VVISYSMPD phage ( $10^{10}$  TU) was added to each well, and the binding assay was performed as described above.

## Peptide Internalization and Visualization

Uptake of biotinylated peptides into cells was monitored as described previously (Derossi et



al. 1994 and Theodore et al. 1995). HUVEC cultures were washed, and the media were replaced with complete media containing 10  $\mu$ g/ml biotinylated peptide. After 2 hr, the cultures were washed with PBS, fixed, permeabilized with ethanol:acetic acid (9:1, v:v) for 5 min at  $-20^{\circ}\text{C}$ , blocked for 30 min with 10% FCS in PBS, incubated for 1 hr with FITC-conjugated streptavidin, and washed with PBS prior to visualization with an inverted fluorescence microscope.

### Double Immunofluorescence

HUVECs were fixed in methanol for 10 min and were incubated with a monoclonal anti- $\beta_5$  antibody (IVA4) (diluted 1/300) and a polyclonal anti-annexin V antibody (diluted 1/200). The secondary antibodies were Cy3-anti-rabbit and FITC-anti-mouse IgG (Jackson ImmunoResearch Laboratories). Cells were examined by fluorescence microscopy (Olympus).

### Proliferation and Cell Viability Assays

Cell proliferation was measured as described previously (Pasqualini and Hemler, 1994). Briefly,  $4 \times 10^4$  HUVECs growing in 24-well plates were starved for 24 hr in unsupplemented EGM-2 media. Twenty-four hours later, the media were supplemented with VEGF (final concentration of 20 nM) and with each peptide (final concentration of 15  $\mu$ M). After incubation for 18 hr, 50  $\mu$ l of media containing [ $^3\text{H}$ ]thymidine (1  $\mu$ Ci/ml; Amersham) was added to each well. Six hours later, the media were removed, and the cells were fixed in 10% trichloroacetic acid (TCA) for 30 min at  $4^{\circ}\text{C}$ , washed with ethanol, and solubilized in 0.5 N NaOH. Incorporation of radioactivity was determined by liquid scintillation counting with an LS 6000SC Beckman scintillation counter. Cell viability was assessed by measurement of cellular metabolism of MTT (Sigma) at  $37^{\circ}\text{C}$ . Cells growing in 24-well plates were treated with penetratin chimeras for 12 hr, washed twice with PBS, incubated in complete media containing MTT (500  $\mu$ g/ml per well) for 2–4 hr, and solubilized with 0.1 N HCl in isopropanol (Mosmann, 1983). Samples were subsequently read at 570 nm in a plate reader (Bio-Tek Instruments). CS-1 and CS-1-b5 cells were grown in 48-well plates and were treated with penetratin or Pen-VVISYSMPD for 12 hr.

Cell viability was performed as described above.

### Apoptosis Assays

Induction of apoptosis was determined by two methods. First, DNA content was analyzed by propidium iodide (PI) staining. Approximately  $1 \times 10^6$  cells were harvested in complete media after incubation in EBM-2 plus VEGF (25 ng/ml) and 15  $\mu$ M penetratin or Pen-VVISYSMPD peptide for 4, 8, or 12 hr. The cells were washed in PBS, resuspended in 0.5 ml of PI solution (50  $\mu$ g/ml PI, 0.1% Triton X-100, and 0.1% sodium citrate), incubated for 24 hr at  $4^{\circ}\text{C}$ , and counted with an XL Coulter System (Coulter Corporation) with a 488 nm laser. Twelve thousand cells were counted for each histogram, and cell cycle distributions were analyzed with the Multicycle program.

Annexin V staining was performed to monitor early stages of apoptosis as described in the ApoAlert Annexin V Technical Bulletin (Clontech). Briefly, HUVECs growing in  $35 \times 10$  mm plates were incubated with the indicated peptides for various times, harvested, washed,



and resuspended in binding buffer supplemented with anti-annexin V antibody. Samples were incubated for 10–15 min at room temperature and were analyzed by FACS. To inhibit caspase activity, 80  $\mu\text{M}$  z-VAD or z-IETD (Calbiochem) was added to the cells with each peptide. In assays performed with PKC inhibitors, HUVECs were starved in EBM-2 media for 24 hr, the media were supplemented with 20 nM VEGF, 12  $\mu\text{M}$  peptides as indicated in the figure legends, and calphostin C (1  $\mu\text{M}$ , 100 nM, 10 nM, and 1 nM; Sigma), and the cells were incubated for an additional 14 hr.

### Protein-Protein Interaction Assays

GST fusion proteins containing the  $\beta_1$ ,  $\beta_3$ , or  $\beta_5$  cytoplasmic domains or GST alone were coated onto 96-well plates at 5  $\mu\text{g}/\text{well}$  to test the binding of annexin V to the  $\beta$  integrin cytoplasmic domain. Purified annexin V was added at 2  $\mu\text{g}/\text{ml}$  in three different buffers: Tris-buffered saline, a binding buffer (100 mM KCl, 3 mM NaCl, 3.5 mM MgCl<sub>2</sub>, 10 mM PIPES [pH 8]), and a binding buffer containing 2 mM CaCl<sub>2</sub>. After 3 hr, binding of annexin V to the GST fusion proteins was detected with an anti-annexin V antibody (diluted 1/100) followed by HRP-conjugated anti-goat IgG. To confirm that equal amounts of the GST fusion proteins were bound to the plates, parallel experiments were performed by ELISA using a 1:1500 dilution of an anti-GST antibody (data not shown; Amersham Pharmacia Biotech). To evaluate the interaction of PKC and annexin V, purified PKC (Promega) was coated at 250 ng/ml onto a microtiter-well plate and incubated with annexin V alone (2  $\mu\text{g}/\text{ml}$ ) or in combination with GST- $\beta_5$  integrin cytoplasmic domain (1  $\mu\text{g}/\text{ml}$ ) and VVISYSMPD peptide (12  $\mu\text{M}$ ). For the immunocapture assays, PKC was immobilized from HUVEC extracts as described (Park et al., 1999). Specifically, 96-well plates were coated overnight at 4°C with 1  $\mu\text{g}/\text{ml}$  anti-PKC (Ab-2; Oncogene). Wells were subsequently rinsed with wash buffer (PBS, 0.1% Tween), followed by blocking buffer (3% BSA in PBS) for 1 hr at room temperature. Blocking buffer was removed, and sonicated HUVEC cell extracts were added and incubated for 2 hr at room temperature. Wells were washed three times with wash buffer, and 2  $\mu\text{g}/\text{ml}$  of recombinant annexin V was added to the wells, which were incubated overnight at 4°C. Unbound protein was removed by three applications of wash buffer. Binding of annexin V to PKC was detected with an anti-annexin V antibody (diluted 1/100) followed by an HRP-conjugated anti-goat IgG.

### Western Blot Analysis and Immunoprecipitation

For Western blotting, total cell extracts were prepared from MDA-MB-435 breast carcinoma cells and HUVECs by solubilization in SDS sample buffer. Lysates were resolved on 4%–20% gradient SDS-polyacrylamide (SDS-PAGE) gels, and proteins were transferred to nitrocellulose membranes. The membranes were blocked and incubated with primary antibodies diluted in blocking buffer (anti-VVISYSMPD antibody diluted 1:3000; anti-annexin V antibody diluted 1:200). The membranes were washed and were incubated with secondary antibodies, a horseradish peroxidase-linked conjugate of anti-rabbit or anti-goat IgG. Reactive bands were visualized using Enhanced Chemiluminescence (ECL) (Pierce). For immunoprecipitation, cells were lysed in cytoplasmic buffer containing 1% NP-40, 2 mM CaCl<sub>2</sub>, and a protease inhibitor cocktail (Sigma). After a preclearing with protein A-Sepharose (Amersham Pharmacia Biotech), 1  $\mu\text{g}/\text{ml}$  annexin V or  $\beta_5$  integrin antibodies was added to the lysates. Two hours later, antibody complexes were isolated with 30  $\mu\text{l}$  of protein A-Sepharose and washed three times with lysis buffer before addition of loading buffer. Proteins were resolved on 4%–20% gradient SDS-PAGE gels, and annexin V was detected



by Western blot as described above.

## Protein Biochemistry and High-Pressure Liquid Chromatography

We used standard protocols for antigen purification by affinity chromatography (Dean et al. 1985 and Gilbert 1987). MDA-MB-435 cells were lysed in water, sonicated for 1 min, clarified by centrifugation ( $100,000 \times g$  for 1 hr), and treated with a protease inhibitor cocktail (Sigma). The supernate were loaded onto a 200 ml gel filtration Superdex 75 column (Pharmacia LKB Biotech) preequilibrated with 50 mM Tris (pH 7.5), 50 mM NaCl. One-milliliter fractions were collected and analyzed by Western blotting with purified IgG from serum raised against the VVISYSMPD peptide (and it was repeated for every purification stage). Fractions recognized by the anti-VVISYSMPD antibody from the gel filtration step were subjected to Mono-Q (HR 5/5) anion exchange high-pressure liquid chromatography (Pharmacia). The column was loaded with buffer A (10 mM Tris-HCl [pH 7.5]) and was eluted with a linear 0–0.5 M NaCl gradient, and 1 ml fractions were collected. Proteins in fractions positive for the anti-VVISYSMPD peptide were concentrated, separated on 4%–20% gradient SDS-PAGE gels (BioRad), and stained with colloidal Coomassie blue. The reactive bands were excised from the gel and digested with trypsin, essentially as described previously (Shevchenko et al., 1996). The resulting tryptic peptide mixtures were analyzed by microcolumn liquid chromatography-tandem mass spectrometry. The protein was determined to be human annexin V by peptide mass fingerprinting and a BLAST search of the GenPept database (<ftp://ftp.ncbi.nlm.nih.gov/genbank/genpept.fsa.gz>).

## In Vitro and In Vivo Neovascularization Assays

Matrigel (150  $\mu$ l per well; BD Pharmingen) was added to 24-well tissue culture plates and was allowed to solidify at 37°C for 10 min (Montesano et al., 1983). HUVECs were starved in basal EBM-2 media for 18–24 hr. Ten thousand cells were added to triplicate wells and allowed to settle onto Matrigel for 30 min at 37°C. The media were replaced by fresh complete EBM-2 media with or without peptide chimeras (12  $\mu$ M). The plates were photographed with an inverted microscope (Olympus) 24 hr later. In vivo neovascularization assays were carried out by injection of ice-cold Matrigel (250  $\mu$ l) containing VEGF (75 ng/ml) and bFGF (200 ng/ml) plus 12  $\mu$ M penetratin or Pen-VVISYSMPD subcutaneously into the flanks of athymic nude mice (Prewett et al., 1999). Five days later, each mouse was injected intravenously with 20  $\mu$ g FITC-lectin (Vector Laboratories). The plugs were harvested after 30 min and were homogenized in 500  $\mu$ l of RIPA buffer (1 $\times$  PBS, 1% nonidet-40, 0.5% sodium deoxycholate, and 0.1% sodium dodecyl sulfate).

Neovascularization was quantified fluorimetrically by measurement of the uptake of FITC-lectin into plugs (HTS 7000 plus, Bioassay reader, Perkin Elmer). Mice injected with FITC-lectin alone were used as controls to determine the fluorescence background. Data are shown after background subtraction.

## Acknowledgements

We thank Drs. Claudio Joazeiro, Dean Sheppard, and Kristiina Vuori for comments on the manuscript and reagents, and Drs. Carlos Caulin and Ricardo Giordano for helpful insights. This work was supported by a grant from the NCI (CA91134) to R.P. and CA90810 to W.A. and by the Gilson-Longenbaugh Foundation (to R.P. and W.A.). M.C.V. was supported by a predoctoral fellowship from the Department of Defense.



## References

- Andersen, M.H., Berglund, L., Petersen, T.E. and Rasmussen, J.T., 2002. Annexin-V binds to the intracellular part of the beta (5) integrin receptor subunit. *Biochem. Biophys. Res. Commun.* **292**, pp. 550–557.
- Aoudjit, F. and Vuori, K., 2001. Matrix attachment regulates Fas-induced apoptosis in endothelial cells: a role for c-flip and implications for anoikis. *J. Cell Biol.* **152**, pp. 633–643.
- Aplin, A.E. and Juliano, R.L., 2001. Regulation of nucleocytoplasmic trafficking by cell adhesion receptors and the cytoskeleton. *J. Cell Biol.* **155**, pp. 187–191.
- Aplin, A.E., Howe, A., Alahari, S.K. and Juliano, R.L., 1998. Signal transduction and signal modulation by cell adhesion receptors: the role of integrins, cadherins, immunoglobulin-cell adhesion molecules, and selectins. *Pharmacol. Rev.* **50**, pp. 197–263.
- Byzova, V.T., Goldman, K.C., Pampori, N., Thomas, A.K., Bett, A., Shattil, J.S. and Plow, F.E., 2000. A mechanism for modulation of cellular responses to VEGF: activation of the integrins. *Mol. Cell* **6**, pp. 6851–6860.
- Chen, Q., Kinch, M.S., Lin, T.H., Burrige, K. and Juliano, R.L., 1994. Integrin-mediated cell adhesion activates mitogen-activated protein kinases. *J. Biol. Chem.* **269**, pp. 26602–26605.
- Clark, E.A. and Brugge, J.S., 1995. Integrins and signal transduction pathways: the road taken. *Science* **268**, pp. 233–239.
- Clark, E.A. and Hynes, R.O., 1997. Keystone symposium on signal transduction by cell adhesion receptors. *Biochim. Biophys. Acta* **1333**, pp. R9–R16.
- Cookson, B.T., Engelhardt, S., Smith, C., Bamford, H.A., Prochazka, M. and Tait, J.F., 1994. Organization of the human annexin V (ANX5) gene. *Genomics* **20**, pp. 463–467.
- Dean, P.D.G., Johnson, W.S. and Middle, F.A., 1985. *Affinity Chromatography: A Practical Approach*, IRL Press, Arlington, VA.
- Derossi, D., Joliot, A.H., Chassaing, G. and Prochiantz, A., 1994. The third helix of the Antennapedia homeodomain translocates through biological membranes. *J. Biol. Chem.* **269**, pp. 10444–10450.
- Derossi, D., Chassaing, G. and Prochiantz, A., 1998. Trojan peptides: the penetratin system for intracellular delivery. *Trends Cell Biol.* **8**, pp. 84–87.
- Dubois, T., Oudinet, J.P., Russo-Marie, F. and Rothhut, B., 1995. In vivo and in vitro phosphorylation of annexin II in T cells: potential regulation by annexin V. *Biochem. J.* **310**, pp. 243–248.



- Dubois, T., Oudinet, J.P., Mira, J.P. and Russo-Marie, F., 1996. Annexins and protein kinases C. *Biochim. Biophys. Acta* **1313**, pp. 290–294.
- Dubois, T., Mira, J.P., Feliars, D., Solito, E., Russo-Marie, F. and Oudinet, J.P., 1998. Annexin V inhibits protein kinase C activity via a mechanism of phospholipid sequestration. *Biochem. J.* **330**, pp. 1277–1282.
- Eliceiri, B.P. and Cheresch, D.A., 2001. Adhesion events in angiogenesis. *Curr. Opin. Cell Biol.* **13**, pp. 563–568.
- Fadok, V.A., Voelker, D.R., Campbell, P.A., Cohen, J.J., Bratton, D.L. and Henson, P.M., 1992. Exposure of phosphatidylserine on the surface of apoptotic lymphocytes triggers specific recognition and removal by macrophages. *J. Immunol.* **148**, pp. 2207–2216.
- Farishian, R.A. and Whittaker, J.R., 1979. Tyrosine utilization by cultured melanoma cells: analysis of melanin biosynthesis using [<sup>14</sup>C] thiouracil. *Arch. Biochem. Biophys.* **198**, pp. 449–461.
- Filardo, E.J., Deming, S.L. and Cheresch, D.A., 1996. Regulation of cell migration by the integrin  $\beta$  subunit ectodomain. *J. Cell Sci.* **109**, pp. 1615–1622.
- Frisch, S.M. and Francis, H., 1994. Disruption of epithelial cell-matrix interactions induces apoptosis. *J. Cell Biol.* **124**, pp. 619–626.
- Frisch, S.M. and Ruoslahti, E., 1997. Integrins and anoikis. *Curr. Opin. Cell Biol.* **9**, pp. 701–716.
- Frisch, S.M. and Screaton, R.A., 2001. Anoikis mechanisms. *Curr. Opin. Cell Biol.* **13**, pp. 555–562.
- Giancotti, F.G. and Ruoslahti, E., 1999. Integrin signaling. *Science* **285**, pp. 1028–1032.
- Gilbert, M.T., 1987. *High Performance Liquid Chromatography*, John Wright-PSG, Littleton, MA.
- Giordano, R.J., Cardó-Vila, M., Lahdenranta, J., Pasqualini, R. and Arap, W., 2001. Biopanning and rapid analysis of selective interactive ligands. *Nat. Med.* **7**, pp. 1249–1253.
- Howe, A., Aplin, A.E., Alahari, S.K. and Juliano, R.L., 1998. Integrin signaling and cell growth control. *Curr. Opin. Cell Biol.* **10**, pp. 220–231.
- Howe, A.K., Aplin, A.E. and Juliano, R.L., 2002. Anchorage-dependent ERK signaling-mechanisms and consequences. *Curr. Opin. Genet. Dev.* **12**, pp. 30–35.
- Huang, X., Griffiths, M., Wu, J., Farese Jr., R.V. and Sheppard, D., 2000. Normal development, wound healing, and adenovirus susceptibility in beta5-deficient mice. *Mol. Cell. Biol.* **20**, pp. 755–759.
- Hynes, R.O., 1992. Integrins: versatility, modulation and signaling in cell adhesion. *Cell* **69**, pp. 11–25.



Hynes, R.O., 1999. Cell adhesion: old and new questions. *Trends Cell Biol.* **9**, pp. M33–M37.

Klemke, R.L., Yebra, M., Bayna, E.M. and Cheresch, D.A., 1994. Receptor tyrosine kinase signaling required for integrin alpha v beta 5-directed cell motility but not adhesion on vitronectin. *J. Cell Biol.* **127**, pp. 859–866.

Koivunen, E., Gay, D.A. and Ruoslahti, E., 1993. Selection of peptides binding to the alpha 5 beta 1 integrin from phage display library. *J. Biol. Chem.* **268**, pp. 20205–20210.

Koivunen, E., Wang, B. and Ruoslahti, E., 1995. Phage libraries displaying cyclic peptides with different ring sizes: ligand specificities of the RGD-directed integrins. *Biotechnology (NY)* **13**, pp. 265–270.

Koivunen, E., Restel, B.H., Rajotte, D., Lahdenranta, J., Hagedorn, M., Arap, W. and Pasqualini, R., 1999. Integrin-binding peptides derived from phage display libraries. *Methods Mol. Biol.* **129**, pp. 3–17.

Kolonin, M., Pasqualini, R. and Arap, W., 2001. Molecular addresses in blood vessels as targets for therapy. *Curr. Opin. Chem. Biol.* **5**, pp. 308–313.

Lewis, J.M., Cheresch, D.A. and Schwartz, M.A., 1996. Protein kinase C regulates alpha v beta 5-dependent cytoskeletal associations and focal adhesion kinase phosphorylation. *J. Cell Biol.* **134**, pp. 1323–1332.

Liu, S., Calderwood, D.A. and Ginsberg, M.H., 2000. Integrin cytoplasmic domain-binding proteins. *J. Cell Sci.* **113**, pp. 3563–3571.

Meredith Jr., J., Mu, Z., Saido, T. and Du, X., 1998. Cleavage of the cytoplasmic domain of the integrin beta3 subunit during endothelial cell apoptosis. *J. Biol. Chem.* **273**, pp. 19525–19531.

Mira, J.P., Dubois, T., Oudinet, J.P., Lukowski, S., Russo-Marie, F. and Geny, B., 1997. Inhibition of cytosolic phospholipase A2 by annexin V in differentiated permeabilized HL-60 cells. Evidence of crucial importance of domain I type II Ca<sup>2+</sup>-binding site in the mechanism of inhibition. *J. Biol. Chem.* **272**, pp. 10474–10482.

Montesano, R., Orci, L. and Vassalli, P., 1983. In vitro rapid organization of endothelial cells into capillary-like networks is promoted by collagen matrices. *J. Cell Biol.* **97**, pp. 1648–1652.

Mosmann, T., 1983. Rapid colorimetric assay for cellular growth and survival: application to proliferation and cytotoxicity assays. *J. Immunol. Methods* **65**, pp. 55–63.

Nakamura, S. and Nishizuka, Y., 1994. Lipid mediators and protein kinase C activation for the intracellular signaling network. *J. Biochem. (Tokyo)* **115**, pp. 1029–1034.

Park, J.E., Lenter, M.C., Zimmermann, R.N., Garin-Chesa, P., Old, L.J. and Rettig, W.J., 1999. Fibroblast activation protein, a dual specificity serine protease expressed in reactive human tumor stromal fibroblasts. *J. Biol. Chem.* **274**, pp. 36505–36512.



Pasqualini, R. and Hemler, M.E., 1994. Contrasting roles for integrin beta 1 and beta 5 cytoplasmic domains in subcellular localization, cell proliferation, and cell migration. *J. Cell Biol.* **125**, pp. 447–460.

Pasqualini, R., Bodorova, J., Ye, S. and Hemler, M.E., 1993. A study of the structure, function and distribution of beta 5 integrins using novel anti-beta 5 monoclonal antibodies. *J. Cell Sci.* **105**, pp. 101–111.

Pasqualini, R., Koivunen, E. and Ruoslahti, E., 1997.  $\alpha_v$  integrins as receptors for tumor targeting by circulating ligands. *Nat. Biotechnol.* **15**, pp. 542–546.

Prewett, M., Huber, J., Li, Y., Santiago, A., O'Connor, W., King, K., Overholser, J., Hooper, A., Pytowski, B., Witte, L. *et al.*, 1999. Antivascular endothelial growth factor receptor (fetal liver kinase 1) monoclonal antibody inhibits tumor angiogenesis and growth of several mouse and human tumors. *Cancer Res.* **59**, pp. 5209–5218.

Raynal, P., Hullin, F., Ragab-Thomas, J.M., Fauvel, J. and Chap, H., 1993. Annexin 5 as a potential regulator of annexin 1 phosphorylation by protein kinase C. In vitro inhibition compared with quantitative data on annexin distribution in human endothelial cells. *Biochem. J.* **292**, pp. 759–765.

Reed, J.C., 2002. Apoptosis-based therapies. *Nat. Rev. Drug Discov.* **1**, pp. 111–121.

Rothhut, B., Dubois, T., Feliars, D., Russo-Marie, F. and Oudinet, J.P., 1995. Inhibitory effect of annexin V on protein kinase C activity in mesangial cell lysates. *Eur. J. Biochem.* **232**, pp. 865–872.

Schlaepfer, D.D. and Hunter, T., 1998. Integrin signalling and tyrosine phosphorylation: just the FAKs?. *Trends Cell Biol.* **8**, pp. 151–157.

Schlaepfer, D.D., Jones, J. and Haigler, H.T., 1992. Inhibition of protein kinase C by annexin V. *Biochemistry* **31**, pp. 1886–1891.

Schwartz, M.A., Schaller, M.D. and Ginsberg, M.H., 1995. Integrins: emerging paradigms of signal transduction. *Annu. Rev. Cell Dev. Biol.* **11**, pp. 549–599.

Shattil, S.J. and Ginsberg, M.H., 1997. Perspectives series: cell adhesion in vascular biology. Integrin signaling in vascular biology. *J. Clin. Invest.* **100**, pp. 1–5.

Shevchenko, A., Wilm, M., Vorm, O. and Mann, M., 1996. Mass spectrometric sequencing of proteins silver-stained polyacrylamide gels. *Anal. Chem.* **68**, pp. 850–858.

Smith, G.P. and Scott, J.K., 1993. Libraries of peptides and proteins displayed on filamentous phage. *Methods Enzymol.* **217**, pp. 228–257.

Sopkova, J., Renouard, M. and Lewit-Bentley, A., 1993. The crystal structure of a new high-calcium form of annexin V. *J. Mol. Biol.* **234**, pp. 816–825.

Stupack, D.G., Puente, X.S., Boutsaboualoy, S., Storgard, C.M. and Cheresch, D.A., 2001. Apoptosis of adherent cells by recruitment of caspase-8 to unligated integrins. *J. Cell Biol.*



155, pp. 459–470.

Tang, S., Gao, Y. and Ware, J.A., 1999. Enhancement of endothelial cell migration and in vitro tube formation by TAP20, a novel beta 5 integrin-modulating, PKC theta-dependent protein. *J. Cell Biol.* **147**, pp. 1073–1084.

Theodore, L., Derossi, D., Chassaing, G., Llirbat, B., Kubes, M., Jordan, P., Chneiweiss, H., Godement, P. and Prochiantz, A., 1995. Intraneuronal delivery of protein kinase C pseudosubstrate leads to growth cone collapse. *J. Neurosci.* **15**, pp. 7158–7167.


Thomas, L., Chan, P.W., Chang, S. and Damsky, C., 1993. 5-Bromo-2-deoxyuridine regulates invasiveness and expression of integrins and matrix-degrading proteinases in a differentiated hamster melanoma cell. *J. Cell Sci.* **105**, pp. 191–201.

Vuori, K. and Ruoslahti, E., 1993. Activation of protein kinase C precedes alpha 5 beta 1 integrin-mediated cell spreading on fibronectin. *J. Biol. Chem.* **268**, pp. 21459–21462.

Zetter, B.R., 1997. On target with tumor blood vessel markers. *Nat. Biotechnol.* **15**, pp. 1243–1244.

Zhu, D.M., Narla, R.K., Fang, W.H., Chia, N.C. and Uckun, F.M., 1998. Calphostin C triggers calcium-dependent apoptosis in human acute lymphoblastic leukemia cells. *Clin. Cancer Res.* **4**, pp. 2967–2976.

---

 Corresponding author. Correspondence: Renata Pasqualini, (713) 792-3873 (phone), (713) 745-2999 (fax)

---

## Molecular Cell

Volume 11, Issue 5 , May 2003, Pages 1151-1162

### This Document

- [SummaryPlus](#)
- ▶ **Full Text + Links**
  - [Full Size Images](#)
  - [PDF \(811 K\)](#)

### Actions

- [E-mail Article](#)

---

[Home](#)
[Journals](#)
[Books](#)
[Abstract Databases](#)
[My Profile](#)
[Alerts](#)
[? Help](#)

[Feedback](#) | [Terms & Conditions](#) | [Privacy Policy](#)

Copyright © 2005 Elsevier B.V. All rights reserved. ScienceDirect® is a registered trademark of Elsevier B.V.



# Steps toward mapping the human vasculature by phage display

WADIH ARAP<sup>1,2</sup>, MIKHAIL G. KOLONIN<sup>1</sup>, MARTIN TREPEL<sup>1</sup>, JOHANNA LAHDENRANTA<sup>1</sup>,  
MARINA CARDÓ-VILA<sup>1</sup>, RICARDO J. GIORDANO<sup>1</sup>, PAUL J. MINTZ<sup>1</sup>, PETER U. ARDELT<sup>1</sup>,  
VIRGINIA J. YAO<sup>1</sup>, CLAUDIA I. VIDAL<sup>1</sup>, LIMOR CHEN<sup>1</sup>, ANNE FLAMM<sup>3</sup>,  
HELI VALTANEN<sup>9</sup>, LISA M. WEAVIND<sup>5</sup>, MARSHALL E. HICKS<sup>6</sup>, RAPHAEL E. POLLOCK<sup>7</sup>,  
GREGORY H. BOTZ<sup>5</sup>, CORAZON D. BUCANA<sup>2</sup>, ERKKI KOIVUNEN<sup>9</sup>, DOLORES CAHILL<sup>10</sup>,  
PATRICIA TRONCOSO<sup>8</sup>, KEITH A. BAGGERLY<sup>4</sup>, REBECCA D. PENTZ<sup>3</sup>, KIM-ANH DO<sup>1</sup>,  
CHRISTOPHER J. LOGOTHETIS<sup>1</sup> & RENATA PASQUALINI<sup>1,2</sup>

Departments of <sup>1</sup>Genito-Urinary Medical Oncology, <sup>2</sup>Cancer Biology, <sup>3</sup>Clinical Ethics, <sup>4</sup>Biostatistics, <sup>5</sup>Critical Care,  
<sup>6</sup>Diagnostic Radiology, <sup>7</sup>Surgical Oncology and <sup>8</sup>Pathology,

The University of Texas M.D. Anderson Cancer Center, Houston, Texas, USA

<sup>9</sup>Department of Biosciences, Division of Biochemistry, University of Helsinki, Helsinki, Finland

<sup>10</sup>Max Planck Institute of Molecular Genetics, Berlin, Germany

M.G.K. and M.T. contributed equally to this study.

Correspondence should be addressed to W.A.; email: warap@notes.mdacc.tmc.edu,  
or R.P.; email: rpassqual@notes.mdacc.tmc.edu

The molecular diversity of receptors in human blood vessels remains largely unexplored. We developed a selection method in which peptides that home to specific vascular beds are identified after administration of a peptide library. Here we report the first *in vivo* screening of a peptide library in a patient. We surveyed 47,160 motifs that localized to different organs. This large-scale screening indicates that the tissue distribution of circulating peptides is nonrandom. High-throughput analysis of the motifs revealed similarities to ligands for differentially expressed cell-surface proteins, and a candidate ligand–receptor pair was validated. These data represent a step toward the construction of a molecular map of human vasculature and may have broad implications for the development of targeted therapies.

Despite major progress brought about by the Human Genome Project<sup>1,2</sup>, the molecular diversity of blood vessels has just begun to be uncovered. Many therapeutic targets may be expressed in very restricted but highly specific and accessible locations in the vascular endothelium. Thus potential targets for intervention may be overlooked in high-throughput DNA sequencing or in gene arrays because these approaches do not generally take into account cellular location and anatomical and functional context.

We developed an *in vivo* selection method in which peptides that home to specific vascular beds are selected after intravenous administration of a phage-display random peptide library<sup>3</sup>. This strategy revealed a vascular address system that allows tissue-specific targeting of normal blood vessels<sup>4,5</sup> and angiogenesis-related targeting of tumor blood vessels<sup>6–10</sup>. Although the biological basis for such vascular heterogeneity remains unknown, several peptides selected by homing to blood vessels in mouse models have been used by several groups as carriers to guide the delivery of cytotoxic drugs<sup>9</sup>, proapoptotic peptides<sup>6</sup>, metalloprotease inhibitors<sup>7</sup>, cytokines<sup>11</sup>, fluorophores<sup>12</sup> and genes<sup>13</sup>. Generally, coupling to homing peptides yields targeted compounds that are more effective and less toxic than the parental compound<sup>6,9,11</sup>. Moreover, vascular receptors corresponding to the selected peptides have been identified in blood vessels of normal organs<sup>14</sup> and in tumor blood vessels<sup>15,16</sup>. Together, these results show that it is possible

to develop therapeutic strategies based on selective expression of vascular receptors<sup>17</sup>.

Although certain ligands and receptors isolated in mouse models have been useful to identify putative human homologs<sup>10,15</sup>, it is unlikely that targeted delivery will always be achieved in humans using mouse-derived probes. Data from the Human Genome Project indicate that the higher complexity of the human species relative to other mammalian species derives from expression patterns of proteins at different tissue sites, levels or times rather than from a greater number of genes<sup>1,2</sup>. In fact, several examples of species-specific differences in gene expression within the human vascular network have recently surfaced. The divergence in the expression patterns of the prostate-specific membrane antigen (PSMA) between human and mouse illustrates such species specificity. Selective expression of PSMA occurs in the human prostate, but not in the mouse prostate; instead, the mouse homolog of PSMA is expressed in the brain and kidney<sup>18</sup>. Additionally, PSMA is a marker of endothelial cells of tumor blood vessels in humans<sup>19</sup>, whereas the mouse homolog of PSMA is undetectable in tumor-associated neovasculature in the mouse (W.D. Heston, pers. comm.). Another example of such divergence is the *TEM7* gene, which is highly expressed in a selective manner in the endothelium of human colorectal adenomas<sup>20</sup>. By contrast, mouse *Tem7* is expressed not in tumor blood vessels but in Purkinje cells instead<sup>21</sup>. Thus, striking species-specific differ-



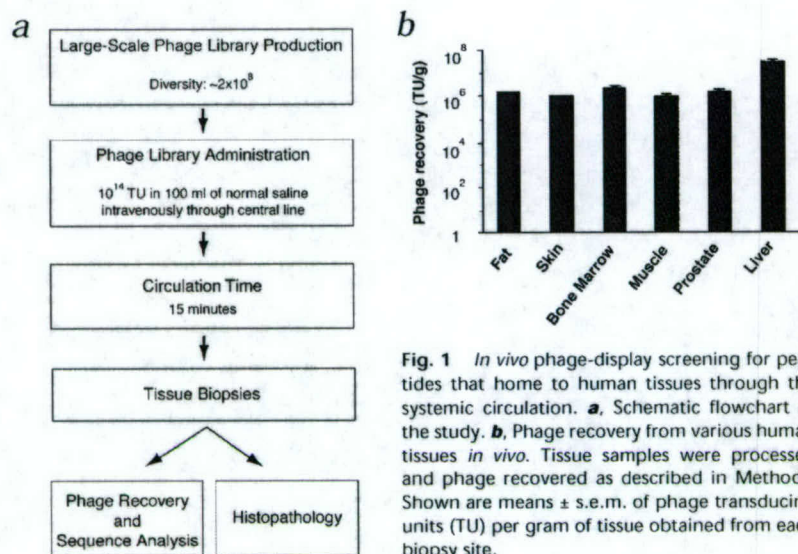


**Fig. 1** *In vivo* phage-display screening for peptides that home to human tissues through the systemic circulation. **a**, Schematic flowchart of the study. **b**, Phage recovery from various human tissues *in vivo*. Tissue samples were processed and phage recovered as described in Methods. Shown are means  $\pm$  s.e.m. of phage transducing units (TU) per gram of tissue obtained from each biopsy site.

ences in protein expression and ligand–receptor accessibility dictates that vascular targeting data obtained in animal models must be carefully evaluated before extrapolating to human studies.

#### Screening phage-display libraries in humans

We reasoned that *in vivo* selection of phage-display random peptide libraries in humans would advance the identification of human vascular targeting probes and facilitate development of targeted delivery of therapeutic and imaging agents to the vasculature. This study reports the initial step toward developing an *in vivo* phage display-based, ligand–receptor map of human blood vessels.

A large-scale preparation of a phage random peptide library containing the insert CX<sub>7</sub>C (C, cysteine; X, any amino-acid residue) and designed to display a constrained cyclic loop within the pIII capsid protein was optimized to create the highest possible insert diversity<sup>3</sup>. The diversity of the library was approximately  $2 \times 10^8$  and its final titer was approximately  $1 \times 10^{12}$  transducing units (TU) per ml.

A patient (see Methods) received an intravenous infusion of the unselected random phage library, and 15 min after infusion tissue biopsies were obtained to provide histopathological diagnosis and to recover phage from various organs (Fig. 1a).

Here we demonstrate the feasibility of producing phage-display random peptide libraries on a very large scale and of selecting phage clones that home to different human organs *in vivo* through the systemic circulation (Fig. 1b).

#### High-throughput analysis of selected peptides

To analyze the distribution of inserts from the random peptide library, we designed a high-throughput pattern recognition software to analyze short amino-acid residue sequences. This automated program allowed surveillance of peptide inserts recovered from the phage library screening.

Based on SAS (version 8; SAS Institute) and Perl (version 5.0), the program conducts an exhaustive amino-acid residue sequence count and keeps track of the relative frequencies of *n*

distinct tripeptide motifs representing all possible  $n_3$  overlapping tripeptide motifs in both directions ( $n \ll n_3$ ). This analysis was applied for phage recovered from each target tissue and for the unselected CX<sub>7</sub>C random phage-display peptide library. Counts were recorded for all overlapping interior tripeptide motifs, subject only to reflection and single-voting restrictions. No peptide was allowed to contribute more than once for a single tripeptide motif (or a reversed tripeptide motif). Tripeptide motifs in both directions are chemically nonsymmetrical and not necessarily equivalent. However, because we often recovered forward and reverse tripeptides recognizing the same receptor by *in vivo* phage display, we chose to take reflection into account, with the understanding that this is not a general feature that is applicable to every ligand–receptor pair interaction. Each peptide contributed five tripeptide motifs. Tripeptide motif counts were conditioned on the total number for all motifs being

held fixed within a tissue. The significance of association of a given allocation of counts was assessed by the Fisher's exact test (one-tailed). Results were considered statistically significant at  $P < 0.05$ . In summary, to test for randomness of distribution, we compared the relative frequencies of a particular tripeptide motif from each target to those of the motifs from the unselected library; such an approach is intrinsically a large-scale contingency table association test.

#### Distribution of tripeptide motifs *in vivo*

To determine the distribution of the peptide inserts homing to specific sites after intravenous administration, we compared the relative frequencies of every tripeptide motif from each target tissue to those from the unselected library. We analyzed 4,716 phage inserts recovered from representative samples of five tissues (bone marrow, fat, skeletal muscle, prostate and skin) and from the unselected library. Tripeptide motifs were chosen for the phage insert analysis because three amino-acid residues seem to provide the minimal framework for structural formation and protein–protein interaction<sup>22</sup>. Examples of such biochemical recognition units and binding of ligand motifs to their receptors include RGD, LDV and LLG to integrins<sup>23,24</sup>, NGR to aminopeptidase N/CD13 (refs 11,15) and GFE to membrane dipeptidase<sup>4,14</sup>. Each phage insert analyzed contained seven amino-acid residues and contributed five potential tripeptide motifs; thus, counting both peptide orientations, a total of 47,160 tripeptide motifs were surveyed.

Comparisons of the motif frequencies in a given organ relative to those frequencies in the unselected library demonstrate the nonrandom nature of the peptide distribution (Table 1); such a bias is particularly noteworthy given that only a single round of *in vivo* screening was performed. Of the tripeptide motifs selected from tissues, some were preferentially recovered in a single site whereas others were recovered from multiple sites. These data are consistent with some peptides homing in a tissue-specific manner and others targeting several tissues. We next adapted the ClustalW software from



the European Molecular Biology Laboratory<sup>25</sup> to analyze the original cyclic phage peptide inserts of seven amino-acid residues containing the tripeptide motifs. This analysis revealed four to six amino-acid residue motifs that were shared among multiple peptides isolated from a given organ (Fig. 2). We searched for each of these motifs in online databases (through the National Center for Biotechnology Information (NCBI; <http://www.ncbi.nlm.nih.gov/BLAST/>) and found that some appeared within known human proteins. Phage-display technology is suitable for targeting several classes of molecules (adhesion receptors, proteases, proteoglycans or growth factor receptors). Based on extensive work performed in murine models, the *in vivo* selection system seems to favor the isolation of peptides that recognize receptors that are selectively expressed in specific organs or tissues<sup>17</sup>. As our motifs are likely to represent sequences present in circulating ligands (either secreted proteins or surface receptors expressed on circulating cells) that home to vascular receptors, we compiled a panel of candidate human proteins potentially mimicked by selected peptide motifs (Table 2).

**Table 1** Peptide motifs isolated by *in vivo* phage display screening

Target organ and motif	Motif frequency (%)	P value
Unselected library		
None	NA	NA
Bone marrow		
GGG*	2.3	0.0350
GFS*	1.0	0.0350
LWS*	1.0	0.0453
ARL	1.0	0.0453
FGG	1.1	0.0453
GVL	2.3	0.0137
SGT	1.1	0.0244
Fat		
EGG*	1.3	0.0400
LLV*	1.0	0.0269
LSP*	0.9	0.0402
EGR	1.1	0.0180
FGV	0.9	0.0402
Muscle		
LVS*	2.1	0.0036
GER	0.9	0.0036
Prostate		
AGG*	2.5	0.0340
EGR	1.0	0.0340
GER	0.9	0.0382
GVL	2.3	0.0079
Skin		
GRR*	2.9	0.0047
GGH*	0.9	0.0341
GTV*	0.8	0.0497
ARL	0.8	0.0497
FGG	1.3	0.0076
FGV	1.0	0.0234
SGT	1.0	0.0234

Peptide motifs isolated by *in vivo* phage display screening. Motifs occurring in peptides isolated from target organs but not from the unselected phage library (Fisher's exact test, one-tailed;  $P < 0.05$ ). Number of peptide sequences analyzed per organ: unselected library, 446; bone marrow, 521; fat, 901; muscle, 850; prostate, 1,018; skin, 980. \*, Motifs enriched only in a single tissue. Motif frequencies represent the prevalence of each tripeptide divided by the total number of tripeptides analyzed in the organ.

### Validation of candidate ligands

It is tempting to speculate on a few biologically relevant homology hits. For example, a peptide contained within bone morphogenetic protein 3B (BMP-3B) was recovered from bone marrow. BMP-3B is a growth factor known to regulate bone development<sup>26</sup>. Thus, this protein may be mimicked by the isolated ligand homing to that tissue. We also isolated from the prostate a potential mimotope of interleukin 11 (IL-11), which has been previously shown to interact with receptors within endothelium and prostate epithelium<sup>27,28</sup>. In addition to secreted ligands, motifs were also found in several extracellular or transmembrane proteins that may operate selectively in the target tissue, such as sortilin in fat<sup>29</sup>. We have also recovered motifs from multiple organs; one such peptide is a candidate mimic peptide of perlecan, a protein known to maintain vascular homeostasis<sup>30</sup>.

To test the tissue specificity of the peptides selected, we developed a phage-overlay assay for tissue sections. Because of the availability and well-characterized interaction between the candidate ligand (IL-11) and its receptor (IL-11R $\alpha$ ), we chose the motif RRAGGS, a peptide mimic of IL-11 (Table 2), for validation. We show by phage overlay on human tissue sections (see Methods) that a prostate-homing phage displaying an IL-11 peptide mimic specifically bound to the endothelium and to the epithelium of normal prostate (Fig. 3a), but not to control organs, such as skin (Fig. 3b). In contrast, a phage selected from the skin (displaying the motif HGGVG; Table 2), did not bind to prostate tissue (Fig. 3c); however, this phage specifically recognized blood vessels in the skin (Fig. 3d). Moreover, the immunostaining pattern obtained with an antibody against human IL-11R $\alpha$  on normal prostate tissue (Fig. 3e) is undistinguishable from that of the CGRRAGGSC-displaying phage overlay (Fig. 3a); a control antibody showed no staining in prostate tissue (Fig. 3f). These findings were recapitulated in multiple tissue sections obtained from several different patients.

Finally, using a ligand-receptor binding assay *in vitro*, we demonstrate the interaction of the CGRRAGGSC-displaying phage with immobilized IL-11R $\alpha$  at the protein-protein level (Fig. 4a). Such binding is specific because it was inhibited by the native IL-11 ligand in a concentration-dependent manner (Fig. 4b). Preliminary results indicate that serum IL-11 is elevated in a subset of prostate cancer patients (C.J.L., unpublished observations) and that the expression of IL-11R $\alpha$  in tumors is upregulated in some cases of human prostate cancer (M.G.K., unpublished observations); these data may have clinical relevance.

### Discussion

Aside from *in vivo* phage display, use of methods such as serial analysis of gene expression (SAGE) clearly shows that the genetic progression of malignant cells is paralleled by epigenetic changes in nonmalignant endothelial cells induced by angiogenesis of the tumor vasculature<sup>20</sup>. Because SAGE is based on differential expression levels of transcripts, it fails to address functional interactions (for example, binding) at the protein-protein level. The complexity of the human endothelium is also apparent from recent studies showing that the profile of certain endothelial cell receptors can vary depending on ethnic background<sup>31</sup>. In fact, *in vivo* phage-display in humans might reveal diversity of receptors expressed in the blood vessels even at the level of individual patients.



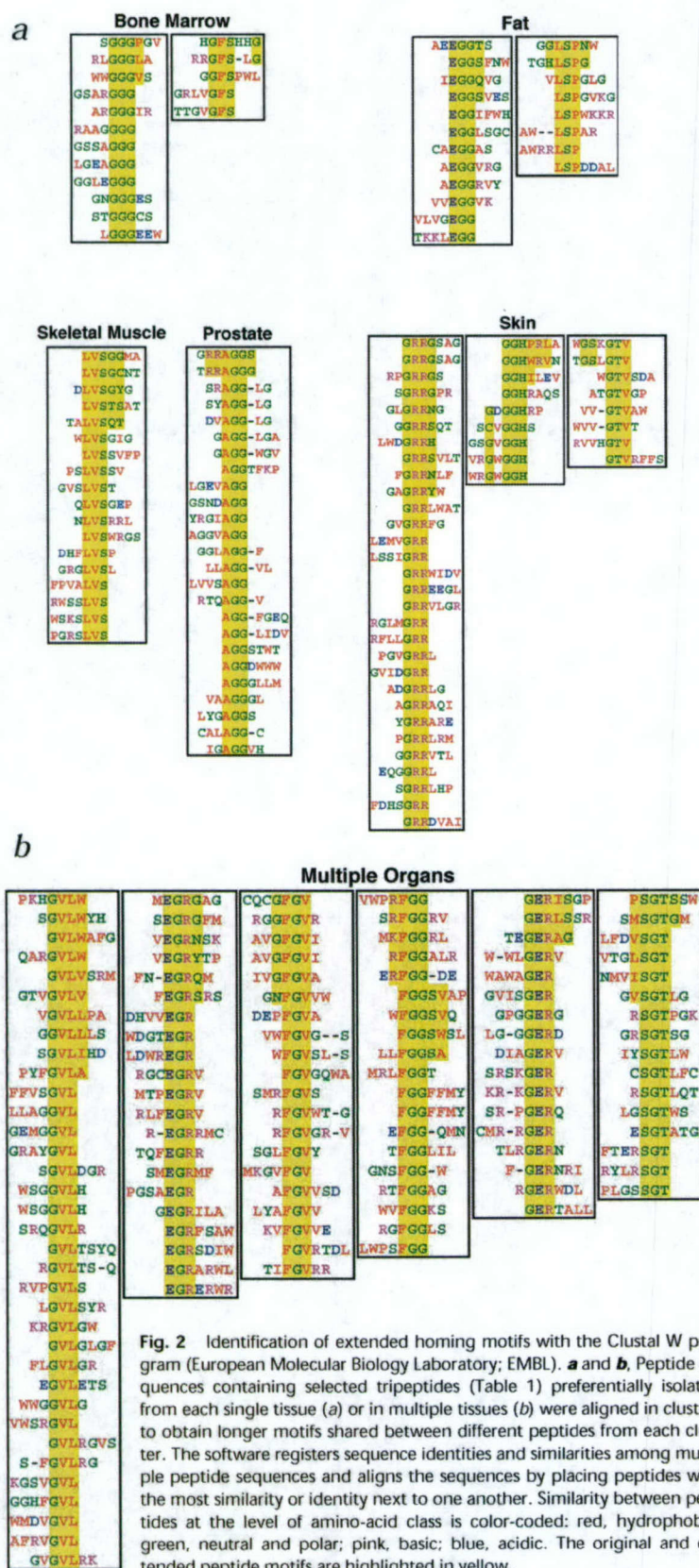


**Fig. 2** Identification of extended homing motifs with the Clustal W program (European Molecular Biology Laboratory; EMBL). **a** and **b**, Peptide sequences containing selected tripeptides (Table 1) preferentially isolated from each single tissue (**a**) or in multiple tissues (**b**) were aligned in clusters to obtain longer motifs shared between different peptides from each cluster. The software registers sequence identities and similarities among multiple peptide sequences and aligns the sequences by placing peptides with the most similarity or identity next to one another. Similarity between peptides at the level of amino-acid class is color-coded: red, hydrophobic; green, neutral and polar; pink, basic; blue, acidic. The original and extended peptide motifs are highlighted in yellow.

However, our validation studies show that at least some ligand-receptor pairs are detectable in multiple unrelated subjects. Another advantage of the method described here is that selected targeting peptides bind to native receptors as they are expressed *in vivo*. Even if a ligand-receptor interaction is mediated through a conformational rather than a linear epitope, it is possible to select binders in the screening. Furthermore, it is often difficult to ensure that proteins expressed in array systems maintain the correct structure and folding. Thus, peptides selected *in vivo* may be more suitable to clinical applications.

Precedent exists to suggest that phage can be safely administered to patients, as bacteriophage were used in humans during the pre-antibiotic era<sup>32</sup>. Ultimately, it may become possible to determine molecular profiles of blood vessels in specific conditions; infusing phage libraries systemically before resections of lung, prostate, breast and colorectal carcinomas, or even regionally before resection of limb sarcomas may yield useful vascular targets. Exploiting this experimental paradigm systematically with the analytical tools developed here may permit the construction of a molecular map outlining vascular diversity in each human organ, tissue or disease. Translation of high-throughput *in vivo* phage-display technology may provide a contextual and functional link between genomics and proteomics. Based on the therapeutic promise of peptide- or peptidomimetic-targeting probes<sup>33</sup>, clinical applications are likely to follow.

## Methods

**Patient selection and clinical course.** A 48-y-old male Caucasian patient was diagnosed with Waldenström macroglobulinemia (a B-cell malignancy) and previously treated by splenectomy, systemic chemotherapy (fludarabine, mitoxantrone and dexamethasone) and immunotherapy (anti-CD20 monoclonal antibody). In the few months preceding his admission, the disease became refractory to treatment and clinical progression with retroperitoneal lymphadenopathy, pancytopenia and marked bone marrow infiltration by tumor cells occurred. The patient was admitted with massive intracranial bleeding secondary to thrombocytopenia. Despite prompt craniotomy and surgical evacuation of a cerebral hematoma, the patient remained comatose with progressive and irreversible loss of brainstem function until the patient met the formal criteria for brain-based determination of death<sup>34</sup>; such determination was carried out by an independent clinical neurologist not involved in the project. Because of his advanced cancer, the patient was considered and rejected as transplant organ donor. After surrogate written informed consent was obtained from the legal next of kin, the patient was enrolled in the clinical study. Disconnection of the patient from life-support systems followed the pro-



Table 2 Examples of candidate human proteins mimicked by selected peptide motifs

Extended motif *	Human protein containing the motif	Protein description	Accession number
<i>Bone marrow</i>			
PGGG	Bone morphogenetic protein 3B	Growth factor, TGF- $\beta$ family member	NP_004953
PGGG	Fibulin 3	Fibrillin- and EGF-like	Q12805
GHHSFG	Microsialin	Macrophage antigen, glycoprotein	NP_001242
<i>Fat</i>			
EGGT	LTBP-2	Fibrillin- and EGF-like, TGF- $\beta$ Interactor	CAA86030
TGGE	Sortilin	Adipocyte differentiation-induced receptor	CAA66904
GPSLH	Protocadherin gamma C3	Cell adhesion	AAD43784
<i>Muscle</i>			
GGSVL	ICAM-1	Intercellular adhesion molecule	P05362
LVSGY	Flt4	Endothelial growth factor receptor	CAA48290
<i>Prostate</i>			
RRAGGS	Interleukin 11	Cytokine	NP_000632
RRAGG	Smad6	Smad family member	AAB94137
<i>Skin</i>			
GRRG	TGF- $\beta$ 1	Growth factor, TGF- $\beta$ family member	XP_008912
HGG+G	Neuropilin-1	Endothelial growth factor receptor	AAF44344
+PHGG	Pentaxin	Infection/trauma-induced glycoprotein	CAA45158
PHGG	Macrophage-inhibitory cytokine-1	Growth factor, TGF- $\beta$ family member	AAB88673
+PHGG	Desmoglein 2	Epithelial cell junction protein	S38673
VTG+SG	Desmoglein 1	Epidermal cell junction protein	AAC83817
<i>Multiple organs</i>			
EGRG	MMP-9	Gelatinase	AAH06093
GRGE	ESM-1	Endothelial cell-specific molecule	XP_003781
NFGVV	CDO	Surface glycoprotein, Ig- and fibronectin-like	NP_058648
GERIS	BPA1	Basement membrane protein	NP_001714
SIREG	Wnt-16	Glycoprotein	Q9UBV4
+GVLW	Sialoadhesin	Ig-like lectin	AAK00757
WLVG+	IL-5 receptor	Soluble interleukin 5 receptor	CAA44081
GGFR	Plectin 1	Endothelial focal junction-localized protein	CAA91196
GGFF	TRANCE	Cytokine, TNF family member	AAC51762
+SGGF	MEGF8	EGF-like protein	T00209
PSGTS	ICAM-4	Intercellular adhesion glycoprotein	Q14773
+TGSP	Perlecan	Vascular repair heparan sulfate proteoglycan	XP_001825

For similarity searches, tripeptide motif-containing peptides (in either orientation) selected by *in vivo* phage display screening were used. \*Extended motifs containing at least 4–6 amino acid residues (Fig. 2) were analyzed using BLAST (NCBI) to search for similarity to known human proteins. Examples of candidate proteins potentially mimicked by the peptides selected in the *in vivo* screening are listed. Sequences correspond to the regions of 100% identity between the peptide selected and the candidate protein. Conserved amino acid substitutions are indicated as (+). Tripeptides shown in Table 1 are highlighted. TGF, transforming growth factor; TNF, tumor necrosis factor.

cedure. This study strictly adheres to current medical ethics recommendations and guidelines regarding human research<sup>35</sup>, and it has been reviewed and approved by the Clinical Ethics Service, the Institutional Biohazard Committee, Clinical Research Committee and the Institutional Review Board of the University of Texas M.D. Anderson Cancer Center.

The University of Texas and researchers (W.A. and R.P.) have equity in NTTX Biotechnology, which is subjected to certain restrictions under university policy; the university manages the terms of these arrangements in accordance to its conflict-of-interest policies.

***In vivo* phage display.** Short-term intravenous infusion of the phage library (a total dose of  $1 \times 10^{14}$  phage TU suspended in 100 ml of saline) into the patient was followed by multiple representative tissue biopsies. Prostate and liver samples were obtained by needle biopsy under ultrasonographic guidance; skin, fat-tissue and skeletal-muscle samples were

obtained by a surgical excision. Bone-marrow needle aspirates and core biopsy samples were also obtained. Histopathological diagnosis was determined by examination of frozen sections processed from tissues obtained at the bedside. Triplicate samples were processed for host bacterial infection, phage recovery and histopathological analysis. In brief, tissues were weighed, ground with a glass Dounce homogenizer, suspended in 1 ml of DMEM containing proteinase inhibitors (DMEM-prin; 1 mM phenylmethylsulfonyl fluoride (PMSF), 20  $\mu$ g/ml aprotinin, and 1  $\mu$ g/ml leupeptin), vortexed, and washed three times with DMEM-prin. Next, human tissue homogenates were incubated with 1 ml of host bacteria (log phase *Escherichia coli* K91kan; OD<sub>600</sub>  $\approx$  2). Aliquots of the bacterial culture were plated onto Luria-Bertani agar plates containing 40  $\mu$ g/ml tetracycline and 100  $\mu$ g/ml of kanamycin. Plates were incubated overnight at 37 °C. Bacterial colonies were processed for sequencing of phage inserts recovered from each tissue and from unselected phage library. Human samples were handled with universal blood and body fluid precautions.



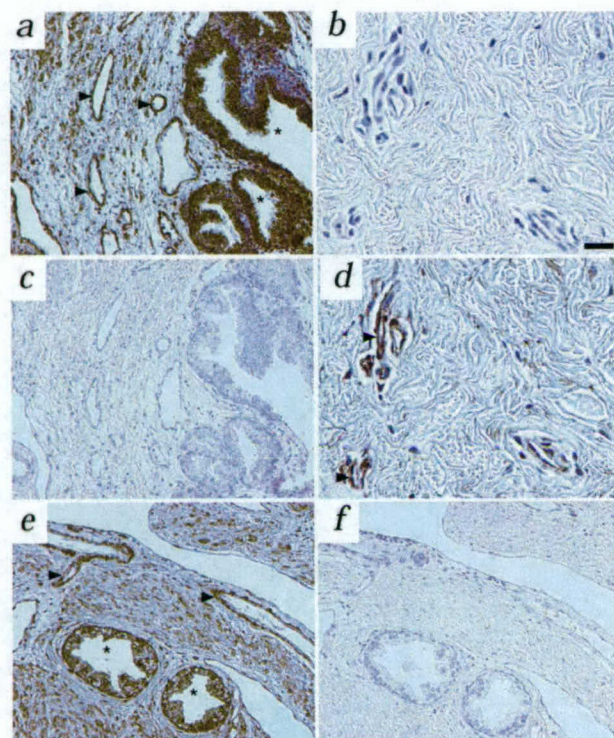


**Fig. 3** Validation of the candidate receptor–ligand pairs resulting from the *in vivo* selection. **a–f**, Phage clones isolated from prostate and from skin were evaluated for binding to human tissues in an overlay assay. Shown are paraffin-embedded tissue sections of human prostate (**a**, **c**, **e** and **f**) and of human skin (**b** and **d**) overlaid with prostate-homing CGRRAGGSC-displaying phage (**a** and **b**) or skin-homing CHGGVGSGC-displaying phage (**c** and **d**). Phage were detected by using an anti-M13 phage antibody. In **e**, IL-11R $\alpha$  expression was determined by conventional immunostaining with an anti-IL-11R $\alpha$  antibody; **a** and **e** show similar immunostaining patterns (brown staining). **f**, Negative control antibody on prostate tissue sections. Arrowheads, positive endothelium; asterisks, positive epithelium. Scale bar, 160  $\mu$ m (**a**, **c**, **e** and **f**); 40  $\mu$ m (**b** and **d**).

ing, the count for each tripeptide motif within each tissue was compared with the count for that tripeptide motif within the unselected library.

**Immunocytochemistry and phage overlays.** Immunohistochemistry on sections of fixed human paraffin-embedded tissues was done using the LSAB+ peroxidase kit (DAKO, Carpinteria, California) as described<sup>3</sup>. For overlay experiments, phage was used at the concentration of  $5 \times 10^{10}$  TU/ml. For phage immunolocalization, a rabbit anti-fd bacteriophage antibody (B-7786; Sigma) was used at 1:500 dilution. For IL-11R $\alpha$  immunolocalization, a goat antibody (sc-1947; Santa Cruz Biotechnology, Santa Cruz, California) was used at 1:10 dilution. Phage binding to tissue sections was evaluated by the intensity of immunostaining relative to controls.

**In vitro protein binding assays.** Recombinant (R&D Systems, Minneapolis, Minnesota) interleukin-11 receptor  $\alpha$  (IL-11R $\alpha$ ), vascular endothelial growth factor receptor-1 (VEGFR1), and leptin receptor (OB-R) were immobilized on microtiter wells (at 1  $\mu$ g in 50  $\mu$ l PBS) overnight at 4°C, washed twice with PBS, blocked with 3% BSA in PBS for 2 h at room temperature, and incubated with  $1 \times 10^9$  TU of CGRRAGGSC-displaying phage in 50  $\mu$ l of 1.5% BSA in PBS. An unrelated phage clone (displaying the peptide CRVDFSKGCG) and insertless phage (fd-tet) were used as controls. After 1 h at room temperature, wells were washed nine times with PBS, after which bound phage were recovered by bacterial infection and plated as described<sup>3</sup>. Either IL-11 or IL-1 (negative control) was used to inhibit phage binding to IL-11R $\alpha$ . Phage were incubated with the immobilized IL-11R $\alpha$  in the presence of increasing concentrations of either IL-11 or IL-1. Binding of CGRRAGGSC-displaying phage on immobilized IL-11R $\alpha$  in the absence of interleukins was set to 100%.

**Statistical analysis.** Let  $p$  be the probability of observing a particular tripeptide motif under total randomness, and  $q = 1 - p$ . Under such parameters, the probability of observing  $K$  sequences characterized as a particular tripeptide motif out of  $n$  total tripeptide sequences is binomial ( $n, p$ ) and may be approximated by the equation  $p_k = \Phi[(k+1)/\sqrt{npq}] - \Phi[k/\sqrt{npq}]$ , where  $\Phi$  is the usual cumulative Gaussian probability. The value  $p_k$  may be treated as a  $P$  value in testing for total randomness of observing exactly  $K$  sequences of a particular tripeptide motif. However, this test requires exact knowledge of the true value of  $p$ , which it is difficult to obtain in practice with certainty. Therefore, to identify the motifs that were isolated in the screen-

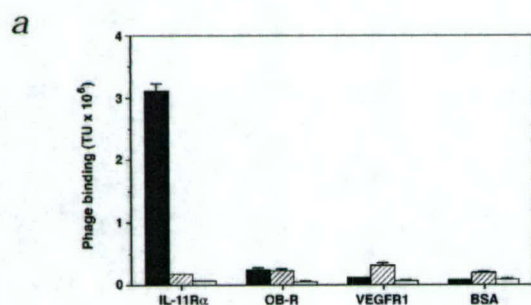
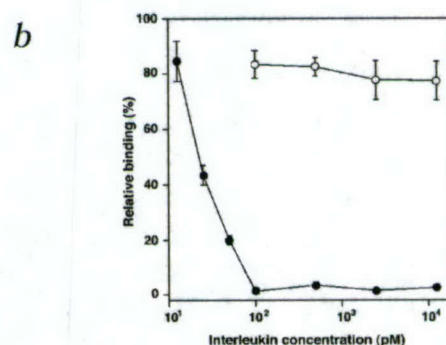


**Fig. 4** Characterization of CGRRAGGSC-displaying phage binding properties by using purified receptors *in vitro*. **a**, Recombinant interleukin-11 receptor  $\alpha$  (IL-11R $\alpha$ ), vascular endothelial growth factor receptor-1 (VEGFR1), or leptin receptor (OB-R) were incubated with the CGRRAGGSC-displaying phage (■). VEGFR1 was used as a representative vascular receptor; OB-R was used because it is homologous to a coreceptor of IL-11R $\alpha$ . An unrelated phage clone (displaying the peptide CRVDFSKGCG, ▨)



and insertless phage (fd-tet, □) were used as controls. Phage binding was evaluated and quantified as described (see Methods). **b**, Specificity of phage binding to the IL-11 receptor. Phage were incubated with the immobilized IL-11R $\alpha$  in the presence of increasing concentrations of either IL-11 (native ligand, ●) or IL-1 (negative control, ○). The experiments were performed three times with similar results. Shown are mean  $\pm$  s.e.m. from triplicate wells.



## Acknowledgements

We thank R.C. Bast, Jr., R.R. Brentani, W.K. Cavenee, A.C. von Eschenbach, J.J. Fidler, W.K. Hong, D.M. McDonald, J. Mendelsohn and L.A. Zwelling for comments on the manuscript; W.D. Heston for sharing unpublished data; C.L. Cavazos, P.Y. Dieringer, R.G. Nikolova, C.A. Perez, B.H. Restel, C.P. Soto and X. Wang for technical assistance. This work was funded in part by grants from NIH (CA90270 and CA8297601 to R.P., CA90270 and CA9081001 to W.A.) and awards from the Gilson-Longenbaugh Foundation and CaP CURE (to R.P. and W.A.). M.G.K., J.L. and P.J.M. received support from the Susan G. Komen Breast Cancer Foundation, R.J.G. from FAPESP (Brazil), M.C.V. from the Department of Defense, L.C. from the NCCRA and E.K. from the Academy of Finland.

## Competing interests statement

The authors declare competing financial interests; see the Nature Medicine web site (<http://medicine.nature.com>) for details.

RECEIVED 19 NOVEMBER 2001; ACCEPTED 2 JANUARY 2002

- Lander, E.S. *et al.* Initial sequencing and analysis of the human genome. *Nature* **409**, 860–921 (2001).
- Venter, J.C. *et al.* The sequence of the human genome. *Science* **291**, 1304–1351 (2001).
- Pasqualini, R., Arap, W., Rajotte, D. & Ruoslahti, E. *In vivo* phage display. In *Phage display: a laboratory manual*. (eds. Barbas, C. F., Burton, D.R., Scott, J.K. & Silverman, G.J.) 1–24 (Cold Spring Harbor Laboratory Press, Cold Spring Harbor, New York, 2000).
- Rajotte, D. *et al.* Molecular heterogeneity of the vascular endothelium revealed by *in vivo* phage display. *J. Clin. Invest.* **102**, 430–437 (1998).
- Pasqualini, R. & Ruoslahti, E. Organ targeting *in vivo* using phage display peptide libraries. *Nature* **380**, 364–366 (1996).
- Ellerby, H.M. *et al.* Anti-cancer activity of targeted pro-apoptotic peptides. *Nature Med.* **5**, 1032–1038 (1999).
- Koivunen, E. *et al.* Tumor targeting with a selective gelatinase inhibitor. *Nature Biotechnol.* **17**, 768–774 (1999).
- Burg, M.A., Pasqualini, R., Arap, W., Ruoslahti, E. & Stallcup, W.B. NG2 proteoglycan-binding peptides target tumor neovasculature. *Cancer Res.* **59**, 2869–2874 (1999).
- Arap, W., Pasqualini, R. & Ruoslahti, E. Cancer treatment by targeted drug delivery to tumor vasculature in a mouse model. *Science* **279**, 377–380 (1998).
- Pasqualini, R., Koivunen, E. & Ruoslahti, E.  $\alpha_v$  integrins as receptors for tumor targeting by circulating ligands. *Nature Biotechnol.* **15**, 542–546 (1997).
- Curnis, F. *et al.* Enhancement of tumor necrosis factor  $\alpha$  antitumor immunotherapeutic properties by targeted delivery to aminopeptidase N (CD13). *Nature Biotechnol.* **18**, 1185–1190 (2000).
- Hong, F. D. & Clayman, G. L. Isolation of a peptide for targeted drug delivery into human head and neck solid tumors. *Cancer Res.* **60**, 6551–6556 (2000).
- Trepel, M., Grifman, M., Weitzman, M.D. & Pasqualini, R. Molecular adaptors for vascular-targeted adenoviral gene delivery. *Hum. Gene Ther.* **11**, 1971–1981 (2000).
- Rajotte, D. & Ruoslahti, E. Membrane dipeptidase is the receptor for a lung-targeting peptide identified by *in vivo* phage display. *J. Biol. Chem.* **274**, 11593–11598 (1999).
- Pasqualini, R. *et al.* Aminopeptidase N is a receptor for tumor-homing peptides and a target for inhibiting angiogenesis. *Cancer Res.* **60**, 722–727 (2000).
- Bhagwat, S.V. *et al.* CD13/APN is activated by angiogenic signals and is essential for capillary tube formation. *Blood* **97**, 652–659 (2001).
- Kolonin, M.G., Pasqualini, R. & Arap, W. Molecular addresses in blood vessels as targets for therapy. *Curr. Opin. Chem. Biol.* **5**, 308–313 (2001).
- Bacich, D.J., Pinto, J.T., Tong, W.P. & Heston, W.D. Cloning, expression, genomic localization, and enzymatic activities of the mouse homolog of prostate-specific membrane antigen/NAALADase/folate hydrolase. *Mamm. Genome* **12**, 117–123 (2001).
- Chang, S.S. *et al.* Five different anti-prostate-specific membrane antigen (PSMA) antibodies confirm PSMA expression in tumor-associated neovasculature. *Cancer Res.* **59**, 3192–3198 (1999).
- St Croix, B. *et al.* Genes expressed in human tumor endothelium. *Science* **289**, 1197–1202 (2000).
- Carson-Walter, E.B. *et al.* Cell surface tumor endothelial markers are conserved in mice and humans. *Cancer Res.* **61**, 6649–6655 (2001).
- Vendruscolo, M., Paci, E., Dobson, C.M. & Karplus, M. Three key residues form a critical contact network in a protein folding transition state. *Nature* **409**, 641–645 (2001).
- Ruoslahti, E. RGD and other recognition sequences for integrins. *Annu. Rev. Cell Dev. Biol.* **12**, 697–715 (1996).
- Koivunen, E. *et al.* Inhibition of  $\beta_2$  integrin-mediated leukocyte cell adhesion by leucine-leucine-glycine motif-containing peptides. *J. Cell Biol.* **153**, 905–916 (2001).
- Thompson, J.D., Higgins, D.G. & Gibson, T.J. CLUSTAL W: improving the sensitivity of progressive multiple sequence alignment through sequence weighting, position-specific gap penalties and weight matrix choice. *Nucleic Acids Res.* **22**, 4673–4680 (1994).
- Daluiski, A. *et al.* Bone morphogenetic protein-3 is a negative regulator of bone density. *Nature Genet.* **27**, 84–88 (2001).
- Mahboubi, K., Biedermann, B.C., Carroll, J.M. & Pober, J.S. IL-11 activates human endothelial cells to resist immune-mediated injury. *J. Immunol.* **164**, 3837–3846 (2000).
- Campbell, C.L., Jiang, Z., Savarese, D.M. & Savarese, T.M. Increased expression of the interleukin-11 receptor and evidence of STAT3 activation in prostate carcinoma. *Am. J. Pathol.* **158**, 25–32 (2001).
- Lin, B.Z., Pilch, P.F. & Kandrór, K.V. Sortilin is a major protein component of Glut4-containing vesicles. *J. Biol. Chem.* **272**, 24145–24147 (1997).
- Nugent, M.A., Nugent, H.M., Iozzo, R.V., Sanchack, K. & Edelman, E.R. Perlecan is required to inhibit thrombosis after deep vascular injury and contributes to endothelial cell-mediated inhibition of intimal hyperplasia. *Proc. Natl Acad. Sci. USA* **97**, 6722–6727 (2000).
- Wu, K.K. *et al.* Thrombomodulin Ala455Val polymorphism and risk of coronary heart disease. *Circulation* **103**, 1386–1389 (2001).
- Barrow, P.A. & Soothill, J. S. Bacteriophage therapy and prophylaxis: rediscovery and renewed assessment of potential. *Trends Microbiol.* **5**, 268–271 (1997).
- Latham, P.W. Therapeutic peptides revisited. *Nature Biotechnol.* **17**, 755–757 (1999).
- Wijedicks, E.F. The diagnosis of brain death. *N. Engl. J. Med.* **344**, 1215–1221 (2001).
- Implementing Human Research Regulations; in *President's Commission for the Study of Ethical Problems in Medicine and Biomedical and Behavioral Research*. (The United States of America Government's Printing Office, Washington, DC; 1983).



# Biopanning and rapid analysis of selective interactive ligands

RICARDO J. GIORDANO, MARINA CARDÓ-VILA, JOHANNA LAHDENRANTA,  
RENATA PASQUALINI & WADIH ARAP

*The University of Texas M.D. Anderson Cancer Center, Houston, Texas, USA*

*Correspondence should be addressed to R.P.; email: rpsqual@notes.mdacc.tmc.edu and or W.A.; email: warap@notes.mdacc.tmc.edu*

Here we introduce a new approach for the screening, selection and sorting of cell-surface-binding peptides from phage libraries. Biopanning and rapid analysis of selective interactive ligands (termed BRASIL) is based on differential centrifugation in which a cell suspension incubated with phage in an aqueous upper phase is centrifuged through a non-miscible organic lower phase. This single-step organic phase separation is faster, more sensitive and more specific than current methods that rely on washing steps or limiting dilution. As a proof-of-principle, we screened human endothelial cells (ECs) stimulated with vascular endothelial growth factor (VEGF) and constructed a peptide-based ligand-receptor map of the VEGF family. Next, we validated the motif PQRPL as a novel chimeric ligand mimic that binds specifically to VEGF receptor-1 and to neuropilin-1. BRASIL may prove itself a superior method for probing target cell surfaces with a broad range of potential applications.

Probing the molecular diversity of cell surfaces is required for the development of targeted therapies<sup>1</sup>. However, selections of phage libraries on cell surfaces are often challenging experiments. First, non-specific clones are recovered when phage libraries are incubated with cell suspensions or monolayers. Second, removal of background by phage-repeated washes is both labor-intensive and inefficient. Third, cells and potential ligands are lost during the washing steps required.

To address these obstacles, we adapted a method termed biopanning and rapid analysis of selective interactive ligands (BRASIL) from an assay described to measure receptor binding of specific yet low-affinity ligands<sup>2-5</sup>. BRASIL allows separation of phage-cell complexes from the remaining unbound phage; this is accomplished by a differential centrifugation that drives the cells from a hydrophilic environment into a non-miscible organic phase. Because the organic phase is hydrophobic, it excludes water-soluble materials surrounding cell surfaces. Bound phage are recovered from the cell pellet whereas the unbound phage remain soluble in the upper aqueous phase, eliminating the need for repeated washes. As a single centrifugation step is required, BRASIL is simpler and more convenient than current cell-panning techniques. Mapping ligand-receptors by BRASIL may allow an understanding of binding requirements for receptor families and enable peptide isolation for cell-targeting applications.

## Cell binding to a defined test phage ligand

We set out to study cell binding by using BRASIL to test an established ligand-receptor pair. Experiments were designed using RGD-4C [authors: Ala-Cys-Asp-Cys-Arg-Gly-Asp-Cys-Phe-Cys-Gly OK here?] phage (displaying the motif ACDCRGDCFCG, termed RGD-4C peptide), which is a specific ligand for  $\alpha$ v integrins<sup>6-8</sup>. We reasoned that cell-surface-bound phage could be specifically carried through an organic phase and recovered by infection of the host bacteria.  $\alpha$ v integrin-expressing Kaposi's

sarcoma cells (KS1767) cells were detached, incubated on ice with RGD-4C phage or control insertless phage (termed fd-tet), and the mixture was separated by differential centrifugation through the organic phase. The number of phage transducing units (TU) recovered from the cell pellets is shown in Fig. 1a. Phage recovery correlated directly with increasing phage input and the recovery ratio (phage output from organic lower layer/phage input from aqueous upper layer) decreased with host bacteria saturation (Fig. 1a). Under non-saturating conditions, the ratio of specific (RGD-4C) phage to control (fd-tet) phage (termed 'enrichment') ranged from 100 to 500. We show that the binding of RGD-4C phage to KS1767 cells is specific because such cell-phage binding is inhibited by the corresponding synthetic RGD-4C peptide in a dose-dependent manner; negative control peptides GRGESP (Fig. 1b) or CARAC (data not shown) at the same molar concentrations had no inhibitory effect. No phage were present at the bottom of the tube or in the organic phase in the absence of KS1767 cells (data not shown). Next, we compared BRASIL with conventional cell-panning strategies that require washing steps. The number of RGD-4C phage recovered by BRASIL was significantly higher (*t*-test,  $P < 0.01$ ) than the number of the same phage recovered when a conventional phage-cell binding strategy involving washing was used (Fig. 1c). Conversely, significantly lower background (*t*-test,  $P < 0.01$ ) with the negative control phage was observed (Fig. 1c). Given the significant increase in recovery of specific phage and the substantial decrease in background, the overall accuracy (cell-specific phage recovery) improved consistently by more than one order of magnitude when BRASIL was used relative to conventional cell-panning methods.

## Screening VEGF-stimulated ECs

Once the method was optimized with a well-defined ligand-receptor pair, we tested whether BRASIL could also be used to screen phage display random peptide libraries on cells; ECs stimulated with vascular endothelial growth factor (VEGF) were used. We designed a two-step panning strategy to isolate phage that bind to angiogenic ECs. First, to decrease non-specific binding, we pre-cleared the phage library on starved ECs (before panning on the same cell line stimulated with recombinant VEGF<sub>165</sub>); starved human umbilical vein ECs (HUVECs) were incubated with the phage library and centrifuged through the organic phase (Fig. 2a). Second, the unbound phage pool left in the aqueous phase was transferred to a fresh tube and incubated with VEGF<sub>165</sub>-stimulated HUVECs. After centrifugation through the organic phase, phage bound to the VEGF<sub>165</sub>-stimulated HUVEC pellet were recovered by bacterial infection, amplified and subjected to two more rounds of selection (Fig. 2a).

## Analysis of phage-displayed peptides

To test the selection method, we compared 21 phage clones randomly chosen for binding to starved HUVECs and to VEGF-stim-



ulated HUVECs. Fourteen out of 21 clones (67%) had a greater than 150% enhancement (range, 1.5–8.7-fold; median, 2.2-fold) in the ratio of cell binding upon VEGF stimulation normalized to control insertless phage (data not shown). Sequence alignment analysis of 34 clones randomly chosen from the selected phage revealed that 24 clones (70%) of the phage recovered by BRASIL had peptide motifs that could be mapped to sequences present in VEGF family members (Table 1).

Next, we chose the CPQPRPLC phage and CNIRRQGC phage (a representative phage out of three different clones displaying the motif IRR<sup>E/Q</sup>) for *in vitro* phage binding assay on VEGF receptor-1 (VEGFR-1). The receptor was immobilized on a microtiter well-plate and incubated with CPQPRPLC phage, CNIRRQGC phage or fd-tet as a negative control. Both CPQPRPLC and CNIRRQGC phage bound to VEGFR-1 (Fig. 2*b*). The CPQPRPLC phage bound best with an average of over 1,000-fold enrichment observed over each of the controls used: CPQPRPLC phage binding to VEGFR-1 over bovine serum albumin (BSA) and CPQPRPLC phage over fd-tet phage binding to VEGFR-1 (Fig. 2*b*).

The CPQPRPLC sequence matched motifs found within the VEGF-B isoforms (Fig. 2*c*). VEGF-B has two mRNA splice variants generated by the use of different, but overlapping, reading frames of exon 6 (isoforms 167 and 186), which diverge in sequence in their C termini<sup>9</sup>. The pentapeptide motif PRPLC is found in the recombinant human VEGF B 167 (VEGF-B<sub>167</sub>) C terminus region encoded by exon 6B, starting at the second residue after the boundary between exons 5 and 6B. PRPLC is a neuropilin-1 (NRP-1) binding domain<sup>10</sup>. On the other hand, the tetrapeptide motif PQPR—which overlaps with PRPLC and also with the phage-displayed CPQPRPLC peptide—is found in the C terminal of recombinant human VEGF B 186 (VEGF-B<sub>186</sub>), and encoded by exon 6A. PQPR is embedded within a 12-residue known NRP-1 binding site<sup>10</sup>. The motif IRR<sup>E/Q</sup> also showed ho-

mology to VEGF family members (Table 1) but it was not studied further here.

### CPQPRPLC is a chimeric VEGF mimic

We evaluated the binding of phage displaying the peptide CPQPRPLC to a panel of VEGF receptors (Fig. 3*a*). CPQPRPLC bound to VEGFR-1 and to NRP-1, but not to VEGF receptor-2 (VEGFR-2) or to neuropilin-2 (NRP-2); this pattern is the receptor recognition profile of VEGF-B (ref. 9). We show that the CPQPRPLC phage binding to VEGFR-1 and to NRP-1 was inhibited by pre-incubation with VEGF<sub>165</sub> (Fig. 3*b*) but not with platelet-derived growth factor-β (PDGF-BB [AU: Should this be a 'β'?]; data not shown). These results are consistent with the fact that VEGF<sub>165</sub> and VEGF-B isoforms compete for binding to VEGFR-1 (ref. 9) and suggest that CPQPRPLC and VEGF<sub>165</sub> might recognize closely related or overlapping binding sites. Finally, we show that the binding of CPQPRPLC phage to the immobilized VEGFR-1 and NRP-1 is specific because it can be inhibited by the corresponding synthetic peptides in a concentration-dependent manner (Fig. 3*c* and *d*). These data show that 1) CPQPRPLC is a

**a** Table 1 Alignment of peptide sequences isolated by BRASIL and VEGF family members

VEGF-A	
<p><b>VEGF-A-121</b>            APLH...CHRRVVKFMVQSRVCHP1ETLVDFQYFDEIYFKPS...CHVLR...COO...CHDGL...CVTEESNITMIRIKP            HQO...CHSFLQHRCCKRCKPK...CHVLR...COO...CHDGL...CVTEESNITMIRIKP</p>	
<p>VEGF-A-121 67 CVTTEEN 75            Peptide #3 CVT-HRLQ-8            VEGF-A-121 50 CVT-HRLQ-8 60</p>	<p>Peptide #26 CHVLR-ARC            VEGF-A-121 108 DRANKKSV 118</p>
<p>Peptide #6 CLSHTGC            VEGF-A-121 86 QOQHTGMSF 96</p>	<p>Peptide #32 CHVLR-AYC            VEGF-A-121 3 MHTVQNH 11</p>
VEGF-A-165	
<p><b>VEGF-A-165</b>            APLH...CHRRVVKFMVQSRVCHP1ETLVDFQYFDEIYFKPS...CHVLR...COO...CHDGL...CVTEESNITMIRIKP            HQO...CHSFLQHRCCKRCKPK...CHVLR...COO...CHDGL...CVTEESNITMIRIKP</p>	
<p>VEGF-A-165 67 CVTTEEN 75            Peptide #3 CVT-HRLQ-8            VEGF-A-165 50 CVT-HRLQ-8 60</p>	<p>Peptide #26 CHVLR-ARC            VEGF-A-165 108 DRANKKSV 118</p>
<p>Peptide #6 CLSHTGC            VEGF-A-165 86 QOQHTGMSF 96</p>	<p>Peptide #32 CHVLR-AYC            VEGF-A-165 3 MHTVQNH 11</p>
VEGF-A-189	
<p><b>VEGF-A-189</b>            APLH...CHRRVVKFMVQSRVCHP1ETLVDFQYFDEIYFKPS...CHVLR...COO...CHDGL...CVTEESNITMIRIKP            HQO...CHSFLQHRCCKRCKPK...CHVLR...COO...CHDGL...CVTEESNITMIRIKP</p>	
<p>VEGF-A-189 67 CVTTEEN 75            Peptide #3 CVT-HRLQ-8            VEGF-A-189 50 CVT-HRLQ-8 60</p>	<p>Peptide #26 CHVLR-ARC            VEGF-A-189 108 DRANKKSV 118</p>
<p>Peptide #4 CLSHTGC            VEGF-A-189 116 SVGRKPKK 128</p>	<p>Peptide #32 CHVLR-AYC            VEGF-A-189 3 MHTVQNH 11</p>
VEGF-A-206	
<p><b>VEGF-A-206</b>            APLH...CHRRVVKFMVQSRVCHP1ETLVDFQYFDEIYFKPS...CHVLR...COO...CHDGL...CVTEESNITMIRIKP            HQO...CHSFLQHRCCKRCKPK...CHVLR...COO...CHDGL...CVTEESNITMIRIKP</p>	
<p>VEGF-A-206 67 CVTTEEN 75            Peptide #3 CVT-HRLQ-8            VEGF-A-206 50 CVT-HRLQ-8 60</p>	<p>Peptide #26 CHVLR-ARC            VEGF-A-206 108 DRANKKSV 118</p>
<p>Peptide #4 CLSHTGC            VEGF-A-206 116 SVGRKPKK 128</p>	<p>Peptide #32 CHVLR-AYC            VEGF-A-206 3 MHTVQNH 11</p>

**b**

VEGF-B	
<p><b>VEGF-B-167</b>            PVSGPAPRQHRVVKFMVQSRVCHP1ETLVDFQYFDEIYFKPS...CHVLR...COO...CHDGL...CVTEESNITMIRIKP            HQO...CHSFLQHRCCKRCKPK...CHVLR...COO...CHDGL...CVTEESNITMIRIKP</p>	
<p>Peptide #3 CVT-HRLQ-8            VEGF-B-167 67 CVT-HRLQ-8 77</p>	<p>Peptide #19 CHVLR-AYC            VEGF-B-167 24 TCN...VTV 37</p>
<p>Peptide #17 CAVVYV            VEGF-B-167 93 SLEEK...CKRP 105</p>	<p>Peptide #19 CHVLR-AYC            VEGF-B-167 112 TCN...VTV 123</p>
VEGF-B-186	
<p><b>VEGF-B-186</b>            PVSGPAPRQHRVVKFMVQSRVCHP1ETLVDFQYFDEIYFKPS...CHVLR...COO...CHDGL...CVTEESNITMIRIKP            HQO...CHSFLQHRCCKRCKPK...CHVLR...COO...CHDGL...CVTEESNITMIRIKP</p>	
<p>Peptide #3 CVT-HRLQ-8            VEGF-B-167 67 CVT-HRLQ-8 77</p>	<p>Peptide #19 CHVLR-AYC            VEGF-B-167 24 TCN...VTV 37</p>
<p>Peptide #12 CHVLR-AYC            VEGF-B-167 180 TCN...VTV 186</p>	<p>Peptide #32 CHVLR-AYC            VEGF-B-167 175 TCN...VTV 182</p>
<p>Peptide #17 CAVVYV            VEGF-B-167 93 SLEEK...CKRP 105</p>	<p>Peptide #32 CHVLR-AYC            VEGF-B-167 153 TCN...VTV 161</p>
VEGF-C	
<p><b>VEGF-C</b>            FEGGLDLSAPDAGATATASKDLQEL...CHVLR...COO...CHDGL...CVTEESNITMIRIKP            HQO...CHSFLQHRCCKRCKPK...CHVLR...COO...CHDGL...CVTEESNITMIRIKP</p>	
<p>Peptide #1 CVT-HRLQ-8            VEGF-C 134 CHVLR-AYC 143</p>	<p>Peptide #21 CHVLR-AYC            VEGF-C 190 TCN...VTV 196</p>
<p>Peptide #12 CHVLR-AYC            VEGF-C 27 CHVLR-AYC 37</p>	<p>Peptide #32 CHVLR-AYC            VEGF-C 77 TCN...VTV 86</p>
VEGF-D	
<p><b>VEGF-D</b>            SREHHPVRSQSSTLER...CHVLR...COO...CHDGL...CVTEESNITMIRIKP            HQO...CHSFLQHRCCKRCKPK...CHVLR...COO...CHDGL...CVTEESNITMIRIKP</p>	
<p>Peptide #1 CVT-HRLQ-8            VEGF-D 55 CHVLR-AYC 66</p>	<p>Peptide #21 CHVLR-AYC            VEGF-D 314 TCN...VTV 327</p>
<p>Peptide #7 CHVLR-AYC            VEGF-D 148 CHVLR-AYC 159</p>	<p>Peptide #28 CHVLR-AYC            VEGF-D 169 TCN...VTV 179</p>
<p>Peptide #21 CHVLR-AYC            VEGF-D 177 CHVLR-AYC 190</p>	<p>Peptide #30 CHVLR-AYC            VEGF-D 303 TCN...VTV 313</p>
<p>Peptide #24 CHVLR-AYC            VEGF-D 101 CHVLR-AYC 114</p>	<p>Peptide #36 CHVLR-AYC            VEGF-D 136 TCN...VTV 145</p>

**c**

PLGF	
<p><b>PLGF-1</b>            LPVFPQALSA...CHVLR...COO...CHDGL...CVTEESNITMIRIKP            HQO...CHSFLQHRCCKRCKPK...CHVLR...COO...CHDGL...CVTEESNITMIRIKP</p>	
<p>Peptide #3 CVT-HRLQ-8            PLGF-1 75 CVT-HRLQ-8 85</p>	<p>Peptide #19 CHVLR-AYC            PLGF-1 108 TCN...VTV 120</p>
<p>Peptide #9 CHVLR-AYC            PLGF-1 90 IRSDPKPK 101</p>	<p>Peptide #25 CHVLR-AYC            PLGF-1 115 TCN...VTV 127</p>
PLGF-2	
<p><b>PLGF-2</b>            LPVFPQALSA...CHVLR...COO...CHDGL...CVTEESNITMIRIKP            HQO...CHSFLQHRCCKRCKPK...CHVLR...COO...CHDGL...CVTEESNITMIRIKP</p>	
<p>Peptide #3 CVT-HRLQ-8            PLGF-2 75 CVT-HRLQ-8 85</p>	<p>Peptide #19 CHVLR-AYC            PLGF-2 108 TCN...VTV 120</p>
<p>Peptide #9 CHVLR-AYC            PLGF-2 90 IRSDPKPK 101</p>	<p>Peptide #25 CHVLR-AYC            PLGF-2 115 TCN...VTV 127</p>

Color-coding identifies individual peptide sequences.  
 PLGF, placenta growth factor.



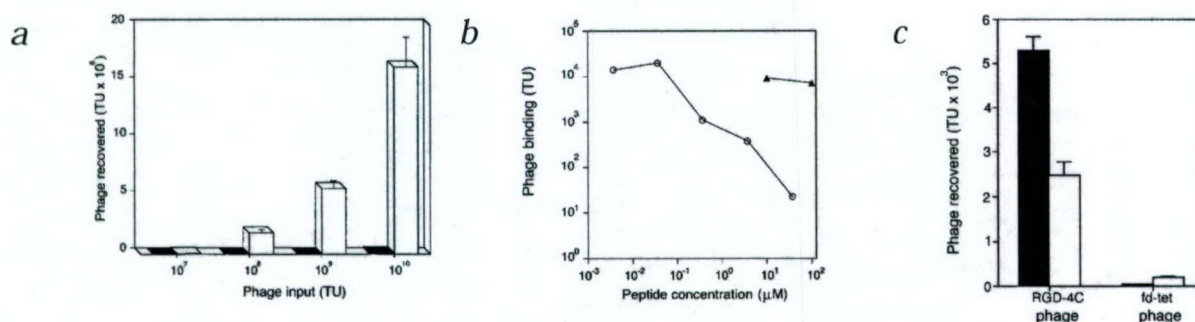


**Fig. 1** Cell-binding assays with a defined  $\alpha_v$  integrin phage ligand and phage-cell-binding optimization with BRASIL. **a**, Amounts of RGD-4C phage (□) and insertless control phage (fd-tet; ■) bound to KS1767 cells at increasing phage inputs were compared. **b**, Specific inhibition of phage binding by the cognate synthetic peptide. RGD-4C phage were incubated with KS1767 cells in the presence of increasing concentrations of RGD-4C peptide (○) or a

control peptide (sequence GRGESP; ▲), and the amounts of phage bound were measured. **c**, Comparison between conventional panning methods and BRASIL (■). RGD-4C or control phage were incubated with KS1767 cells. Bound phage were assayed by passing through the organic phase or by washing the cells 3 times with PBS/0.1% BSA (□). The experiments were performed 3 times with similar results. Bars represent mean  $\pm$  s.e.m. from triplicates.

chimeric VEGF-B-family mimic, and 2) this peptide interacts specifically with VEGFR-1 and NRP-1.

## Discussion

Our results show that organic phase separation is an efficient and convenient method for phage selection. On side-by-side comparison to current protocols, BRASIL was more sensitive and more specific than techniques that rely on washing or limiting dilution steps to eliminate background during successive rounds of selection. BRASIL may represent an improvement over conventional cell-panning methods.

Because of our interest in targeting vascular endothelium<sup>6-8,11,12</sup>, we screened a phage-display random peptide library on VEGF<sub>165</sub>-stimulated ECs. We identified a VEGF-receptor ligand with the sequence CPQPRPLC that resembles the motif PRPLC (an NRP-1 binding site found in VEGF-B<sub>167</sub>) and the overlapping motif PQPR (found embedded within a 12-residue NRP-1-binding epitope of VEGF-B<sub>186</sub>; ref. 10). Thus, the motif PQPRPLC appears to be a chimera between overlapping binding sites on different VEGF-B isoforms. Binding assays using individual

phage on a panel of purified targets confirmed that the CPQPRPLC phage interacts specifically with VEGF receptors in a pattern consistent with VEGF-B-type ligands<sup>9</sup>. These results suggest that the C terminal regions of both VEGF-B isoforms bind to VEGFR-1 and NRP-1 and are in agreement with recent results of deletion and site-directed mutagenesis studies of VEGF-B isoforms<sup>10</sup>. Further mutational experiments are needed to confirm the VEGF-B receptors that are recognized by the motifs PRPLC and PQPR individually. Also of importance is the observed difference in the ability of the synthetic peptide CPQPRPLC to block

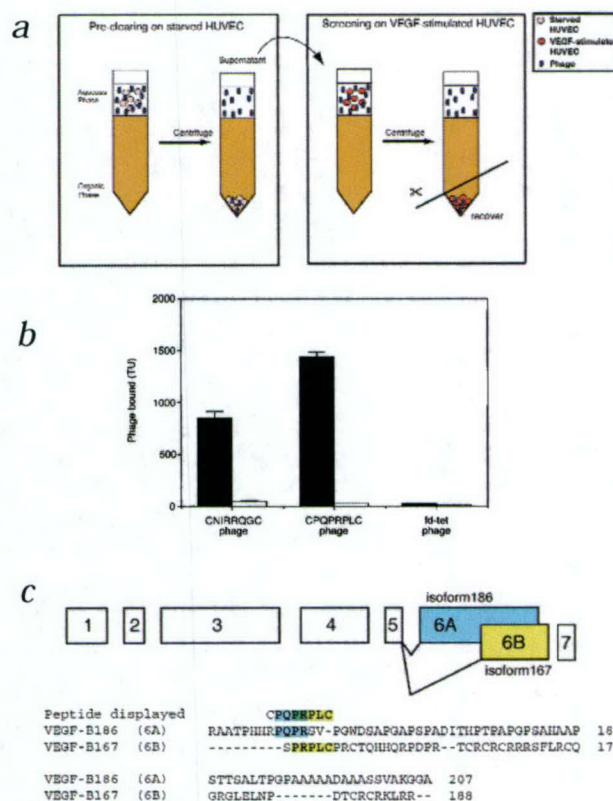


**Fig. 2** Screening VEGF<sub>165</sub>-stimulated HUVECs by BRASIL. **a**, Panning strategy to isolate phage that bind to activated ECs. Starved HUVECs were incubated with the peptide phage library, and the cells were separated by centrifugation through the organic phase. The supernatant containing the unbound phage was transferred to VEGF<sub>165</sub>-stimulated HUVECs and after incubation, cells and bound phage were separated by centrifugation through the organic phase. The cell-bound phage in the pellet were rescued by infection, amplified and used for another round of biopanning. **b**, Binding of the selected phage clones (CPQPRPLC, CNIRRGCG, and control) to the immobilized VEGFR-1 (■) compared with binding to BSA (□). VEGFR-1 was used to coat the microtiter plate. The individual wells were then incubated with equal amounts of each individual phage. Bars represent mean  $\pm$  s.e.m. from duplicate wells. **c**, Homology analysis of the CPQPRPLC sequence. Exon organization of the two VEGF-B isoforms (modified from ref. 32) is shown. Sequences of exon 6A of VEGF-B<sub>186</sub> and of exon 6B of VEGF-B<sub>167</sub> [AU: GenBank #'s removed. Please replace only in Methods.] are compared with the sequence of the phage display-selected peptide. Overlapping motif sequences are shown in colors corresponding to the respective exons of origin (exon 6A, blue; exon 6B, yellow): CPQPRPLC is a chimera between the motifs PQPR (VEGF-B<sub>186</sub>, residues 145–148) and PRPLC (VEGF-B<sub>167</sub>, residues 138–142).



## Methods

**Reagents.** A phage display random peptide library based on the vector FUSE5 (ref. 15) displaying the insert CX<sub>6</sub>C (C, cysteine; X, any amino-acid residue) was constructed with a size between  $1 \times 10^6$  and  $1 \times 10^7$ , as described<sup>16</sup>. Human VEGF<sub>165</sub> (Pharmingen, [authors: city, state location of company]), human VEGFR-1 (Oncogene Research Products, [authors: city, state location of company]), rat NRP-1/Fc, rat NRP-2/Fc, VEGFR-2/Fc (all 3 receptor domains fused to the Fc region of human IgG<sub>1</sub>), PDGF-BB, anti-VEGFR-1 (polyclonal anti-Flt1), and anti-human VEGF polyclonal antibody (R&D Systems, [authors: city, state location of company]), dibutyl phthalate, cyclohexane (Sigma-Aldrich) and synthetic peptides (AnaSpec, [authors: city, state location of company]) were obtained commercially. HUVECs and KS1767 cells were described<sup>6-8,12</sup>.

**BRASIL optimization.** Cells were collected with PBS and 5 mM EDTA, washed with MEM, and re-suspended in MEM containing 1% BSA at  $1 \times 10^6$  cells per ml and incubated with phage within 1.5-ml Eppendorf tubes. To minimize post-binding events such as receptor-mediated internalization, cells and media were kept on ice unless otherwise stated. After 4 h, 100  $\mu$ l of the cell-phage suspension was gently transferred to the top of a non-miscible organic lower phase (200  $\mu$ l [authors:  $\mu$ l? you had  $\mu$ ] in a 400  $\mu$ l-Eppendorf tube) and centrifuged at 10,000g for 10 min. The most suitable organic phase combination was dibutyl phthalate:cyclohexane (9:1 [v:v];  $\rho = 1.03$  g ml<sup>-1</sup> [authors: what is  $\rho$ ?]) but other phthalate combinations with the appropriate density (dibutyl phthalate:diisooctyl phthalate; 4:6 [v:v]) were used with similar results. The tube was snap frozen in liquid nitrogen, the bottom of the tube sliced off, and the cell-phage pellet transferred to a new tube; this optional freeze-cut technique prevents cross-contamination with the phage remaining in the aqueous phase. As part of the method optimization, we have tested the effects of the organic phase and of the optional freeze-thaw phase on phage infectivity. Increasing amounts of phage (ranging from  $1 \times 10^3$  –  $1 \times 10^9$ ) were incubated in 100  $\mu$ l of bacterial culture phase plus organic phase admixture (varying from 0% to up to 20% v:v bacterial culture). After 15 min, bound phage were amplified by the addition of 100  $\mu$ l of *Escherichia coli* K91kan at log-phase. The genes inducing tetracycline resistance in the host bacteria were induced by adding low tetracycline concentrations<sup>12,15,16</sup>, infection and proceeded for 1 h. The triplicates were plated at multiple dilutions, and the number of colonies counted after an overnight incubation of the plates at 37 °C. No significant differences in the phage infection ratios were observed under the conditions tested. We also compared phage recovery with or without the snap-freeze step under each of the conditions. No substantial decrease was noted in the amounts of test phage recovered (data not shown). These data suggest that limited exposure to the organic mixture and a brief freeze-thaw had no measurable adverse affects on the infection of bacteria and recovery of phage. However, because decreases in phage infectivity with other phage-peptide libraries might occur under these conditions, we advise that these results should not be extrapolated without testing. Bound phage were rescued by infection with 200  $\mu$ l of *E. coli* K91kan host bacteria in log phase<sup>12,15,16</sup>. To evaluate binding specificity, phage and cells were incubated with the cognate or control synthetic pep-

tides for competition assays.

**Binding assays with phage clones.** KS1767 cells were detached with cold EDTA and re-suspended in MEM containing 1% BSA.  $\alpha$ v integrin-binding RGD-4C phage were used as defined ligands. The cell suspension was incubated with RGD-4C phage or a control phage with no peptide insert (fd-tet phage). Increasing amounts of either phage were added to the cells in suspension and the cell-phage admixture was then incubated for 4 h on ice. Cells were then separated by centrifugation through the organic phase. Bound phage were recovered and colonies were counted. To compare BRASIL to conventional methods that require an additional washing step, 200  $\mu$ l of the cell suspension were incubated with phage for 4 h on ice. Then, unbound phage from 100- $\mu$ l aliquots were removed either by centrifuging over the organic phase or by washing the cells 3 times with 1 ml PBS containing 0.3% BSA. Competitive inhibition was evaluated by comparing synthetic RGD-4C and control peptides (CARAC or GRGESP) at the same molar ratios.

**Screening assays with phage libraries.** HUVECs at 80% confluence cultured in endothelial basal medium (EBM-2; Clonetics, [authors: city, state location of company]) without supplements for 24 h were defined as 'starved HUVECs'. The medium was then replaced by EBM-2 supplemented with 20 ng ml<sup>-1</sup> VEGF<sub>165</sub>, and the cells, cultured under these conditions for another 18 h, were defined as 'VEGF-stimulated HUVECs'. Cells were collected with ice-cold PBS and 5 mM EDTA, washed once with EBM-2 plus 1% BSA, and re-suspended in the same medium at  $1 \times 10^7$  cells per ml. In the pre-clearing step,  $1 \times 10^6$  starved HUVECs were incubated with  $1 \times 10^9$  transducing units (TU) of unselected library for 2 h on ice; the mixture was then centrifuged through the organic phase. In a screening step, the unbound phage remaining in the aqueous upper phase (supernatant) was transferred to a fresh tube and incubated with  $1 \times 10^6$  VEGF-stimulated HUVECs. After 4 h on ice, the cell-phage complexes were separated by centrifugation through the organic lower phase. Phage were recovered from the pellet by infection of log phase *E. coli* K91kan<sup>12,15,16</sup>.

**Binding assays on purified receptors.** VEGFR-1, VEGFR-2, NRP-1 and NRP-2 (at 1  $\mu$ g in 50  $\mu$ l PBS) were immobilized on microtiter wells overnight at 4 °C. Wells were washed twice with PBS, blocked with PBS/3% BSA for 2 h at room temperature, and incubated with  $1 \times 10^9$  TU of CPQPRPLC phage, CNIRRQGC phage or fd-tet phage in 50  $\mu$ l of PBS/1.5% BSA. After 1 h at room temperature, wells were washed 9 times with PBS and phage were recovered by bacterial infection. Serial dilutions were plated onto Luria-Bertani (LB) medium supplemented with tetracycline<sup>12,15,16</sup>. VEGF<sub>165</sub>, PDGF-BB or synthetic peptides were used to evaluate competitive inhibition of phage binding. ELISA with polyclonal anti-VEGFR-1 serum or anti-human IgG (VEGFR-2, NRP-1 and NRP-2) confirmed the presence and concentration of the receptors on the wells. To show that the VEGF receptors were functionally active, VEGF<sub>165</sub> (50 ng ml<sup>-1</sup>) was incubated with the immobilized receptors for 2 h at room temperature; following three washes, VEGF<sub>165</sub> binding was evaluated by ELISA by using VEGF-specific antibodies (data not shown).



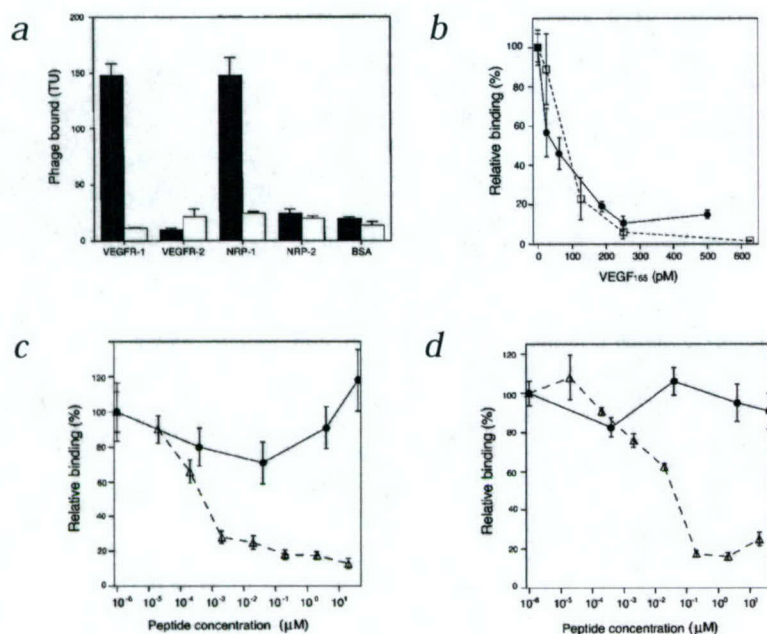


**Fig. 3** Binding of the CPQPRPLC peptide to immobilized VEGF receptors. Recombinant VEGFR-1 and -2 and NRP-1 and -2 were used to coat microtiter plates. CPQPRPLC or control phage were added to the wells. **a**, Binding of CPQPRPLC phage (■) and control phage (□) to the immobilized receptors. **b**, Inhibitory effect of VEGF<sub>165</sub> on the binding of CPQPRPLC phage to VEGF receptors. CPQPRPLC phage were incubated with the immobilized VEGFR-1 (●) or NRP-1 (□) in the absence or presence of VEGF<sub>165</sub> (0–600 pM). No binding inhibition was observed by using PDGF-BB (up to 8 nM) as a negative control (data not shown). **c** and **d**, The binding of CPQPRPLC phage to VEGFR-1 (**c**) and NRP-1 (**d**) is specific. The cognate peptide CPQPRPLC (Δ), but not a control peptide (●) inhibits phage binding to the immobilized receptor. Phage were incubated in the presence of increasing amounts of the synthetic CPQPRPLC peptide or of the negative control peptide CARAC. A specific, dose-dependent inhibition is noted. The experiments were performed 3 times with similar results. Shown are mean ± s.e.m. from triplicate wells.

phage binding to VEGF receptors. Our results suggest that the CPQPRPLC peptide is approximately 100-fold more efficient in blocking phage binding to VEGFR-1 than to NRP-1. It is tempting to speculate that our chimeric motif interacts with VEGF receptors differentially; if so, this may be due to differences in the number of peptide-binding sites on each receptor, or in the affinity of the interaction at each binding site. Alternatively, such ligand-receptor interactions may be dependent on the conditions used for the binding assay. Full understanding of binding mechanisms awaits elucidation of the X-ray crystal structures of VEGFR-1- or NRP-1-CPQPRPLC peptide complexes. Although one can not as yet assert that BRASIL will be well suited for any cell-selection application, our data show that vascular targets<sup>13</sup> can clearly be found in EC membranes.

We also compared BRASIL and conventional cell-panning methods side-by-side to test the specific binding of the recently identified  $\beta_2$  integrin-antagonist peptide CPCFLGCC containing the motif Leu-Leu-Gly (ref. 14). BRASIL was again consistently and reproducibly superior when selection was performed on  $\beta_2$  integrin-expressing cells (unpublished observations). We are adapting the method for use with phage displaying larger polypeptides or folded proteins such as enzymes or antibodies (IAU: Provide initials.), unpublished data).

Importantly, BRASIL is also of value for targeting and isolating ligand-receptor pairs in cell populations derived from clinical samples. The method may be used in tandem with fine-needle aspirates of solid tumors or fluorescence-activated cell sorting of leukemic cells obtained from patients. Moreover, because multiple samples and several rounds of pre-clearing and selection can be performed in a few hours with minimal loss, automation for high-throughput screening, and clinical applications are likely to follow.

#### Acknowledgments

This work was supported by the NIH (CA90270 and CA8297601 to R.P.; CA90270 and CA9081001 to W.A.) and by a Gillson-Longenbaugh Foundation Award (to R.P. and W.A.). R.J.G. was supported by FAPESP (Brazil), M.C.V. by the Department of Defense and J.L. by the Susan G. Komen Breast Cancer Foundation.

- Brown, K.C. New approaches for cell-specific targeting: Identification of cell-selective peptides from combinatorial libraries. *Curr. Opin. Chem. Biol.* **4**, 16–21 (2000).
- Hatzfeld, J.A., Hatzfeld, A. & Maigne, J. Fibrinogen and its fragment D stimulate proliferation of human hemopoietic cells in vitro. *Proc. Natl. Acad. Sci. USA* **79**, 6280–6284 (1982).
- Ouaisi, M.A., Afchain, D., Capron, A. & Grimaud, J.A. Fibronectin receptors on *Trypanosoma cruzi* trypomastigotes and their biological function. *Nature* **308**, 380–382 (1984).
- Levesque, J.P., Hatzfeld, A. & Hatzfeld, J. A method to measure receptor binding of ligands with low affinity. Application to plasma proteins binding assay with hemopoietic cells. *Exp. Cell Res.* **156**, 558–562 (1985).
- Giordano, R., Chammas, R., Veiga, S.S., Colli, W. & Alves, M.J. An acidic component of the heterogeneous Tc-85 protein family from the surface of *Trypanosoma cruzi* is a laminin binding glycoprotein. *Mol. Biochem. Parasitol.* **65**, 85–94 (1994).
- Pasqualini, R., Koivunen, E. & Ruoslahti, E.  $\alpha_v$  integrins as receptors for tumor targeting by circulating ligands. *Nature Biotechnol.* **15**, 542–546 (1997).
- Arap, W., Pasqualini, R. & Ruoslahti, E. Cancer treatment by targeted drug delivery to tumor vasculature in a mouse model. *Science* **279**, 377–380 (1998).
- Ellerby, H.M. *et al.* Anti-cancer activity of targeted pro-apoptotic peptides. *Nature Med.* **5**, 1032–1038 (1999).
- Olofsson, B., Jeltsch, M., Eriksson, U. & Alitalo, K. Current biology of VEGF-B and VEGF-C. *Curr. Opin. Biotechnol.* **10**, 528–535 (1999).
- Makinen, T. *et al.* Differential binding of vascular endothelial growth factor B splice and proteolytic isoforms to neuropilin-1. *J. Biol. Chem.* **274**, 21217–21222 (1999).
- Kolonin, M., Pasqualini, R. & Arap, W. Molecular addresses in blood vessels as targets for therapy. *Curr. Opin. Chem. Biol.* **5**, 308–313 (2001).
- Pasqualini, R., Arap, W., Rajotte, D. & Ruoslahti, E. *In vivo* selection of phage-display libraries. in *Phage Display: A Laboratory Manual* (eds. Barbas, C.F., III, Burton, D.R., Scott, J.K. & Silverman, G.J.) 1–24 (Cold Spring Harbor Laboratory Press, New York, 2000).
- Soker, S., Takashima, S., Miao, H.Q., Neufeld, G. & Klagsbrun, M. Neuropilin-1 is expressed by endothelial and tumor cells as an isoform-specific receptor for vascular endothelial growth factor. *Cell* **92**, 735–745 (1998).
- Koivunen, E. *et al.* Inhibition of  $\beta_2$  integrin-mediated leukocyte cell adhesion by leucine-leucine-glycine motif-containing peptides. *J. Cell Biol.* **153**, 1–13 (2001).
- Smith, G.P. & Scott, J.K. Libraries of peptides and proteins displayed on filamentous phage. *Methods Enzymol.* **217**, 228–257 (1993).
- Koivunen, E. *et al.* Integrin-binding peptides from phage display peptide libraries. *Integrin Protocols. Methods Mol. Biol.* **129**, 3–17 (1999).



# Is annexin 7 a tumor suppressor gene in prostate cancer?

M Cardó-Vila<sup>1</sup>, KC Arden<sup>2</sup>, WK Cavenee<sup>2</sup>, R Pasqualini<sup>1</sup> and W Arap<sup>1</sup>

<sup>1</sup>The University of Texas MD Anderson Cancer Center, Houston, TX; <sup>2</sup>Ludwig Institute for Cancer Research—San Diego Branch, La Jolla, CA, USA

Two features make the prostate and its tumors unusual. First, the prostate gland continues to grow throughout adult life, even doubling in size between the second and fourth decades.<sup>1</sup> As a result, benign prostate hypertrophy affects most aging men to some degree. Second, and much more serious, cancer of the prostate is the most frequent malignant tumor and second leading cause of cancer-related deaths among men in the United States and Europe.<sup>2</sup> While one out of every 11 men will develop prostate cancer during their lifetime, many tumors remain clinically quiescent. Without entirely reliable ways of predicting which tumors will progress, many prostate cancer patients are treated aggressively with radical prostatectomy or radiation therapy on the chance of cure, but often at the price of devastating treatment side-effects such as urinary incontinence and sexual impotence. Thus, there is a clear need for markers of cellular growth potential as new diagnostic and therapeutic targets in prostate cancer.

In 1971, Knudson postulated that tumors arise from as few as two stochastic events;<sup>3</sup> this empirically based hypothesis—known as the ‘two-hit’ model—has been supported by using molecular genetic approaches. A major tool for these studies has been the determination of loss of heterozygosity (LOH) in tumors, which is a refined version of cytogenetic analysis that can sensitively detect genetic alterations and infer subtle chromosomal mechanisms. The method can be used in sporadic tumor types because shared regions of LOH are likely to reflect potential sites for tumor suppressor genes and common mech-

anisms for tumorigenesis. It is now widely accepted that human tumors originate and undergo malignant progression through a multi-step process in which growth-advantageous genetic events accumulate.<sup>2,4–6</sup> Inactivation of tumor suppressor genes is a critical step in the development of human cancer. Gene inactivation is frequently accompanied by the loss of the chromosome or chromosomal region in which the tumor suppressor resides. This hypothesis was developed by using retinoblastoma as a model<sup>7</sup> and has subsequently been tested in a large variety of tumors, perhaps most rigorously in human colorectal cancer<sup>5</sup> and malignant gliomas.<sup>6</sup>

In prostate cancer, the series of genetic events underlying tumorigenesis is still poorly defined but inactivation of multiple tumor suppressor genes appears to be a common genetic alteration. Inactivation of tumor suppressor gene pathways such as p53, PTEN, and CDKN2-RB, as well as inactivation of metastasis suppressor genes such as KAI-1 and E-cadherin have all been the subject of scrutiny in the molecular progression of the disease.<sup>8–13</sup> Perhaps more important, a myriad of deletions and LOH sites in chromosomes 1, 2, 4–11, 13, and 16–18 have been described in prostate cancer<sup>11,14</sup> suggesting the possibility of as yet unidentified tumor suppressor gene loci. In particular, various allelic losses of chromosome 10 loci have been identified in over 70% of prostate cancers.<sup>15</sup> Multiple regions of LOH on chromosome 10 have been implicated in prostate cancer including 10p11, 10q25 (the locus of the candidate tumor suppressor gene MXI-1), 10q23 (the locus of the PTEN tumor sup-

pressor gene), and 10q21. While chromosome 10q21 losses are frequently observed in prostate cancer and many other tumors, the chromosomal region harbors several potential growth suppressors, so it has been difficult to pinpoint the actual target gene of the LOH.

The annexins (formerly known as calmedins, calelectrins, calpactins, calphobindins, endonexins, lipocortins, synexins) are a complex family of proteins implicated in a number of cellular processes involving calcium signaling. The structural hallmark of the annexins is a conserved 34-kDa C-terminal domain generally comprised of four conserved repeats of 70 residues each. Such repeats contain calcium- and phospholipid-binding sites. All of them hold the area known as the ‘endonexin fold’ with the identifying motif GXGTDE. In contrast to its homologous protein core, the N-terminus of annexins is diverse in sequence and length and appears to be responsible for the specificity of each family member.<sup>16</sup> Several annexins have been implicated in the pathogenesis of benign and malignant neoplasms of different origins.<sup>17</sup> Annexin 7 (ANX7) is the most evolutionarily conserved member of this gene family and it is located on human chromosome 10 in the q21 region.<sup>18</sup> ANX7 encodes a calcium-activated GTPase, which is a protein that fuses membranes in a calcium-dependent manner and localizes to secretory vesicles and plasma membranes.<sup>19</sup>

Established genetic models provide interesting clues to the biological function of the human ANX7 gene. The organism *Dictyostelium discoideum* can be used for selection and testing of growth suppressor genes. Studies of the homologue *anx7* gene mutants in this experimental system suggest that a relative decrease in the *anx7* product favors growth and proliferation at the expense of calcium-dependent differentiation functions.<sup>20</sup> Candidate tumor suppressor genes in mammalian development and tumorigenesis may also be studied by genetic knockouts in mice; indeed, elimination of the *anx7* gene by homologous recombina-



nation results in embryonic lethality while heterozygous mice display defects in calcium signaling and insulin secretion in pancreatic islet cells, but no tumors.<sup>21</sup> Later, in as yet unpublished work (Srivastava *et al*, *Dis Markers* 2001; in press), various developmental defects and tumors were noted as the heterozygous mice aged.

The genetic criteria for tumor suppressor genes include inactivation by mechanisms such as homozygous chromosomal deletions, LOH with mutations in the remaining allele<sup>22</sup> or epigenetic inactivation by promoter methylation and transcriptional silencing.<sup>23</sup> Additional evidence can be provided by functional studies showing cell growth suppression *in vitro* and *in vivo*.

In a notable recent study, Srivastava *et al* tested whether ANX7 might be the gene targeted by 10q21 deletions.<sup>24</sup> Using tissue microarray technology, they showed tumor stage-specific losses in the expression of ANX7 in over 300 prostate cancer specimens. Also, to specifically address the hypothesis that ANX7 is a growth suppressor gene in human prostate cancer cells, the authors transfected full-length ANX7 cDNA into cultured prostate cancer cells. Satisfyingly, this led to a dose-dependent growth suppression of the cells. Taken together, these structural and functional data provide strong support for the candidacy of the ANX7 gene as a growth suppressor in prostate cancer.

A few points still remain to be addressed to definitively establish this role for ANX7: First, the ANX7 gene was transfected into cell lines whose endogenous ANX7 gene status was not described. Are the endogenous alleles absent or present? If present, are the endogenous ANX7 genes defective or functional? Each of these possibilities would have an impact on the interpretation of the present experiments. In addition, while the growth inhibition displayed dose-dependence for the amount of DNA transfected, the amounts of ANX7 proteins expressed need to be determined as well to show that an alternate explanation for the results (for example, toxicity) is unlikely.

Second, the LOH studies implicating ANX7 use microsatellite markers 'on 10q21 at or near the ANX7 locus';<sup>24</sup> however, it is unclear how close they really are. The four markers used in this study span an approximately 6.3-Mb distance and are spaced at approximately 2-Mb intervals (from the G3 map of Human Genome Center at Stanford University; <http://www-shgc.stanford.edu/>). Chromosomal regions of this size may contain several genes. While one marker that shows homozygous loss appears to be the marker closest to ANX7, the authors speculate that ANX7 is homozygously deleted. Because the physical proximity of this locus to ANX7 appears not to be known, it is possible that there is loss at this particular marker but that ANX7 remains heterozygous—this can be easily tested by probing a Southern blot of DNA from the tumor with ANX7 cDNA. This reservation assumes importance since at least one of the examples of LOH presented appears to fall outside the critical chromosome region corresponding to the ANX7 locus.<sup>24</sup> In the absence of a detailed physical mapping, the possibility remains that the actual target may be another gene located near to the ANX7 locus such as SFT (Stimulator of Fe Transport) gene, PPP3CA (calcineurin A alpha), or TCF6 (mitochondrial transcription factor A).

Third, the sequence of the remaining ANX7 allele in the tumors showing LOH at chromosome 10q21 has not been reported. If an intragenic mutation was identified that had a predicted (eg a nonsense or frame-shift mutation) or functional (eg caused alleviation of ANX7 growth-suppressive abilities) consequence, this would provide powerful evidence in support of the candidacy of ANX7 as a tumor suppressor.

The ANX7 gene appears to be an attractive candidate tumor suppressor gene in prostate cancer and, perhaps, other tumors. If it survives the rigorous testing required to move from a candidate to bona fide status, the manuscript by Srivastava *et al* will be considered a landmark study in the genetic basis for this important tumor.

## ACKNOWLEDGEMENTS

WA and RP are recipients of a CaP CURE Award.

## DUALITY OF INTEREST

None declared.

## Correspondence should be sent to

R Pasqualini or W Arap, The University of Texas MD Anderson Cancer Center, 1515 Holcombe Avenue, Houston, TX 77030, USA.  
E-mail: [rpasqual@notes.mdacc.tmc.edu](mailto:rpasqual@notes.mdacc.tmc.edu) or [warap@notes.mdacc.tmc.edu](mailto:warap@notes.mdacc.tmc.edu)

## REFERENCES

- 1 Folkman J. Is tissue mass regulated by vascular endothelial cells? Prostate as the first evidence. *Endocrinology* 1998; **139**: 441–442.
- 2 DeVita VT Jr, Hellman S, Rosenberg SA. *Cancer. Principles and Practice of Oncology*, 5th edition. Lippincott-Raven Publishers: 1997.
- 3 Knudson AG. Mutation and cancer: statistical study of retinoblastoma. *Proc Natl Acad Sci USA* 1971; **68**: 820–823.
- 4 Lasko D, Cavenee W, Nordenskjold M. Loss of constitutional heterozygosity in human cancer. *Annu Rev Genet* 1991; **25**: 281–314.
- 5 Vogelstein B, Fearon ER, Hamilton SR, Kern SE, Preisinger AC, Leppert M *et al*. Genetic alterations during colorectal-tumor development. *N Engl J Med* 1988; **319**: 525–532.
- 6 Nagane M, Huang HJ, Cavenee WK. Advances in the molecular genetics of gliomas. *Curr Opin Oncol* 1997; **9**: 215–222.
- 7 Cavenee WK, Dryja TP, Phillips RA, Benedict WF, Godbout R, Gallie BL *et al*. Expression of recessive alleles by chromosomal mechanisms in retinoblastoma. *Nature* 1983; **305**: 779–784.
- 8 Navone NM, Troncoso P, Pisters LL, Goodrow TL, Palmer JL, Nichols WW *et al*. p53 protein accumulation and gene mutation in the progression of human prostate carcinoma. *J Natl Cancer Inst* 1993; **85**: 1657–1669.
- 9 McMenamin ME, Soung P, Perera S, Kaplan I, Loda M, Sellers WR. Loss of PTEN expression in paraffin-embedded primary prostate cancer correlates with high Gleason score and advanced stage. *Cancer Res* 1999; **59**: 4291–4296.
- 10 Halvorsen OJ, Hostmark J, Haukaas S, Hoisater PA, Akslen LA. Prognostic significance of p16 and CDK4 proteins in localized prostate carcinoma. *Cancer* 2000; **82**: 416–424.
- 11 Verma RS, Manikal M, Conte RA, Godec CJ. Chromosomal basis of adenocarcinoma of the prostate. *Cancer Invest* 1999; **17**: 441–447.
- 12 Ueda T, Ichikawa T, Tamaru J, Mikata A, Akakura K, Akimoto *et al*. Expression of the KAI1 protein in benign prostatic hyperplasia and prostate cancer. *Am J Pathol* 1996; **149**: 1435–1440.
- 13 Paul R, Ewing CM, Jarrard DF, Isaacs WB. The cadherin cell-cell adhesion pathway in prostate cancer progression. *Br J Urol* 1997; **79**: 37–43.



- 14 Cher ML, Bova GS, Moore DH, Small EJ, Carroll PR, Pin SS *et al*. Genetic alterations in untreated metastases and androgen-independent prostate cancer detected by comparative genomic hybridization and allelotyping. *Cancer Res* 1996; **56**: 3091–3102.
- 15 Trybus TM, Burgess AC, Wojno KJ, Glover TW, Macoska JA. Distinct areas of allelic loss on chromosomal regions 10p and 10q in human prostate cancer. *Cancer Res* 1996; **56**: 2263–2267.
- 16 Raynal P, Pollard HB. Annexins: the problem of assessing the biological role for a gene family of multifunctional calcium- and phospholipid-binding proteins. *Biochem Biophys Acta* 1994; **1197**: 63–93.
- 17 Bastian BC. Annexins in cancer and autoimmune diseases. *Cell Mol Life Sci* 1997; **53**: 554–556.
- 18 Shirvan A, Srivastava M, Wang MG, Cultraro C, Magendzo K, McBride OW *et al*. Divergent structure of the human synexin (annexin VII) gene and assignment to chromosome 10. *Biochemistry* 1994; **33**: 6888–6901.
- 19 Kuijpers GAJ, Lee G, Pollard HB. Immunolocalization of synexin (annexin VII) in adrenal chromaffin granules and chromaffin cells: evidence for a dynamic role in the secretory process. *Cell Tissue Res* 1992; **269**: 323–330.
- 20 Doring V, Schleicher M, Noegel AA. *Dictyostelium* annexin VII (synexin). cDNA sequence and isolation of a gene disruption mutant. *J Biol Chem* 1991; **266**: 17509–17515.
- 21 Srivastava M, Atwater I, Glasman M, Leighton X, Goping G, Caohuy H *et al*. Defects in inositol 1,4,5-trisphosphate receptor expression, Ca(2+) signaling, and insulin secretion in the *anx7* (+/–) knockout mouse. *Proc Natl Acad Sci USA* 1999; **96**: 13783–13788.
- 22 Hansen MF, Cavenee WK. Tumor suppressors: recessive mutations that lead to cancer. *Cell* 1988; **53**: 173–174.
- 23 Merlo A, Herman JG, Mao L, Lee DJ, Gabrielson E, Burger PC *et al*. 5' CpG island methylation is associated with transcriptional silencing of the tumour suppressor p16/CDKN2/MTS1 in human cancers. *Nature Med* 1995; **1**: 682–692.
- 24 Srivastava M, Bubendorf L, Srikantan V, Fossum L, Nolan L, Glasman M *et al*. ANX7, a candidate tumor suppressor gene for prostate. *Proc Natl Acad Sci USA* 2001; **98**: 4575–4580.